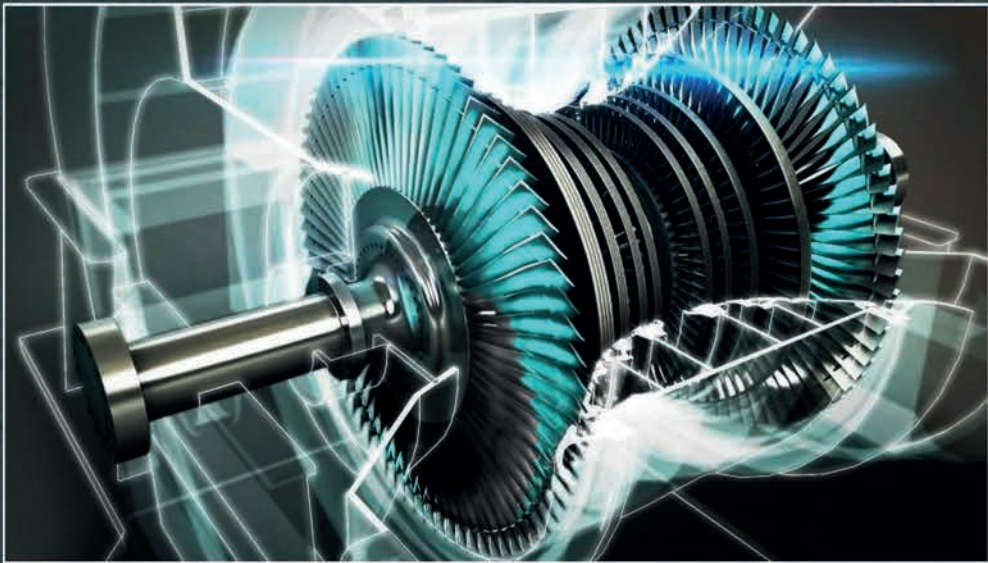


Anatoly
TARELIN

**HEAT-
ELECTROPHYSICAL
PROCESSES
IN STEAM
TURBINES**



NATIONAL ACADEMY OF SCIENCES OF UKRAINE
A. PIDHORNYYI INSTITUTE OF MECHANICAL
ENGINEERING PROBLEMS OF THE NAS OF UKRAINE

НАЦІОНАЛЬНА АКАДЕМІЯ НАУК УКРАЇНИ
ІНСТИТУТ ПРОБЛЕМ МАШИНОБУДУВАННЯ
і.м. А.М. ПІДГОРНОГО НАН УКРАЇНИ

Анатолій
ТАРЕЛІН

**ТЕПЛО-
ЕЛЕКТРОФІЗИЧНІ
ПРОЦЕСИ
В ПАРОВИХ
ТУРБІНАХ**

ПРОЄКТ
«УКРАЇНСЬКА НАУКОВА КНИГА
ІНОЗЕМНОЮ МОВОЮ»

КИЇВ
АКАДЕМПЕРІОДИКА
2024

Anatoly
TARELIN

**HEAT-
ELECTROPHYSICAL
PROCESSES
IN STEAM
TURBINES**

*PROJECT
«UKRAINIAN SCIENTIFIC BOOK
IN A FOREIGN LANGUAGE»*

KYIV
AKADEMPERIODYKA
2024

Reviewers:

O.L. SHUBENKO, Corresponding Member of the NAS of Ukraine, Dr. Tech. Sci., Prof., Head of the Department of Optimization of Processes and Turbomachinery Designs of the A. Pidhornyi Institute of Mechanical Engineering Problems NAS of Ukraine

N. M. FIALKO, Corresponding Member of the NAS of Ukraine, Engineering Sci. Dr, Prof., Honored Worker of Science and Engineering of Ukraine, Laureate of the State Prize of Ukraine in Science and Technology, Head of Thermophysics of Energy-Efficient Heat Technologies Department of the IETP NAS of Ukraine

Approved for publication by the Scientific Council of the A. Pidhornyi Institute of mechanical engineering problems NAS of Ukraine (September 21, 2023, Protocol No. 7)

The publication was funded within the framework of the Targeted Complex Program of the NAS of Ukraine “Scientific Bases of Functioning and Providing for Conditions for the Development of the Scientific and Publishing Complex of the NAS of Ukraine”

Tarelin A.O.

T21 Heat-electrophysical processes in steam turbines / A.O. Tarelin; A. Pidhornyi Institute of Mechanical Engineering Problems of the NAS of Ukraine. — Kyiv: Akadempriodyka, 2024. — 140 p.

ISBN 978-966-360-512-8

The monograph deals with comprehensive research in the field of electrization of wet steam flow in a turbine. An analysis is presented, the experience of studies conducted on laboratory stands and full-scale facilities (CHP and TPP) in Ukraine, the USA is summarized, post-factorial phenomena of electrization and their influence on the operational characteristics of the turbine are considered, and specific recommendations are proposed to improve its efficiency and reliability. The most widely presented are studies on establishing the main electrophysical factors of influence the surface strength of the blade, such as electric fields, charge density, and their polarity. Water chemistry regimes (WCM) are also considered in the context of their influence on the flow charge formation process, reliability, and efficiency indicators of the turbine. The monograph may be useful to energy specialists working in the field of research, development, and operation of steam turbines.

UDC 621.165

FOREWORD

Steam turbines are heat engines in which the thermal energy of steam is converted into mechanical energy. High-temperature high-pressure steam, passing through the flow path of the turbine, expands while maintaining near and supersonic speeds, contacting (being in touch) with the metal structures of the flow path of the LPC. As a result, the flow of wet steam is electrified. The high charge density in the flow path of the turbine's LPC is accompanied by electrical discharges and ionization of the steam flow, which can have a noticeable effect on the properties of steam, heat exchange processes, and, given the presence of an aggressive electrified working medium, can intensify erosion-corrosion degradation phenomena in metal structures. In fact, in this part of the turbine, the ongoing processes should be considered as heat-electrophysical, in which the effect of electrization cannot be ignored.

The phenomenon of electrization was first described by Thales around 600 BC as the property of rubbed amber to attract light bodies, and only 2200 years later, the study of the phenomenon of electrization was continued by Hilbert, who in 1600 showed that this property is inherent for other solids and introduced the concept "electricity". Then Otto von Guericke in 1663 built the first electrical device, consisting of a sulfur ball, which, when rotated, could rub against the palm and become electrified at the same time. He was the first who observed (in 1672) electrical repulsion. The distinction between two kinds of electricity was discovered by Du Fay in 1734. At the end of the 19th century, Ken showed that already touching and then separating two bodies was enough to electrify them. Thus, the study of the phenomenon of electrization was unsystematic and proceeded extremely slowly.

The fact that electrical phenomena arise in wet steam installations has been known for a long time from observations at industrial installations and experimental stands. Historically, these phenomena were first discovered at the end of the 19th century in England, where steam engines were widely introduced into production.

The first observations of the electrization of a steam jet on a steam boiler were announced by A. Anderson. In late September 1840, an unusual incident occurred on a 28-horsepower steam engine that was driving trolleys in a coal mine near Newcastle. The driver noticed

a flow of steam leaking under the flange of the safety valve. Thinking that the pressure in the evaporator had risen too high, he decided to manually open the safety valve. As soon as he touched the safety valve, he felt a strong tingling sensation in his fingertips. This experiment was repeated many times, and it was found that the strongest spark was observed when the experimenter was standing in a flow of steam, and not in a surrounding cloud of steam, and if he was standing on the brickwork of the base of the boiler, then he could communicate strong sparks to the surrounding observers when they brought their hands to his hand.

The stories about the phenomena observed by the drivers attracted the attention of the scientific community. Lord William Armstrong, in a letter to Michael Faraday, described the phenomenon of steam electricity. Faraday replied to Armstrong that he investigated the incident and, using an electrometer, found a positive electric charge in the steam flow. Faraday determined that the water used in the boiler was acidic due to accumulated deposits. In another boiler, filled with clean rainwater, Faraday did not find the electric charge of the steam flow. As a result, Faraday suggested that the chemical composition of the evaporated water affects the charge of the steam.

The study of the phenomenon of electrization of a flow of wet steam was continued by other researchers. Shortly after Armstrong's work, Pattinson discovered that the length of the sparks from the discharge of an electrified flow of steam was proportional to the pressure in the boiler.

As new experimental facts were obtained, ideas about the nature of the electrization of wet steam flow gradually changed. In 1843, the hypothesis about the leading role of triboelectric phenomena in the electrization process began to prevail. After probes inserted inside the boiler did not allow detecting electrization inside, Armstrong expressed his belief that the source of electricity was concentrated in a place where wet steam moves with friction, but he had great difficulty in substantiating the hypothesis that steam friction (triboelectricity) was exceptionally the cause of electrization. Faraday's studies did not contradict the hypothesis of the leading role of friction phenomena, since they demonstrated that the electrization of the liquid did not occur during evaporation, condensation, or a change in the state of the liquid, at the same time, it was possible to change the amount of charge of the steam flow by changing the nozzle material without changing the regime of evaporation. These results also contributed to a change in Faraday's point of view on the chemical properties of water as a source of steam electrization in favor of the hypothesis of contact electrization when a flow of wet steam (liquid particles in a steam flow) friction against the nozzle wall. Faraday confirmed the results of Armstrong's work that dry steam is not electrified, but distilled water entering the steam flow is charged positively, and the boiler itself is negatively charged. When a small amount of alkali was added to distilled water, the steam acquired a positive charge. Ammonia added to the distilled water led to an increase in electrical charges in the steam flow, but the charge disappeared after a small amount of sulfuric acid was added to the boiler water. From studies of the electrization of steam at the end of the 19th century, only in the experiments of M. Faraday were measurements of the pH of electrified steam and the effect of changes in acid-base properties on electrization.

To explain the observed facts, Faraday proposed a hypothesis of triboelectric pairs: impurities on the surface of distilled water droplets and the nozzle material form triboelectric pairs. The sign of the charge was determined by the mutual position of the rubbing substances in the triboelectric row.

However, even this point of view did not allow for explaining the results of several experiments, in particular, the sign of the droplet charge in a liquid flow sprayed with compressed air.

A detailed study of the influence of nozzle materials on the electrization process was carried out by Lord Armstrong on an experimental steam boiler mounted on glass insulators. Armstrong found that the amount of electrization was influenced by the pressure in the boiler and the material of the nozzle. In addition, the material of the nozzle and the chemical composition of the liquid also affect the sign of the electric charge of the wet steam flow. However, Armstrong did not offer a theory explaining the relationship between the sign of the steam charge and the nozzle material, as well as the effect of chemical additives on electrization.

Researchers have noted a certain similarity between the processes of electrization of wet steam and electrization when sprayed or sprinkled with water droplets. The model of electrization of drops, considering the features of the structure of the water surface, was proposed in 1892 by Lennard. The model used a new concept — a double electric layer on the surface of the water. The model explained the sign of the droplet charge not by triboelectric phenomena, but by the structural features of the surface of the dispersed liquid. However, this model was more suitable for describing the process of liquid spraying, and the processes occurring during the electrization of wet steam are much more complicated.

Summing up the general picture that developed in the study of steam electrization at the end of the 19th century, it can be noted that there was an initial accumulation of experimental facts, and also primary scientific theories that underwent significant evolution arose. However, neither purely chemical nor purely physical models proposed by scientists at the end of the 19th century allow explaining the entire complex of observed phenomena, especially the processes taking place in steam turbines.

The practical application of electrization of steam in steam engines was tried to be realized in some designs of steam electrostatic generators with multiple nozzles. By 1843, a gigantic 46-nozzle machine was built for the Polytechnic Institute of London. Steam generators made it possible to obtain a high voltage with a spark discharge in the air over 50 cm, but had extremely low efficiency and huge dimensions. However, despite numerous studies in this direction, steam electrostatic generators of this type did not receive wide distribution in the future.

Studies carried out at the end of the 20th century have shown that the phenomenon of electrization in wet steam turbines is a complex multicomponent process that occurs mainly due to the electrization of droplets. Water droplets in the stream can collide with the working surface of the blades or be detached from it during movement, large droplets can be crushed into small ones, etc. In general, these processes can include bioelectric and electrolytic mechanisms, as well as the effect of the destruction of the double electric layer [1], the last one, as shown by numerous studies, is prevalent.

The first demonstration of the electrization of wet-steam turbines can be considered the phenomenon of electrization of the rotors of wet-steam turbines, discovered at the beginning of the 20th century, and, as a result, damage (due to electro-corrosion) of bearings.

In the domestic scientific and technical literature, publications devoted to this phenomenon appeared in the 30s. To explain the phenomenon of electrization, hypotheses were put forward in two directions: «electromechanical» and «heat-mechanical». The electromechanical direction combines hypotheses related to the mechanism of electromagnetic induction arising in the elements of a turbine plant. In the thermo-mechanical direction, the hypotheses are based on the study of the features of static electrization during friction of steam on the surface of the turbine rotor. Unfortunately, the explanations for the causes of electro-corrosive wear of bearings presented in the literature are contradictory and insufficiently substantiated.

In the middle of the 20th century, publications appeared in which attention was drawn not only to the rotor charge but also to the electrization of the steam flow in the turbine. So in 1980, the authors D. Rayleigh and F. Loftus published a paper [2] devoted to a comprehensive experimental study of electrostatic phenomena associated with the flow of wet steam in wet steam turbines. The investigations were carried out on an experimental stand in a wet-steam channel, the processes of condensation, the relative velocities of the phases, the rupture of the liquid-vapor interface, and the formation of droplets were studied. Steam was charged with a dry steam flow with primary and secondary spraying of a liquid film. The results of the study showed that electrization depends on the parameters of steam, and vacuum in the condenser, and the presence of a positive potential on the turbine shaft indicates active erosion of the blades. According to the authors, the electrization of wet vapor occurs mainly due to the impact of drops on an obstacle and the subsequent destruction of the liquid surface into small drops, which become charged, as well as from the sudden separation of the liquid film from the solid surface. In this case, there is no electrization of dry steam and contamination of the surface of the flow channel, and impurities in the wet steam change the polarity of its charge. The article does not attempt to associate electrostatic charges in the steam flow with the characteristics of the turbine; in the authors' opinion, their influence on the efficiency of working processes should be investigated separately. Electrical charges are expected to contribute insignificantly to performance degradation but can have a significant effect on blade erosion. The article points out the need for a further comprehensive study of the effect of the electrization of wet steam in a turbine to improve the design of bearing assemblies for increasing the working life of the rotor and turbine blades.

A new stage in the study of the phenomena of static electrization, which was carried out both on experimental stands, which is very important, and on full-scale steam turbine installations of CHP and TPP, was the work begun at IPMash NAS of Ukraine in 1980. First of all, it was found that static electrization not only the turbine rotor is exposed, but also the wet-steam flow in the section from the phase transition zone to the exhaust pipe. Moreover, the strongest electrization of the wet steam flow is observed in the zone of the last stage and the exhaust pipe of the turbine.

Static electrization of a wet steam flow has a significant effect on the phase transition process, on the flow of wet steam in the LPC stages and in the exhaust pipe. It was discovered for the first time that behind the last stage of the turbine, a high-speed flow of wet steam can contain a significant volumetric electric charge, not only affecting gas-dynamic processes but also generating a broad-spectrum electromagnetic field with a power of up to tens of kW.

The presence of such complex electrical and magnetic phenomena accompanying thermal processes in a turbine makes it possible to consider them together as a complex thermoelectrodynamic system and to study the effect of natural and artificial electrization of a wet steam flow on the reliability and efficiency of a turbine plant. Such studies in the theory of turbomachines can be characterized as a new scientific direction — heat-electrophysics.

The presented work summarizes and systematizes all the studies conducted under the guidance of the author [1] with a more expanded presentation of the material on the effect of electric charges and fields on the surface strength of blades, as well as water-chemical modes on the reliability and efficiency of the turbine.

ELECTROSTATIC CHARGE IN WET STEAM FLOW WITHIN A TURBINE

1.1. An experimental set-up for the study of electrostatic charge build-up in wet steam flows

Contact electrization of steam droplets causes the build-up of electrostatic charge in wet steam flows.

The collision of a droplet of water with the working surface of a blade or nozzle causes a charge build-up on all surfaces, including the droplet itself. Water droplets acquire an electric charge when they are detached from solid «separation charging» or when a large droplet is crushed/evaporated while moving in a stream.

In a wet steam flow within a steam turbine, moisture serves as a main charge carrier where volume charge is proportional to moisture concentration. Despite many significant differences in essential electrodynamic processes occurring in humidified air flow at atmospheric pressure and within a steam flow at reduced pressure, the mechanisms of charge build-up on water droplets remain the same. Therefore a study of the electrostatic charge build-up in humidified airflow would allow for a better understanding of electrostatic processes occurring within a flow section of the steam turbine. Fig. 1.1 represents a diagram of the experiment and includes the following main systems:

- a system for organizing airflow and air humidification;
- a system for charging the flow and measuring the flow charge.

To organize the air -droplet flow behind the nozzle 22, an air humidification system was installed.

The drop flow generated by the nozzle is exposed to the accelerating air flow and electric field. In this case, further

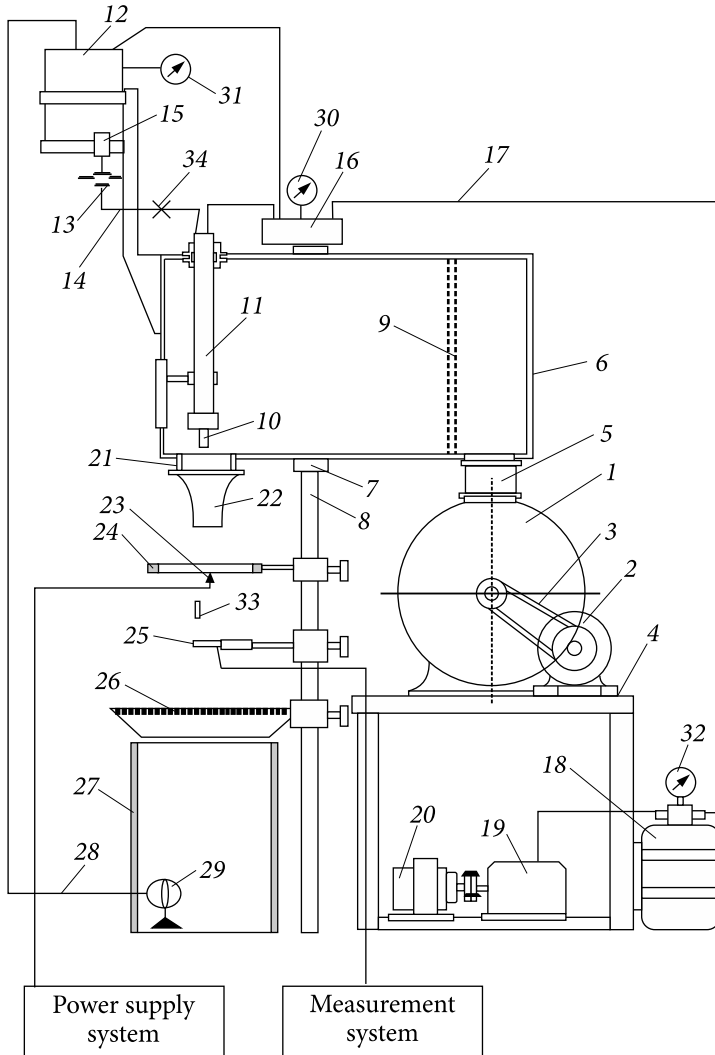


Fig. 1.1. Layout of the stand for testing and calibrating electrical probes: 1— fan; 2 — electric drive; 3— V-belt transmission; 4 — platform; 5 — inlet pipe; 6 — receiver; 7 — receiver support; 8 — racks; 9 — lattice; 10 — pneumatic nozzle; 11 — nozzle attachment; 12 — tank; 13 — throttle washer; 14 — pipeline; 15 — filter; 16 — adjustable pneumatic device; 17 — air duct; 18 — compressor receiver; 19 — compressor; 20 — compressor electric drive; 21 — outlet branch pipe; 22 — nozzle; 23 — corona electrode; 24 — screen ring; 25 — electric probe; 26 — collector; 27 — tank; 28 — pipeline; 29 — pump; 30, 31, 32 — pressure gauges; 33 — pitot tube; 34 — clamp

crushing of the droplets occurs. The average droplet diameter behind the nozzle is $\sim 30 \mu\text{m}$. During the experiments, the volumetric charge density was measured (per unit volume of the air droplet flow).

At the stand, it is necessary to create conditions that are adequate to those existing in steam turbines, first of all, in terms of the amount of moisture per unit volume. Therefore, in order to approximate the results to real conditions in the turbine, we used the parameter not «moisture degree», but «water content» — the amount of water in 1 m³ of the medium — a parameter widely used in meteorology.

Subsequently, conductivity W , corresponding to a certain moisture steam, will be called the equivalent humidity Y . The water content of steam at the turbine exhaust depends on its moisture content and pressure in the condenser. An analysis of the operating modes of several turbine units showed that the water content of the steam flow after the last low-pressure stages is $\sim 2\text{--}4.5\text{ g/m}^3$. As the initial water content about bench conditions, its value was taken equal to 3.5 g/m^3 . This water content of the steam flow occurs at the exhaust of a turbine operating at a pressure in the condenser of $\sim 4.5\text{ kPa}$ and a steam humidity of 10 %. Fig. 1.2 shows the dependences of the water content of steam at the turbine exhaust on the moisture content of the steam at various pressures in the condenser.

The stand makes it possible to study the dependence of the removal current (electrization) and charge polarity on the water content, flow rate, chemical composition of water, and material of the surface washed by the flow, as well as to study the effect of the electric field on the electrization process.

To study the dependence of electrization current on the flow parameters, the diagram shown in Fig. 1.3 was used.

The airborne stream 1 flows out through nozzle 2 and passes through electrode 3, which is a ring 100 mm in diameter with a grid having a permeability of 0.8. When moving through the grid, part of the droplets contained in the flow settles on the grid. When droplets are detached from the grid of electrode 3, electrification of the flow occurs, i.e. removal current I_s . The amount of carry-over current is controlled by a micro ammeter. With the help of a static voltmeter, the potential arising on electrode 3, when the flow passes through it, can also be measured. At a distance of 100—300 mm from electrode 3, a collector electrode 4 is installed, which is a ring 300 mm in diameter with a grid having a permeability of 0.98 made of stainless steel. Due to the high permeability, as well as the distance from the nozzle 2, the electrization of the collector 4 practically does not affect the results of the experiment. Collector 4 allows you to

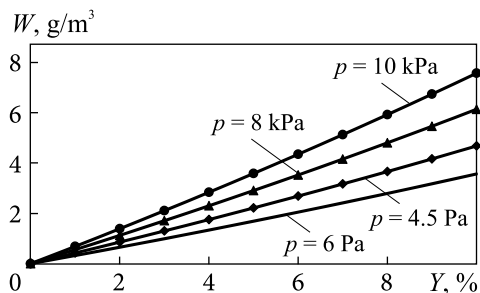


Fig. 1.2. Dependence of the water content of the steam flow at the turbine exhaust on humidity at various pressures

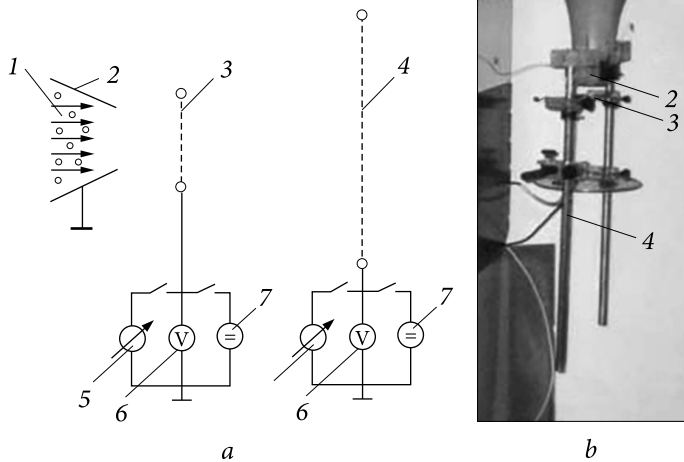


Fig. 1.3. Electrical diagram (a) and a general view of the device for measuring the air-droplet flow discharge current (b). 1 — Airborne droplet flow; 2 — nozzle; 3 — grid electrode; 4 — collector electrode; 5 — microammeter; 6 — voltmeter; 7 — capacitor

control the amount of the carry-over current from electrode 3, as well as create an electric field due to an additional high-voltage source.

1.2. Methods for measuring the density of charges in a wet steam flow of a turbine

To study the processes of flow electrization in steam turbines, it is necessary to have a reliable and simple method that makes it possible to measure or control the real-time value of the volumetric charge in the flow.

The specificity of the research object does not allow direct use of the experience gained in measuring charges in the atmosphere.

When measuring volumetric charges in fogs and clouds, one has to deal with charge densities of $10^{-9} - 10^{-7} \text{ C/m}^3$ [1]. For such measurements, in practice, methods based on measuring the probe potential are most often used. At the same time, the required insulation resistance of $10^{11} - 10^{15} \text{ Ohm}$ is easily provided with simple techniques. A decrease in the insulation resistance caused by the presence of moisture leads to an increase in the potential measurement error. In this case, an error in measuring the potential of 1% leads to an error in determining the volumetric density of charges up to 30% or more.

Providing the required insulation resistance for a probe placed in a wet steam flow is extremely difficult. This is because the water film formed on the surfaces in the wet steam flow of the turbine is a concentrated solution of impurities contained in the water supply. In this case, the most appropriate method is to determine the volumetric charge by shorting the current circuit on the probe [3, 4].

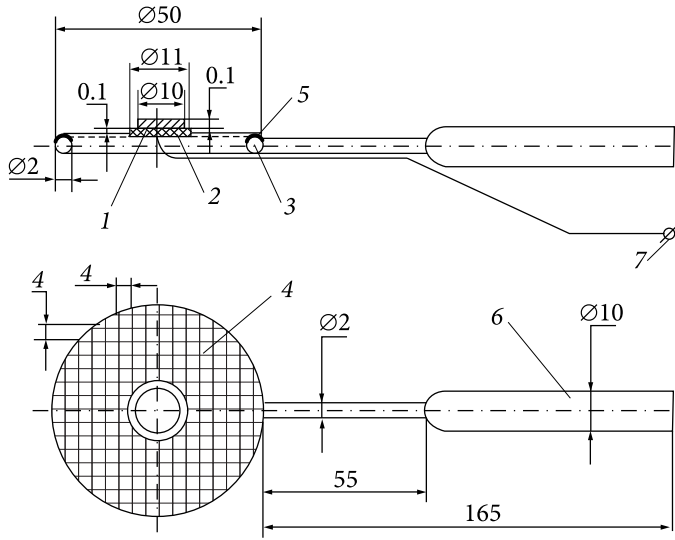


Fig. 1.4. Standard probe: 1 — electrode; 2 — insulator; 3 — ring; 4 — grid; 5 — compound; 6 — holder; 7 — probe terminal

If steam flow with a certain volumetric charge q_v moves at a speed C through the area S , then a current flows through it [5]

$$I_s = C \cdot q_v \cdot S$$

Having measured the value of the current I_s , as well as knowing the area S and the flow rate C , we can find the volumetric charge density q_v . The magnitude of the current can be measured with any required accuracy. The flow rate C can also be determined using standard methods with the required accuracy. Thus, to measure the volumetric charge density in the flow, it is necessary to know a precise value of the effective cross-sectional area S_{eff} of the probe since when measuring the short-circuit current of the probe in a pair, the electric field of the volumetric charge is distorted, due to which the S_{eff} of the probe increases, i.e. $S_{\text{eff}} = K_s \cdot S$. The effective cross-section of the probe depends on the flow rate, charge density, flow moisture and can be found experimentally, while the probe configuration should not distort the flow in any way. To determine the influence of flow parameters on the effective section of the probe, special studies were performed in a laboratory setting.

K_s is determined by comparing the currents of the probes under test, with the currents of the reference probe, measured at the same flow parameters.

Fig. 1.4 shows the design of the probe used as a standard for calibration of the test probes.

To determine the effective surface area of the measuring probe, the standard (see Fig. 1.4) and the tested probes (Fig. 1.5, 1.6) were alternately installed

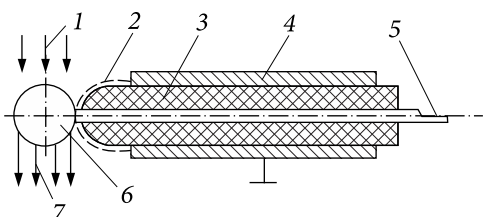


Fig. 1.5. Diagram of an electrical probe placed in a wet steam flow: 1 — flow coming to the probe; 2 — water film; 3 — insulator; 4 — body; 5 — output of the probe; 6 — receiving surface of the probe; 7 — flow, breaking off from the surface of the probe

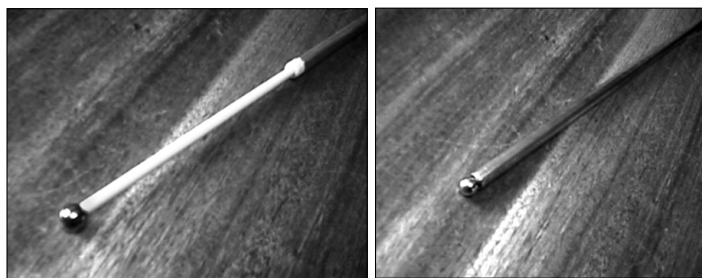


Fig. 1.6. The electric probes used in experiments

in the same place in the charged flow. Then the current of each probe was measured at speeds from 30 to 90 m/s.

The performed studies have shown that the effective section of a spherical probe with a diameter of 10 mm can be approximated to 1.25 of the probe surface area S . Fig. 1.5 shows a schematic of a probe placed in a flow of wet steam.

1.3. The main factors affecting the magnitude and polarity of charges in the steam-water flow

The Studies describing the influence of various factors on charges in a wet steam flow are described in detail in [1]. This monograph is set to describe the laboratory stand and general final results of various experiments, including full-scale ones, which will be used in subsequent studies presented further. Below are the main trends that influence the charge formation in the steam flow concerning various factors (speed, moisture, electric field, and pH).

The dependence of the electrization current on the flow rate is shown in Fig. 1.7. It can be seen that the electrization current grows proportionally to an increase in the flow rate. An increase in the discharge current with an increase in the flow rate is associated with a decrease in the film thickness and, as a consequence, an increase in the amount of charges carried away by the drops from the Gui layer, upon stripping from a washed surface.

The dependence of the electrization current on the water content of the flow is shown in Fig. 1.8. The water content of the flow was controlled by changing the water flow rate through the nozzle.

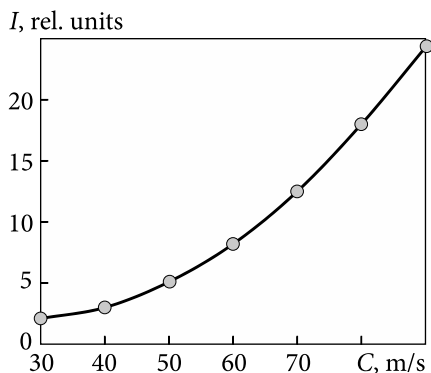


Fig. 1.7. Dependence of the electrization current on the flow rate

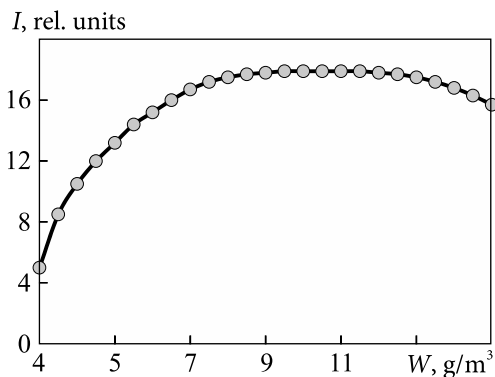


Fig. 1.8. Dependence of the electrization current on the water content of the air droplet flow

It can be noted that an increase in water content is accompanied by an increase in the electrization current of the air-droplet stream until the saturation occurs, i.e. with a further increase in water content, the electrization current does not increase (Fig. 1.8). Due to a fact that the water content in a wet stream zone of a turbine typically does not exceed 5g/m^3 , the electrization of a steam flow, and subsequently the volumetric charge density of the flow will increase accordingly to an increase in stream moisture. To illustrate the above, Fig. 1.9. shows the dependence of the electric probe current on the steam moisture obtained during a full-scale experiment on the T-37/50-8.8 turbine. Where the moisture of a steam flow is the only variable parameter, other parameters are unchanged (steam flow rate, pressure in the condenser, steam consumption, etc.).

With a change in moisture from 1.3 to 1.75 %, the probe current changed almost linearly, which is associated with a slight change in moisture (Fig. 1.8).

During the study, the influence of the material on the polarity of charges in the flow was also considered.

The polarity of the charges acquired by droplets upon separation from the surface in a two-phase flow depends primarily on the direction of the electric field in the electric double layer. With the same chemical composition of water in an air or vapor-droplet flow, the polarity of the charges formed on the droplets will be determined by the material of the surface in the flow. Stainless steel, black steel, and brass alloys are mainly used in the flow path of the turbine and the condenser of the turbine unit. Therefore, during the research, the polarity of the charges was determined only for these materials. For this purpose, stainless steel, black steel, and brass nets were installed in the air-droplet flow downstream of the nozzle of the laboratory experimental unit. As a result of the re-

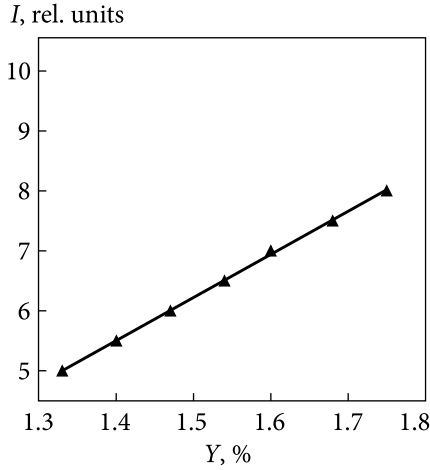


Fig. 1.9. Dependence of the probe current on the moisture of the steam flow (turbine T-37/50-8.8)

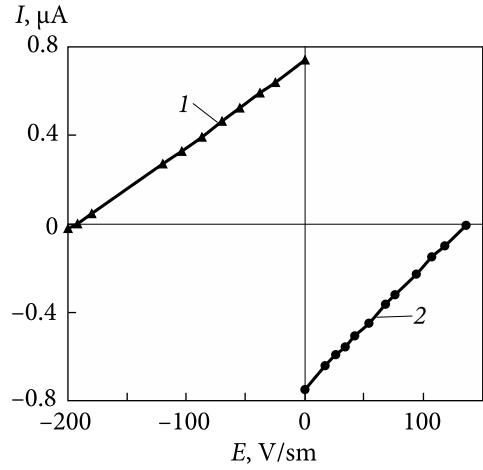


Fig. 1.10. Dependences of the removal current on the electric field strength: 1 — brass grid; 2 — stainless steel grid

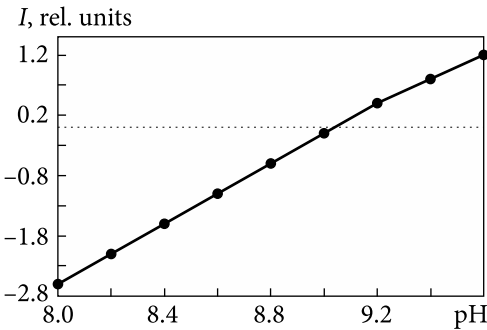


Fig. 1.11. Dependence of the current measured on the probe to water PH (lab results)

search, it was found that for distilled water the polarity of the charges formed when flowing around a stainless steel grid (+), and for a black steel and brass grid (-).

Fig. 1.10 shows the dependence of the removal current from electrode 3, made of stainless steel and brass, on the strength of the electric field created by electrode 4 at a constant flow rate.

It can be seen that for an electric field strength of $E = 0$, the removal current takes on a maximum value regardless of the material of the grid in the air-droplet flow (Fig. 1.10). For the brass grid, the polarity of the current to ground is positive. This indicates that negatively charged drops are carried away from the brass grid by the flow. For the stainless steel grid, the polarity of the removal current is opposite. With an increase in the electric field strength (due to an increase in the voltage on electrode 4), the removal current decreases almost linearly. To completely stop the electrization process, it is sufficient to create a counter-electric field with an intensity of $E = -192 \text{ V}/\text{cm}$ for the case of a brass grid and $+136 \text{ V}/\text{cm}$ for a stainless steel grid.

Thus, the flow of the carryover current from the working surface can be controlled by changing the electric field strength near the surface on which electrization occurs.

The dependence of the electrization current on the pH of water is shown in Fig. 1.11. With an increase in water pH from 8 to ~9 units, the electrization current decreases to zero, and with a further increase in pH to 9.2, the electrization current reverses its polarity (Fig. 1.11.).

Similar studies to determine the dependence of the electrization current on the pH of the feed water were also obtained during an experiment carried out on an 800 MW turbine at the Navajo station (Arizona, USA) [1].

1.4. Brief chronology of the studies carried out to determine the charge density in the wet steam flow of the turbines of TPP and TPP

In 1992, the researchers of IPMash NAS of Ukraine during research on the steam turbine T-37/50-8.8 (TPP-2 «Eskhar») for the first time discovered the presence of charges in the steam flow of the turbine. The measured charge density downstream the last stage of the turbine turned out to be an order of magnitude higher than in a thundercloud and amounted to 10^{-3} C/m^3 at an electric field strength of up to $2 \cdot 10^5 \text{ V/m}$. The measurements were carried out with a stationary electric probe installed in the peripheral zone of the last stage impeller. The fact of the existence of an electromagnetic field in the turbine branch pipe was also established and its spectral composition was measured [6].

It was found that the measured charge density at the beginning of the phase transition zone depends on the water-chemical regime and measured $10^{-10} - 10^{-8} \text{ C/m}^3$. Both positive and negative charges appear in the steam flow, the concentration of which sharply increases when coarse moisture appears in the flow. Under different water-chemical regimes, an increase in the density of charges in the steam flow is accompanied by a decrease in the supercooling of the steam. The studies performed allow us to conclude that it is possible to reduce the supercooling of steam in the flow path due to ionization [7].

In 1997, in the USA, on a steam turbine of 800 MW at the Navajo TPP (Arizona), the steam flow was traversed in the flow path of the turbine with movable electric probes (see Fig. 1.12).

The possibility of controlling the process of electrization of the steam flow by changing the water-chemical regime has been investigated (see Fig. 1.12 c). It was found that before the last stage, the charge density was $10^{-8} - 10^{-6} \text{ C/m}^3$, and after the last stage — 10^{-4} C/m^3 . With the help of an optical probe, a glow of

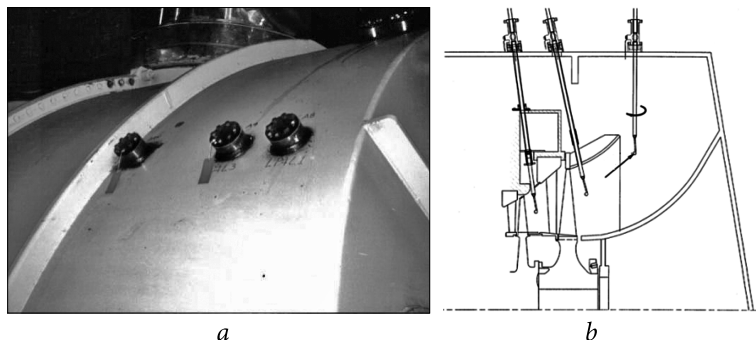


Fig. 1.12. Traversing the steam flow with electric probes: *a* — installation of special valves; *b* — movable probes; *c* — results of measurements of charges in the flow path of the turbine

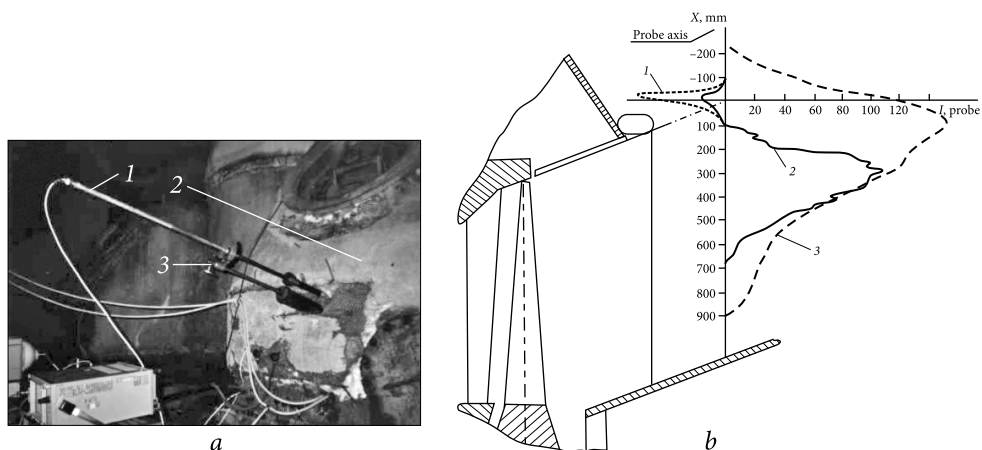


Fig. 1.13. Traversing the flow downstream of the last stage with an electric probe: *a* — installation of a movable combined probe with a coordinate device for measuring the density of charges in the steam flow at the turbine exhaust; *b* — distribution of charges in the flow from the side of the regulator (1 — $I \cdot 0.5 \cdot 10^8$ A, $T_{min} = 542$ °C, $N = 200$ MW; 2 — $I \cdot 10^7$ A, $T_{min} = 512$ °C, $N = 200$ MW; 3 — $I \cdot 10^6$ A, $T_{min} = 512$ °C, $N = 250$ MW in heating mode)

steam was detected directly downstream of the impeller of the last stage, which confirms the presence of discharge phenomena in the steam flow of the turbine.

Similar studies were carried out on the T-250/300-23.5 cogeneration steam turbine (see Fig. 1.13). The density of charges was fixed in the range of 10^{-8} — 10^{-6} C/m³. The fact of an increase in the concentration of hydrogen at the turbine exhaust with an increase in the density of charges in the steam flow has been established.

Using movable probes on a 400 MW turbine (USA, Conesville), the charge density measured downstream the last stage of the turbine was within 10^{-8} —

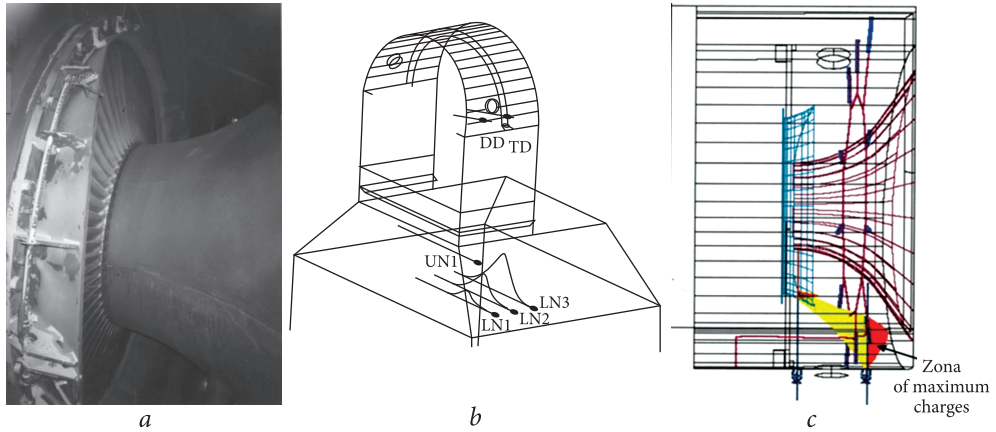


Fig. 1.14. Flow traversing in the exhaust and condenser zone: *a* — turbine exhaust with a capacity of 400 MW (USA, Conesville); *b* — a diagram of the installation of movable electric probes in the turbine exhaust pipe (in the lower part of the figure, the distribution of charges along the axes of the probes in the condenser zone is shown); *c* — charge distribution in the diffuser area

10^{-6} C/m^3) the measurements obtained in the condenser were within 10^{-9} — 10^{-7} C/m^3 range (see Fig. 1.14)¹.

It was found that the charge density in the condenser zone is several orders of magnitude lower than that near the turbine impeller.

A comparative analysis of spontaneous electrization of droplets in turbines at a nuclear power plant (NPP) and at a fossil fuel power plant was presented in 2001 at the 14th International Conference in Kyoto, the authors of the report were V. Petr and M. Kolovrantik from the University of Prague [8]. The studies were carried out by the probe method, the authors used a combined probe with an optical and electrical channel. In this work, a study was made of the relationship between the size of droplets and their electric charge on a 1000 MW nuclear turbine and a 210 MW turbine running on hydrocarbon fuel. The spectra of the droplet size of the nuclear and thermal turbines were obtained downstream the last stage at the level of the middle of the blade length represented in Fig. 1.15.

It can be seen from the graphs that the spectrum of droplets in a nuclear turbine is much wider, and the main part of the droplets is larger than in a thermal turbine.

The charge density in these studies at the NPP at the exit from the last stage was 10^{-3} C/m^3 , i.e. results of the same order as those previously obtained by the author in 1992 [1].

¹ All US studies were commissioned by EPRI with input from Sonoma Research.

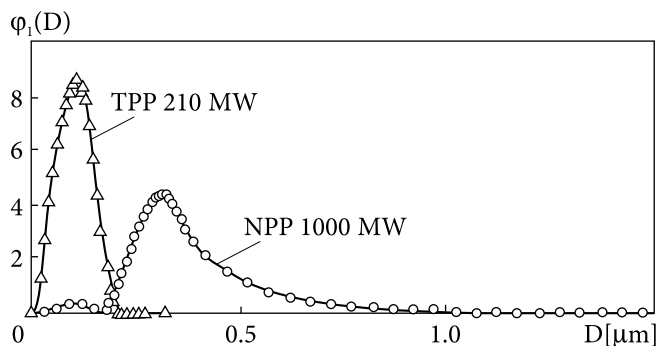


Fig. 1.15. Droplet size spectrum after the last stage for NPP and TPP: $\Pi\epsilon_1(D)$ — optical sensor signal, D (μm) — droplet diameter

Thus, the developed instrumentation in the form of electric probes made it possible to carry out large-scale research on turbines of various purposes (heating and condensing) and capacities (50; 100; 200; 300; 320; 400; 800 MW).

Summarizing the results of all studies in this area, it can be summarized that the distribution of the charge density in the flow path and the condenser of humid steam turbines is represented as:

- at the beginning of the phase transition zone $10^{-11}—10^{-8} \text{ C/m}^3$;
- before the last stage $10^{-8}—10^{-6} \text{ C/m}^3$;
- after the last stage $10^{-6}—10^{-3} \text{ C/m}^3$;
- in the condenser area $10^{-9}—10^{-7} \text{ C/m}^3$.

The fact of the electrization of a wet steam flow in a turbine predetermined the need for research on the influence of these phenomena on the reliability and efficiency of turbines.

1.5. Influence of electrization of steam flow on electric currents and potential of the turbine rotor shaft

It is known that during the operation of a turbine, an electric potential arises on the rotor shaft. If the turbine shaft is not grounded, this potential increases until the oil film breaks down in the bearings. The removal current causes electrical erosion of the bearings. This harmful phenomenon is fought by grounding the turbine rotor shaft using special current-collecting brushes [9].

The emergence of potential and currents on the turbine rotor shaft is usually associated with a whole range of phenomena — electromagnetic induction, triboelectrification, thermoelectric, electrochemical and electromechanical processes, pickups, and leaks from the electrical circuits of a turbine generator [10].

Unfortunately, as noted in [11], the explanations of the causes of electrical discharge damage presented by various specialists are contradictory and insufficiently substantiated.

In our opinion, among the large number of factors noted above that affect the electrical erosion of the elements of a turbine unit, it is necessary, first of all, to distinguish those phenomena that relate to the root causes of these negative processes. Taking into account that the overwhelming number of cases of electrical discharge damage observed during operational use of the turbine occurs not on generator units, but on turbine units and parts, the main reason should be sought precisely in the phenomena occurring in this part of the turbine unit.

Among the various/multiple phenomena leading to the emergence of an electric potential on the rotor shaft, electromagnetic induction, due to the magnetization of the turbine rotor, is usually singled out as the main cause [12]. If the phenomena of axial rotor magnetization occur in a turbine, the turbine now technically becomes a Faraday generator. However, the voltage generated this way on the rotor shaft is not enough to break/leak through the oil film. This is because the dielectric strength of the oil is about 20 kV/mm, and a breakdown voltage of 120V is required to leak through the 6-micron film. A unipolar Faraday generator is capable of creating a voltage of no more than a few volts (up to 10 V). Accordingly, a tension of no more than 1.6 V/ μm will be created in the 6 μm gap, which is not enough to break down an oil film.

At the same time, it is known [10] that in a real turbine operating on wet steam, a constant electric potential appears on a non-grounded rotor, continuously growing to a value of several hundred or more volts (depending on the specific turbine unit and its operating mode). The electric potential growth is ultimately limited by the properties of the electrical insulation of the rotor. Such an increase in electric potential, as well as the dependence of its charge (+/-) on the water-chemical regime, is characteristic of the electrostatic electrization of the rotor. In this case, electrostatic electrization has a relatively low discharge current. Since the electrostatic discharge current from the turbine rotor does not exceed 1-10mA, the oil film breakdown can't cause any significant damage to the bearings. At the same time, the ESD breakdown channel can become a conductive path for currents coming from the rotor caused by electromagnetic induction and other reasons mentioned above. The magnitude of these currents is significantly higher than the electrostatic discharge current and can, under certain conditions, reach hundreds or more amperes, which is sufficient to seriously damage the bearing. Thus, it is precisely as a result of the mutual static electrization of wet steam and the turbine rotor that a high electrostatic potential can arise on the rotor shaft, providing an electrical breakdown, followed by a large current arising from the rotor magnetization leaking

through the formed channel, thereby creating a potential electrical discharge hazard. In turn, the static electrization of the steam flow depends on the degree of steam moisture when high moisture leads to higher electrization of the steam flow. Therefore, on a full-scale turbine, one can expect an electric charge build-up downstream the last stage of a turbine, as well as an electrization of a turbine's rotor proportional to the steam moisture, subsequently leading to a change in the turbine's rotor electric potential.

An experiment carried out on the T-37/50-8.8 turbine at TPP-2 Eskhar confirmed this point of view. Investigations of the electrization of wet steam and the turbine rotor were carried out at different moisture levels of the steam flow. For the experiment, the initial steam temperature at the turbine inlet was reduced from 500 °C to 460 °C, which significantly increased the electric charge density in the flow. The static electrization of the rotor was estimated by the magnitude of the constant component of the rotor grounding current, which was removed using the grounding brush assembly. The ground current also had an alternating component due to pickups, the value of which was about 70 mA and remained unchanged during the experiment. The power of the turbine unit also did not change and amounted to 31 MW.

The electrization of the wet steam flow was recorded using an electrical probe installed downstream of the last stage by measuring the short-circuit current on it. The results of the experiment are presented in the Table 1.1.

As can be seen from Table 1.1, the current of the probe and the current of the brush vary significantly depending on the values of the temperature of the steam, and therefore indirectly on its moisture, while the probe is positively charged, and the brushes are negatively charged. This circumstance means that the reason for the increase in current is the process of electrostatic charge formation in the flow path of the turbine. The inequality of the currents of the probe and the rotor in this case is since an insignificant part of the volumetric charge of the vapor stream flows down the probe. This is due to the significant difference in the geometric dimensions of the probe and rotor, as well as the difference in their electrical insulation. The main result of the experiment is the demonstration of a significant increase in electrization with increasing steam moisture, which is directly related to an increase in the rotor potential, as noted above.

Table 1.1. Change in the current of the probe and brushes from the initial temperature of the steam

Experience number	Probe current, μA	Brush current, mA	t, °C
1	+0.4	-4	500
2	+1.40	-92	460

It can be seen from the Table 1.1 above that an increase in steam moisture significantly increases the rotor charge current (by 23 times), and this, in the event of a malfunction of the grounding brush as-

sembly, will lead to an intensive charge accumulation on the rotor and a corresponding increase in potential.

Thus, the intensification of the process of electrization of the steam flow in the turbine due to an increase in moisture leads to an increase in the intensity of the rotor charge current and to increase in the electric potential of the rotor. The risk of electro-erosion damage increases proportionally to an increase in the moisture of the steam.

In connection with the above, to reduce the risks of electro-erosive damage to bearings, it is advisable to take measures to minimize the effects of electrization of the steam flow, for example, by neutralizing charges or choosing a rational/adequate water-chemical regime. At the same time, it is also necessary to demagnetize the rotor in case of exceeding the permissible limits (240 A/m).

1.6. Electrostatic generator operational mode of the last stage and branch pipe of the turbine

The general principle underlying the operation of various types of electrostatic generators is to increase the potential of electric charges when they are moved by mechanical forces in an electric field against the action of the forces of the latter. Charges are carried by solid, liquid, or gaseous bodies.

A steam turbine in the last stage + branch pipe zone can be considered as an electrostatic generator [13] with a flow of charged particles. After, for example, a positively charged drop has detached from a negatively charged turbine blade, the Coulomb force begins to act on the drop, which is proportional to the magnitude of the drop charge. This force is directed towards the movement of the drop, which causes the drop to slow down. In this case, the mechanical energy of the flow, driving the droplets, is converted into the energy of the electric field. With distance from the blades of the last stage of the turbine, the potential of charged water droplets increases. This occurs as a result of a decrease in the electrical capacity of the charged droplet while maintaining the amount of charge. The growth of the potential can continue until the Rayleigh decay of the drop occurs, or its discharge through the ionization of the environment. The forces caused by the presence of an increasing electric field are directed towards the main steam-water flow, due to which there is a partial deceleration of the flow, and an increase in pulsations in the zone of the last stage and the turbine branch pipe. This ultimately leads to an increase in energy losses.

To assess the effect of the volumetric charge on the steam flow, an experiment was carried out on the T-37/50-8.8 turbine. It was found that downstream the last stage of the turbine, the density of charges of the steam flow was $\sim 6 \cdot 10^{-4} \text{ C/m}^3$, and the electric field strength was $2 \cdot 10^5 \text{ V/m}$. The voltage

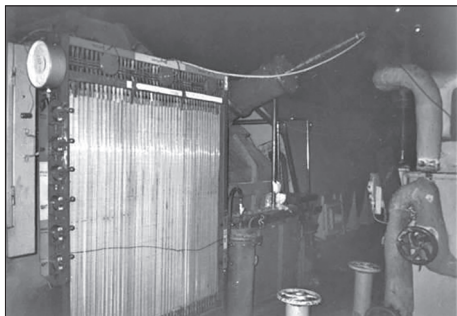


Fig. 1.16. Manometric shield

measured at the electrodes installed downstream of the last stage of the T-37/50-8.8 turbine at a distance of 0.15 m from the impeller was ~ 29 kV, which means that the electric field energy will hinder the steam flow and increase pressure downstream the last stage.

In the course of this experiment, the static pressure downstream the last stage was measured using pressure taps installed on special visors, 6 pieces evenly around the circumference in the peripheral region of the last stage. The secondary instruments used were differential water gauges mounted on the gauge panel (see Fig. 1.16).

The pressure measurements were carried out with neutral and charged steam flow. To change the density of charges in the steam flow, high-voltage electrodes were installed downstream of the last stage of the turbine, with the help of which it was possible to neutralize the flow [1, 14]. With the neutralizer turned off in this experiment, the local charge density in the peripheral zone of the impeller corresponded to the natural state of the steam flow, i.e. $\sim 6 \cdot 10^{-4}$ C/m³. With the neutralizer turned on, the local charge density in the flow decreased by $10^3 - 10^4$ times and, as a consequence, this led to a decrease in the flow deceleration by the electric field. When the volumetric charge was neutralized, the static pressure decreased by 80—150 Pa after the last stage. At the same time, the power losses from an electrostatic generation of a steam flow from a vacuum deterioration in the condenser by 150 Pa are approximately 140 kW for a given turbine, i.e. 0.4%. This fact indicates a noticeable effect of the volumetric charge on the efficiency of steam flow in the pipe. For the sake of fairness, it should be noted that this turbine is of a very old design, not operating at its full capacity of 35 MW. It is not equipped with modern dehumidification systems, and therefore, for new -generation turbines, energy losses from electrization of the steam flow will be significantly less, approximately 0.25—0.30%.

During the experiment, a noticeable effect of the volumetric charge on the character of the steam flow in the exhaust compartment was also established. In some modes, at the maximum charge density in the flow, pulsation of liquid levels in the tubes of the manometric shield ± 5 mm was observed. When the flow was neutralized, a decrease in the amplitude of pulsations was observed up to their complete cessation. This is due to the following circumstances. As shown by numerous experimental field studies, the volumetric charge density and the electric field strength both in the axial and radial direc-

tions are very uneven, and the electric fields and currents resulting from electrization have a pulsating character. All this, in addition to increasing the pressure downstream the last stage, also causes additional flow pulsations, which also negatively affects the turbine efficiency indicators, while the dynamic load on the blades of the last stage increases.

Thus, the last stage of the turbine and the branch pipe work as an electrostatic generator. Therefore, to reduce energy losses and improve reliability in this part of the turbine, it is necessary to take appropriate measures to control the modes of electrostatic generation, for example, to neutralize the flow charges, as shown in [14].

1.7. Generation of hydrogen in a steam turbine unit during electrization of a wet steam flow

It is known [15] that during the operation of a turbine unit, hydrogen is formed in the steam flow. Although the concentration of hydrogen gas is negligible, its presence can affect the reliability of the turbine unit.

Traditionally, it is believed that hydrogen in a steam turbine plant is formed in a boiler due to the dissociation of water during heating, as well as due to chemical reactions. However, the fact [1, 14] of electrization of a wet steam flow, as well as the presence of a significant volumetric electric charge in a wet steam flow, allows us to take a fresh look at the possible reasons for the formation of hydrogen in the flow path and the exhaust pipe of the turbine.

Electrization of a wet steam flow in a turbine is accompanied by electrochemical phenomena, which lead to the appearance of gaseous hydrogen and hydrogen saturation of the structural materials of the turbine.

So, as a result of electrophysical processes occurring on the elements of the turbine flow path, the steam-water flow will acquire a charge of the same polarity, and the elements of the flow path structure, on the surface of which the flow is electrified (for example, turbine blades), will acquire a charge opposite in sign to the steam charge. Consequently, between the areas of the surface of the turbine elements participating in the electrization of the working fluid, and the areas of surfaces on which electrically charged particles of the working fluid are discharged, a pulsed constant electric current flows, the value of which (all other things being equal) is largely determined by the chemical composition of water, gas-dynamic parameters and the moisture of the steam flow.

By Faraday's law, when a direct electric current flows on the electrodes, the chemical constituents of the electrolyte are released. In this case, as the main component of the electrolyte acts as water, therefore at its electrolytic dissociation on the cathode will release hydrogen H^+ or other positively charged ions at

the anode and — ions OH^- and other negatively charged ions. As a result, the cathode sections of the surface of the parts of the flow path of the turbine will be exposed to hydrogen saturation, which, as is known, leads to a decrease in the level of reliability of the elements of turbomachines.

The dissociation of water droplets and the formation of free hydrogen can also be carried out under the influence of a high-intensity electric field directly in the volume of the steam flow.

As noted earlier, in the zone of wet steam, when a film of water leaves the working and guide vanes, the electrization of drops occurs. Charged water droplets in the steam flow form an electric field, the strength of which rapidly increases with distance from the working or guide blades, reaching the limiting value at which an independent electric discharge occurs from the water droplets. In this case, the field strength at the surface of charged droplets can reach 10^{10} V/m [12]. At such a field strength, field evaporation of H^+ ions occurs, i.e. dissociation of water. A field with such intensity is created at the surface of a drop with a radius of curvature of $\sim 10^{-6}$ m at a voltage of $\sim 10^4$ V. The limiting value of the electric field strength in the vapor flow depends on the pressure and moisture of the vapor. As noted above, the measured electric field strength downstream the last turbine stage reaches $\sim 2 \cdot 10^5$ V/m. Stress was measured at a distance of 150 mm from the surface of the wheel of the last stage of the turbine, $\sim 3 \cdot 10^4$ V. During the operation of the turbine in the steam flow, droplets with a radius of $10^{-8} - 10^{-5}$ m are formed [16]. Thus, in the turbine,

due to the natural electrization of the steam flow, conditions are created under which field evaporation of hydrogen ions H^+ can occur. The amount of generated hydrogen will depend on the density of charges in the vapor stream.

To test the effect of electrization of the steam flow on the hydrogen con-

Table 1.2. Influence of charge density on hydrogen concentration

t_{op} , °C	Hydrogen concentration, %	Charge density, C/m ³
542	0.0235	$1.23 \cdot 10^{-4}$
509	0.0275	$1.6 \cdot 10^{-4}$

Table 1.3. Influence of the steam flow charge on the hydrogen concentration

Measurement Mode	Hydrogen concentration, %
Original	0.022
Neutralizer grounded	0.02
The voltage of the corona electrodes -13 kV	0.0243
Voltage of corona electrodes - 16 kV	0.0235

centration, an experiment was carried out on a T-250/300-23.5 turbine unit (Kharkiv CHPP-5). The experiment was carried out in partial mode at a load of 200 MW and a condenser pressure of 3.8 kPa. To change the charge density in the steam flow was changed by reducing the moisture vapor reheating temperature $t_{\text{of claims}}$ from 542 °C to 509 °C. The hydrogen concentration was determined at the exhaust of the main ejector from the side of the regulator using a Gasochron 3101 gas analyzer with a sensitivity of 0.000443%.

In the temperature decreasing time $t_{\text{of claims}}$ from 542 °C to 509 °C simultaneously with the hydrogen concentration varied charge density of the last turbine stage. The density of charges in the vapor flow was measured using a stationary electric probe installed downstream of the exhaust diffuser. With a decrease in temperature, the hydrogen concentration and the charge density in the flow gradually increased. The measurement results are presented in the Table. 1.2.

During the second experiment, at the temperature $t_{\text{of}} = 509$ °C density of charges after the last turbine stage was reduced by grounding the electrode catalyst. To increase the charge density in the capacitor zone, a voltage was applied to the corona electrodes from an external high-voltage source. The experimental results are shown in Table 1.3. Artificial ionization of the steam flow in the last two variants leads to an increase in the hydrogen concentration.

Since the experiments were carried out in a partial mode with low steam moisture, the hydrogen concentration and charge density were insignificant. With an increase in moisture, it can be expected that the concentration of hydrogen due to dissociation in an electric field will noticeably increase, and will lead to an intensification of the process of hydrogen absorption of metal structures.

Experimental studies have shown that natural electrization is one of the reasons for the formation of hydrogen in the steam flow of the turbine flow path.

1.8. Electromagnetic fields in the exhaust pipe of a steam turbine

As already noted, in a humid steam turbine plant, starting from the Wilson zone and further to the last stages of the turbine, there is an electrization of droplet moisture in the flow of the working fluid. The causes and mechanisms of electrization are considered in sufficient detail in [1].

One of the consequences of electrization can be the emergence of electromagnetic radiation (EMR) of wet steam in the zone of the last stages and in the exhaust pipe. The most probable sources of EMR are pulsed currents arising during charge-discharge of water droplets, crushing and merging of charged droplets, impact of charged droplets on grounded elements of the flow path, close (of the order of the droplet size) flight of a charged droplet near a grounded metal surface, corona formation of droplets, spark discharges inside

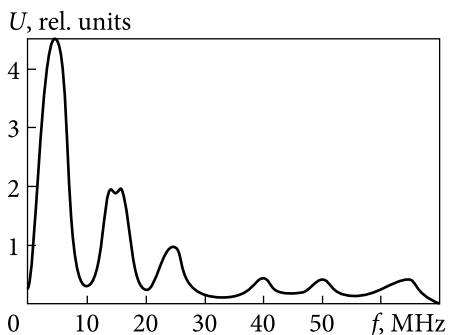


Fig. 1.17. General view of the spectral composition of the signal

the humid steam flow and between the steam flow and grounded surfaces. Experimental studies carried out in the early 1990s confirmed the presence of EMR in the exhaust pipe of a humid steam turbine [1].

As a radiation receiver, we used two parallel-connected linear antennas in the form of steel strings suspended on insulators between the walls of the branch pipe above the tube bundle at a height of 800 mm. To measure the spectral composition, an S4-59 spectrum

analyzer with a measurement range of 10—110 MHz was used. The general view of the signal distribution over the spectrum is shown in Fig. 1.17 (here the X-axis indicates the frequencies in MHz and the Y-axis voltage in relative units).

For measurements in the higher-frequency region, an S4-27 spectrum analyzer with a measurement range of 0.01 — 40 GHz was used. As a result, radiation was detected in the vicinity of 2 GHz. However, this result should be considered preliminary, since the antenna used in the experiment had a narrow bandwidth, and the charged humid-vapor flow strongly absorbs EMR.

In general, the measurements showed that the EMR detected in the branch pipe of a humid steam turbine is of a noisy nature. The recorded amplitude varied continuously over a wide range, and the frequency range was distributed from units of kHz to units of GHz. According to preliminary estimates, the total radiation power can reach several kW.

In addition to the direct registration of radiation in the turbine condenser with the appropriate equipment, damage (melting) of the insulation of the high-voltage cables of the PVV type installed in the capacitor was detected (Fig.1.18) (the high-voltage cable system was installed to conduct experiments to study the effect of additional ionization of steam in the condenser on the efficiency of its operation). The type of damage to the cable system was similar to the thermal effect of a standing electromagnetic wave that occurs in cable conductors under the influence of external electromagnetic radiation.

The cable bundles had areas of boiling and carbonization of the insulation, in which the insulating sheath of several cables was sintered into one piece (see Fig. 1.18).

In all likelihood, a similar spectrum of radiation, including frequencies up to a few GHz, can also be found in the exhaust pipe of a humid steam turbine.

For an experimental study of the qualitative picture of damage to the cable insulation by high-frequency electromagnetic radiation in a capacitor (Fig. 1.18),

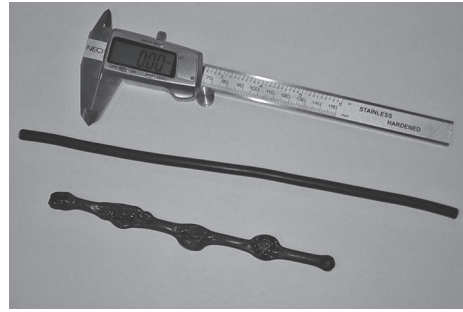
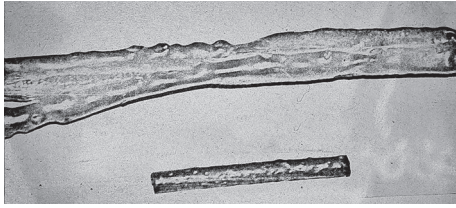


Fig. 1.18. Photo of the melted section of the cable harness, below is a fragment of the whole cable

Fig. 1.19. Photo of a cable exposed to radiation in a microwave oven

an experiment was carried out in a microwave oven. A piece of high-voltage cable PVV placed in a microwave oven for 4 minutes had insulation damage with periodic melting (see Fig. 1.19) qualitatively identical to the damage of the same cable in the turbine condenser. The difference, of course, was in the periodicity of the damage zones, located with a period of 45 mm, which corresponds to the gigahertz radiation frequency range (2.4 GHz).

Thus, the experiment carried out qualitatively confirms that the reason for the melting of the cable insulation in the branch pipe may be the presence of electromagnetic radiation, which excites high-frequency standing electromagnetic waves in the cable conductor.

In general, we can say that electromagnetic radiation of a noisy nature exists in the exhaust pipe of a humid steam turbine plant. The spectrum of radiation covers a wide range — from hundreds of hertz to units of gigahertz. Spark discharges can be one of the most important radiation mechanisms. Radiation can be absorbed by ionized vapor and condenser surfaces, which can lead to higher temperatures and degraded turbine condenser efficiency. The above data on electromagnetic radiation in the branch pipe and condenser of a humid steam turbine are preliminary and require further research based on modern power plants.

At the same time, the studies carried out once again confirmed the need to take measures during the operation of the turbine unit to reduce the level of coarse moisture in the steam flow, on which the degree of electrization of the flow largely depends. These include several well-known methods and technological methods, such as various methods of moisture removal, including by heating the shelves of the guide blades [17, 18]; neutralization of charges [1, 16]; rational choice of a water-chemical regime (WRC) [1, 19] and the use of surfactants (surfactants) [13].

1.9. Influence of electrization of the steam flow on the thermodynamic characteristics of the turbine unit

The presence of high-density charges in the flow path of the turbine in a steam flow moving at a transonic speed initiates the onset of electric discharges, ionization of the working fluid, and the appearance of electric fields. All this, as is known from the theoretical foundations of physics, can have a noticeable effect on the properties of steam. Therefore, the question of assessing their influence on the thermodynamic processes occurring in the turbine becomes relevant.

The effect of an electric field on water and water vapor should be considered as a factor of additional work being done on the thermodynamic system. Then, the joint equation of the I and II laws of thermodynamics will have the form

$$Tds = du + pdv - \sum \zeta dx, \quad (1.1)$$

where $\sum \zeta dx$ — reflects the impact of physical fields of various nature; \int — generalized force; x — generalized coordinate.

If we consider (1.1) only taking into account the work of the extension, then

$$T \cdot ds = du + p \cdot dv. \quad (1.2)$$

This equation connects the 5 unknowns T , S , u , p , and v . Therefore, having set two independent variables out of 5 unknowns, to determine the rest, two more equations should be added, which can be the thermal and caloric equation of state: $p = p(v, T)$; $u = u(v, T)$. If we consider (1.1) taking into account one more type of work, for example, the action of an electric field, then

$$T \cdot ds = du + p \cdot dv - P_d \cdot dE, \quad (1.3)$$

where E — is the field strength; P_d — dielectric polarization.

In this case, two more unknowns E , P_d appear.

Having set the variable E , and bearing in mind the dependence $P_d = (\Sigma - 1)\Sigma_0 E$ known from electrostatics, we obtain a closed system of equations. Here $\Sigma = f(T)$ — is the dielectric constant of the medium; $\Sigma_0 \approx 8.854 \cdot 10^{-12}$ F/m — electrical constant. Thus, in the case of exposure to an electric field, the equation of state of the working fluid will be determined not by two independent variables, for example, $p = f(T, V)$, but by three $p = f(T, V, E)$.

In this case, it becomes incorrect to use directly tables of thermodynamic properties of water and steam.

The derivation of the relations for determining the change in the heat capacity $C_{E,p}$ and the entropy S_v of the working fluid under the influence of an electric field of intensity E is described in detail in [1]. Finally, these dependencies look like this:

$$C_{E,p}(E, T, p) - C_p(T, p) = \frac{T\epsilon_0 E^2}{2} \frac{d^2\epsilon}{dT^2}, \quad (1.4)$$

$$S_{v_2} - S_{v_1} = \epsilon_0 \frac{E_2^2 - E_1^2}{2} \frac{d\epsilon}{dT}. \quad (1.5)$$

The aspects of the effect of electric fields on the thermophysical properties of working media, considered in the literature and studied by the author, make it possible to conclude that it is necessary to take these phenomena into account when studying the thermodynamic processes occurring in steam turbine installations. The above dependences can be used to numerically estimate the effect of electric fields on changes in the entropy and isobaric heat capacity of water and steam. The question of determining the value of the dielectric constant of a wet-steam mixture carrying a large volumetric charge in the low-potential part of powerful steam turbines remains open. In the literature, the author's knowledge, reference data for Σ in specified conditions such mixtures are not present, and estimate Σ , in this case, the results of experiments extremely difficult. At the same time, in some works, the change in ϵ in various mixtures under the influence of an electric field is considered. For example, in [20] it is stated that the dielectric constant of polyelectrolytes will increase with an increase in the density of this charge and reach ~ 1300 . From the dependence $d\epsilon/dT$ given in [21], it follows that as the temperature of the working fluid decreases, ϵ also increases; $d\epsilon/dT > 0$. Analyzing dependencies 1.4 and 1.5, with some precaution, it can be assumed that with an increase in the electric field strength, both the entropy and the heat capacity of water steam tend to increase, but it is too early to speak of a quantitative assessment.

Consequently, especially for theoretical studies, the importance of the issue of determining Σ , due to the establishment of a reliable quantitative assessment of the result of the effect of electric fields on the thermodynamic properties of the working (steam-water) medium in a turbine, remains relevant and this problem should be given primary attention in further research.

The appearance of electric charges in a two-phase flow also affects its stream. If the charges in the flow are formed due to electrization when flowing around grounded surfaces, the charged particles are acted upon by the force F [22, 23] directed to these surfaces, ie. not in the direction, but often against the flow, creating a back pressure

$$F = q_M E_{oc} = neE_{oc} = 4\pi\Sigma_0 E_{oc} E_3 r^2 \delta, \quad (1.6)$$

where E_{oc} — is the strength of the electric field in which the particle moves, V/m; r — is the radius of the drop; δ — is a coefficient depending on the conductivity of the drop.

Moving in an electric field, a charged particle experiences resistance depending on its size and speed, as well as on the viscosity of the medium. According to Stokes' law, the resistance force is

$$F_c = 6\pi\mu r C_e, \quad (1.7)$$

where μ — is the coefficient of dynamic viscosity of the medium (N · s)/m²; C_e — particle velocity, m/s.

When a charged particle moves, the force of the action of an electric field on it is quickly balanced by the force of resistance of the medium

$$4\pi\epsilon_0 E_{oc} E_3 r^2 \delta = 6\pi\mu r C_e, \quad (1.8)$$

wherefrom the particle velocity

$$C_e = (4\epsilon_0 E_{oc} E_3 \delta r) / 6\mu, \quad (m/s). \quad (1.9)$$

As a result, under the action of an electric field, charged particles (droplets) tend to move at a speed of C_e to grounded surfaces and entrain steam with them, creating additional resistance to the movement of the mainstream. It can be seen from formula (1.9) that with an increase in the electric field strength, the velocity of the charged droplet to the grounded surfaces increases, which contributes to an increase in the backpressure and a decrease in the velocity of the main flow.

Under real conditions, the electrization of a steam flow is accompanied by an increase in the electric field strength of the volumetric charge. In the case of a low conductivity of the medium, the electric field strength of the volumetric charge increases until an electrical removal occurs. For example, downstream the last stage of the turbine, the removal electric field strength for the steam flow is $\sim 2 \cdot 10^5$ V/m. This means that already at a distance of 0.1 m from the impeller, the potential in the steam flow can reach 20 kV. In reality, the voltage measured at the electrodes installed downstream of the last stage of the T-37/50-8.8 turbine at a distance of 0.15 m from the impeller was ~ 29 kV. Under the action of the stresses arising in two-phase flows and an electric field directed against the flow of the stream, charged particles can be decelerated. Thus, the electrization of the two-phase flow is accompanied by the conversion of kinetic energy into the energy of the electric field, which reduces the speed of the steam flow and causes an increase in energy losses.

The transformation of the kinetic energy of the steam flow into the energy of the electric field occurs whenever electrization occurs in the flow. Charged

water droplets in the steam flow form an electric field, which grows with distance from the charge formation zone, quickly reaching its limiting value. In this case, the energy density of the electric field is equal to

$$W_v = \frac{\varepsilon \cdot \varepsilon_0 \cdot E^2}{2}. \quad (1.10)$$

As seen from (1.10), the energy density depends on the strength of the electric field and the dielectric constant of the medium. In this case, the ultimate electric field strength is limited by the removal strength of the medium and is a function of pressure.

If the dielectric constant of the steam, as is commonly believed, is taken close to one, then the limiting energy density of the electric field of the volumetric charge of the steam flow will be $W_v = 0.177 \text{ J/m}^3$. The dielectric constant of the uncharged steam is close to one. However, if the steam has a high-density volumetric charge, its dielectric constant may differ significantly from that of a neutral steam.

If the dielectric constant of the charged steam flow increases, the limiting energy density of the electric field will also increase (1.10). As noted earlier, there is no information in the literature on the dielectric constant of a charged steam flow. However, the performed studies give reason to believe that in the presence of a volumetric charge in the steam flow, its dielectric constant can increase tens of times. This means that the limiting energy density of the electric field in the steam flow can reach $\sim 1 \div 10 \text{ J/m}^3$. This energy of the electric field arises as a result of the transformation of the kinetic energy of the flow, i.e. by reducing its speed. Thus, when the steam flow is electrified, losses from moisture are added to losses due to the presence of a natural electric field directed against the flow.

In our opinion, it is quite appropriate to present further the experimental results obtained during studies on the T-37/50-8.8 turbine on the effect of steam electrization on the speed, pressure, and energy losses, which partially confirm the above conclusions and conclusions.

To determine how the electrization of steam after the last stage of the T-37/50-8.8 turbine can affect the flow rate and pressure, an electric probe and a total pressure sensor were installed in the upper part of the nozzle, and a neutralizer of volumetric charge was installed downstream the impeller.

The electric probe is an insulated rod with a diameter of 5 mm and a length of 100 mm. The total pressure sensor is standard (pitot tube with diffuser). The probe and sensor were mounted on a movable rod, which was installed into the branch pipe through the airlock. The bar could move along the radius of the wheel at a distance of 350 mm from its plane. In the course of the ex-

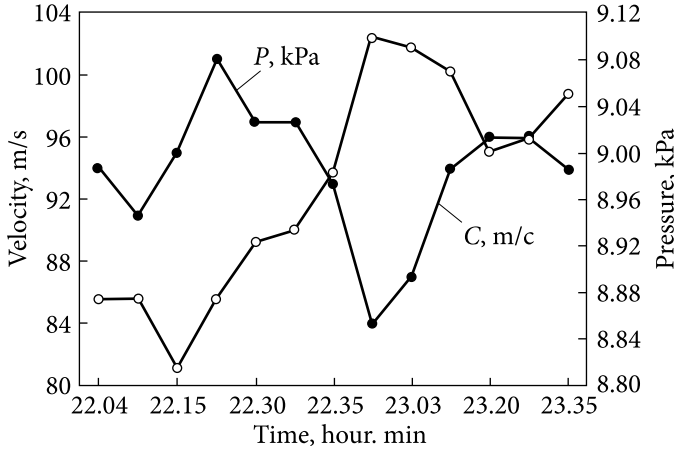


Fig. 1.20. Changes in the flow rate and pressure in the condenser of the T-37 / 50-8.8 turbine when the neutralizer is turned on

periment, the total and static pressures of the flow were measured, as well as the short-circuit current of the electric probe at different voltages on the electrodes of the neutralizer downstream of the stage. Fig. 1.20 shows the dependences of pressure P and speed C versus time after the last stage of the turbine at voltages on the electrodes downstream the stage, allowing neutralization of the steam flow.

It can be seen that after supplying at 22.10. voltage -16 kV across the neutralizer electrodes, the flow rate increases, and the pressure in the branch pipe decreases. The turbine operating mode during the experiment was unstable, and the pressure in the condenser was constantly increasing. This explains the fact that after turning on the neutralizer, the pressure in the condenser first decreased, and then gradually increased. In the period from 22.30 to 23.03, when the neutralizer was turned off, the pressure in the condenser increased and the flow rate decreased. When a voltage of -15 kV was applied to the neutralizer at

23.03, the flow rate increased, and the pressure in the condenser decreased. From the above graph (Fig. 1.20), the change in speed and pressure is visible

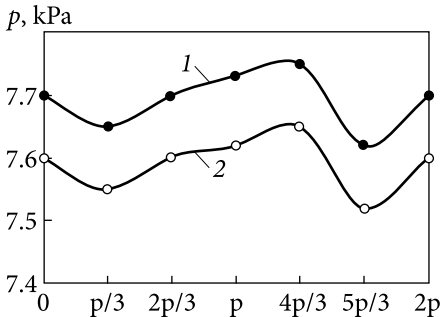


Fig. 1.21. Distribution of pressure along the circumference of the impeller of the T-37/50-8.8 turbine at different densities of the volumetric charge: 1 — electrified flow; 2— neutral

when the neutralizer is turned on. As a result of this experiment, it was found that the electrization of steam leads to an increase in pressure downstream of the last stage by 100 Pa, a local decrease in speed by 12 m/s, and an increase in energy losses in the turbine by $\sim 0.35\%$.

Similar results were obtained with this turbine under more stable operating conditions using passive neutralization methods (see Fig. 1.21). It can be seen that neutralization leads to a decrease in pressure along the entire perimeter of the flow, although the circumferential irregularity does not change in this case. At different operating modes of the turbine, the pressure drop from neutralization of the flow was 8–15 mm of water column and the speed increased from 10 m/s to 20 m/s.

The above experiments confirm the previously obtained theoretical conclusions on the negative effect of steam electrization on the thermodynamic characteristics of the turbine.

Conclusions for Section 1:

- the fact of electrization of the wet steam flow in the turbine has been established. The dynamics of charge formation in the flow path have been determined: the charge density at the beginning of the phase transition is from 10^{-11} C/m³ to 10^{-8} C/m³, and after the last stage — from 10^{-6} C/m³ to 10^{-3} C/m³, which is an order of magnitude higher than in a thundercloud;
- natural electrization of the wet steam flow has, in the main, a negative effect on the operation of the turbine unit;
- the risk of electro-erosion damage to bearings in a turbine when working on steam with high moisture is much higher than when working on steam with low moistening;
- the phenomenon of electrostatic generation of high-speed steam-droplet flow in the exhaust zone (last stage + branch pipe) reduces the efficiency of the turbine unit;
- electrochemical processes and dissociation of water droplets in the electric field of a high-intensity steam flow can lead to hydrogen saturation of the blade metal, which requires special case studies in this direction;
- the fact of the presence of electromagnetic radiation with a wide spectrum in the turbine branch pipe has been established;
- electrization of the steam flow increases energy losses, reduces the flow rate, and increases the pressure downstream of the last stage, i.e. hurts the thermodynamic characteristics of the flow;
- to increase the efficiency and reliability of the turbine unit, it is necessary to control the density of charges in the flow and, if possible, to minimize the process of electrization of coarse moisture.

Based on the above problems that arise in the theoretical substantiation and taking into account all the components of the effect of steam electrization on the thermodynamic characteristics of turbine plants, especially when determining the dielectric constant, the main emphasis should now be placed on experimental studies.

Thus, the various physical phenomena discussed above, arising from the natural electrization of a wet-steam flow, mainly harm the efficiency and reliability of the turbine unit. It also follows from the above conclusions that electrophysical phenomena should be considered in the context of their influence on the strength indicators of the blades, including the effect of an electrically charged steam medium and electromagnetic fields. These processes have not previously been considered in the theory of turbomachines and can certainly be of both scientific and practical interest.

**INFLUENCE OF ELECTRIC
STEAM FLOW ON SURFACE
STRENGTH OF BLADE STEEL**

2.1. Justification of physicochemical factors of the influence of a charged steam flow on the strength of the blades

The main reason for the destruction of the surface of the working blades of the last stages of wet steam turbines is erosion damage. The erosion process develops gradually, successively going through three stages: the incubation period, the non-stationary period, and the stationary one. An important stage, from the point of view of the service life of the rotor blades, is the incubation period since at this moment there is an accumulation of damage in the structure of the material without destroying the surface of the blades. The leading mechanism of erosion damage to the surface layer of the material is currently considered to be fatigue phenomena arising from the impact of erosion-hazardous drops. The main role in the accumulation of damage in this case is played by Rayleigh waves [24—26]. The accumulation of fatigue damage as a result of repeated wave action leads to the appearance of annular cracks and the development of erosional entrainment of the material.

However, the data presented earlier give grounds to assert that the operation of moisture steam turbines, as a rule, is accompanied by both spontaneous electrization of wet steam and electrization of droplet moisture under the influence of an electric field. These phenomena are not taken into account in either physical or mathematical models of the processes of destruction of the surface layer of the blades.

Due to the presence of electrical phenomena on the charged surfaces of the flow path, as well as on the surfaces exposed to the flow of charged droplets, electrochemical processes similar to anodic and cathodic ones in electrochemical

systems can occur, and metal parts can be exposed to negative factors, in particular, anodic dissolution and cathodic hydrogen saturation.

The main carriers of charges (ions) in the flow of the working fluid are the particles of droplet moisture in the steam flow. In this case, large drops are predominantly charged positively, and small drops negatively. The flow of charged droplets generates a volumetric electric charge in the flow path of the turbine and a total ionic current. The flow of such a current in the flow path of the turbine is accompanied by the appearance of a magnetic current field and the induction of stray currents in the details of the flow path by the law of electromagnetic induction.

The magnetic field of an ionic current element in a steam flow is determined per the Bio-Savart-Laplace's law:

$$dB = \frac{\mu_0}{4\pi} \cdot \frac{I dl \sin\alpha}{r^2}$$

where B — is the magnetic induction of the charged steam current element; μ_0 — $4\pi \cdot 10^{-7}$ H/m — magnetic constant; r — the distance between the current element and the point of determining the magnetic induction; I — current; dl — length of the current element; α — is the angle between dl and r .

Changes in the magnetic field of the flow of charged steam associated with the uneven movement of the ion current, and changes in the density of the space charge in time generate an EMF, inducing stray currents in the metal surfaces of the flow path [27]:

$$e_i = \frac{d\Phi}{dt},$$

where e_i — is the EMF induced by a time-varying magnetic field; Φ — magnetic flux; t — time.

Stray currents are capable of activating electrochemical processes of destruction of a metal surface, which, in combination with a mechanical load, will lead to accelerated accumulation of damage and destruction of the blade surface [28].

On the whole, the electrochemical processes in the last stages of the LPC, caused by the charged droplets, represent a complex system, which is significantly different from the systems traditionally considered in electrochemistry.

A conventional image of a fragment of the electrochemical system for the last stage is shown in Fig. 2.1.

The peculiarity of the electrochemical system shown in this scheme is that the electrolyte is a stream of individual droplets with ions moving in a steam

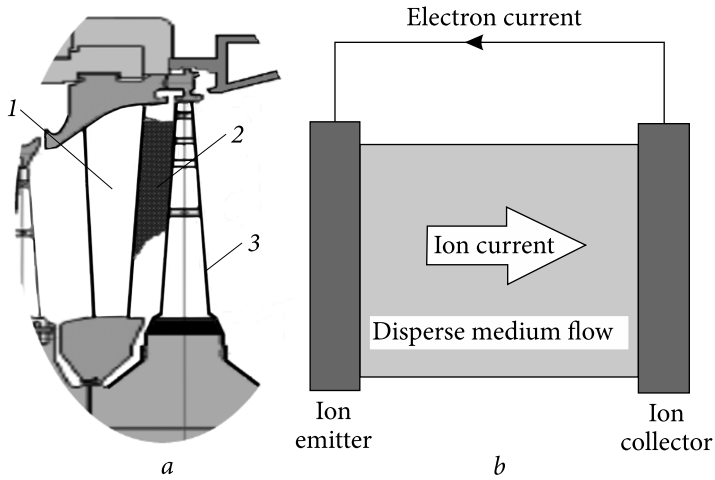


Fig. 2.1. Scheme of the last stage with sections of electrization, transfer, and neutralization of ions: *a*: 1 — guide blade surface (dispersion region), 2 — flow with charged particles, 3 — rotor blade surface (deposition region); *b* — equivalent diagram of processes

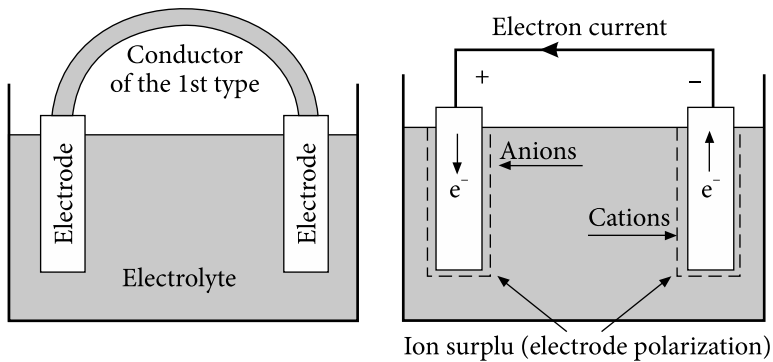


Fig. 2.2. Traditional electrochemical system

(dielectric) flow from the electrization zone to the grounded parts in one direction. In this case, there is no counter-movement of anions and cations in the electrolyte; the transfer of charged particles occurs due to the mechanical energy of the steam flow, and not under the action of an electric field; areas of polarization of the electrodes do not appear on the electrode surfaces due to the blowing of the electrodes with a flow of condensing steam; electrochemical currents arising in the system are pulsed; mechanical shocks cause local damage to oxide films on the metal surface, which intensifies the course of electrochemical processes [29]. Electrochemical systems of this type, as a rule, are not considered within the framework of traditional electrochemistry [30]. The view of a classical electrochemical system is shown in Fig. 2.2.

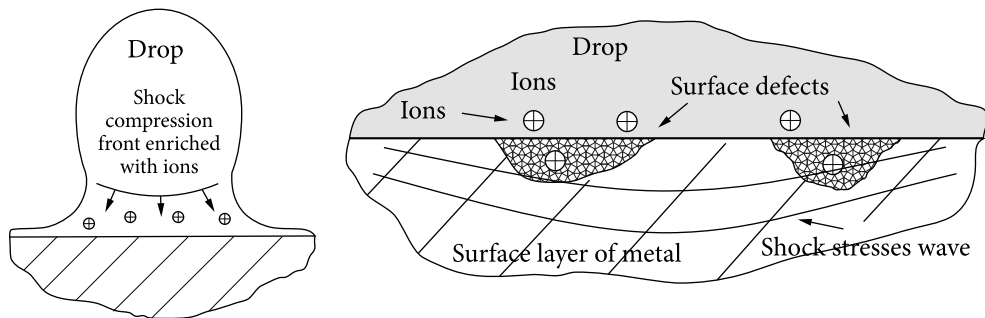


Fig. 2.3. Scheme of the process of ion penetration into the metal surface upon impact of a charged drop

Table 2.1. Hydrogen content in samples impacted by water droplets

Parameter	Sample number				Control sample	Note
	1	2	3	4		
15X11MΦ + niobium-carbon coating						
Sample weight, g	2,940	3,920	5,320	7,360	3,740	
Concentrator. hydrogen (C _{H₂}), Ppm	7.8	4.35	5.37	4.04	1.96	
15X11MΦ in delivery condition						
Sample weight, g	2,730	2,560	2,150	7,290	5,180	
Concentrator. hydrogen (C _{H₂}), Ppm	5.31	7.91	4.52	2.92	1.15	
Satellite insert + 40 A						
Sample weight, g	8.580*	7.570**	5.320	7.360	1.89	* — satellite insert ** — base metal
Concentrator. hydrogen (C _{H₂}), Ppm	6.418	29.6	5.37	4.04	2.52	
Wire X18H9T						
Sample weight, g	1.130	1.58			1.89	
Concentrator. hydrogen (C _{H₂}), Ppm	25.62	31.54			2.52	

In the considered electrochemical system (see Fig. 2.1), together with the mechanical erosion process, as well as the intrusion of ions and chemically active particles into the surface, the processes of dissolution and leaching of the products of electrochemical transformations from the surface can take place.

Fig. 2.3 schematically shows the effect of the contact of a charged droplet with a metal surface and the introduction of hydrogen ions into surface defects.

Experimental confirmation of the possibility of hydrogenation of turbine parts during electrization of the working fluid is the data given in the monograph [1] and article [31].

In particular, work was carried out to study the comparative content of hydrogen in the samples installed on the stand for the study of erosive wear of materials and exposed in dry air after testing for at least 3 months. Tests were carried out on plant samples with dimensions of 5×20×30 mm, made of steel 15X11MF; samples with niobium-carbon coating; and samples with a satellite insert. The eroded sections of plant samples were mechanically cut into several different parts and weighed, and then the hydrogen content in them was determined by melting in a carrier gas on a PTAK001 unit. Similar studies on the hydrogen content were also carried out on a full-scale T-37/50-8.8 turbine at the Eskhar CHPP for wire X18H10T. In this case, we investigated the hydrogen content in a wire with a diameter of 2 mm made of steel Kh18N9T, which was used for the bandage fastening of parts of the system of electro-physical effects and installed in the nozzle of a 50 MW turbine unit during field tests [1]. A wire sample was exposed to a positively charged wet-steam flow in a nozzle for 18 days; after exposure, the wire became brittle and collapsed from slight deformation. The results of tests to determine the hydrogen content are presented in Table 2.1.

The results are given in Table 2.1. show that areas of the metal surface exposed to erosive wear under the impact of water droplets are highly hydrogenated (in some cases, the hydrogen concentration increases more than tenfold).

The residual hydrogen concentration is maintained for a long time. Thus, the hydrogen content in the samples, even after aging, is 3—10 times higher than in the initial state. Similar results were obtained for the shroud wire. Based on the results obtained, it was concluded that the impact of water droplets on a metal surface leads to the occurrence of tribo-chemical and electrolytic processes, as a result of which the metal surface is significantly saturated with hydrogen, and electrophysical phenomena in the flow path can enhance this effect.

The data presented in the monograph [1] and the above-mentioned articles are the basis for further studies of the effect of steam flow with charged droplets on samples of structural materials for the turbine flow path.

In addition to electrochemical factors, electrophysical phenomena (EMP, electric, and magnetic fields) accompanying steam electrization affect the metal surface in a turbine [32]. In this regard, it is necessary to study their influence on the strength properties of the surface layer of blade materials.

2.2. Experimental evaluation of the effect of a charged dispersed medium on the strength properties of blade steel

2.2.1. Description of the Experimental Installation

When electrization of the working fluid in the turbine occurs, a specific electrochemical system arises in the blade apparatus, in which the surface of the working blades plays the role of an electrode. A stream of ions is deposited on this electrode from the charged droplet moisture of the working fluid flow and is affected by the electric field of the space charge of the steam. It is known, that during electrochemical processes in an electrochemical system, chemical transformations can occur on the surface of electrodes with a change in the chemical composition and mechanical properties of the surface of the electrodes. Taking this into account, the solution of the number of research tasks should begin with determining the nature of the change in the strength properties of the electrode surface (sample section of the blade) in a specific electrochemical system, with a steam-droplet medium with charged droplets as a carrier of ion currents.

To solve this problem, a test installation was designed and manufactured that creates an electric field and a low-speed steam flow of water mist with charged droplets in contact with the surface of the blade steel sample under study.

The experimental installation made it possible to obtain moist, condensing steam outflowing into the atmosphere. A laboratory boiler with a capacity of 8 liters, operating at an excess pressure of not more than 0.1 kg/cm^2 , was used as a wet steam generator. Distilled water was used as a working fluid. Fig. 2.4 shows the installation scheme.

he productivity of the wet steam generator was up to 1 kg/h (0.28 g/s) with a steam temperature at the exit from the steam pipeline to the atmosphere in

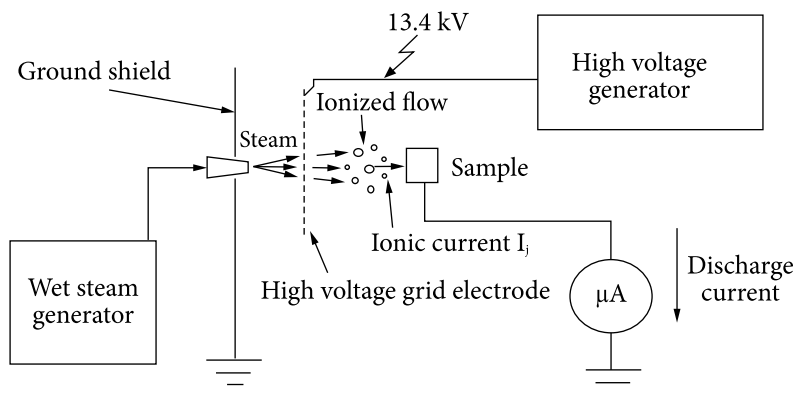


Fig. 2.4. Experimental installation scheme

the range of $100 \div 102$ °C. The flow rate was about 300 mm/s (0.3 m/s). From the boiler through a heated steam line, steam entered the guide glass tube and, passing through a fine-meshed stainless grid, to which a voltage of 13.4 kV was applied, was charged and out flowed the atmosphere in the form of a stream of mist. The most probable mechanism of droplet charging, in this case, is the transfer of electrons from the droplets to the grid electrode with the formation of positive hydroxonium ions in the droplets H_3O^+ :

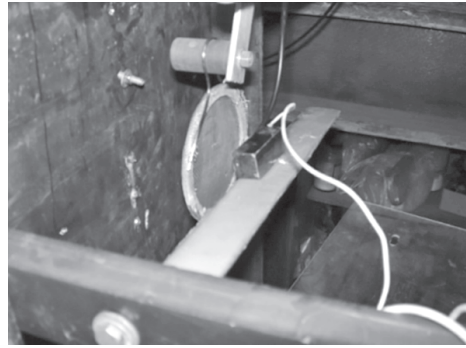
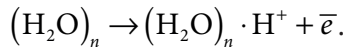


Fig. 2.5. Arrangement of the sample and mesh electrode



An insulator in the form of a plate was installed behind the grid, on which the processed blade steel sample was placed, Fig. 2.5. The sample was grounded through a system for recording the current of charged particles deposited on the sample. The potential of the high-voltage mesh electrode was positive. Steam has partially condensed on the mesh, and a small amount of moisture droplets are formed, which are retained on the mesh. Behind the mesh, the flow of steam was in the form of a jet of mist. Since the diameter of droplets in a mist is usually from 2 to 120 μm , the average diameter of droplets deposited on the sample was considered equal to 60 μm .

The distance from the sample surface to the high-voltage electrode was 15 mm. The area of the high-voltage electrode was significantly larger than the

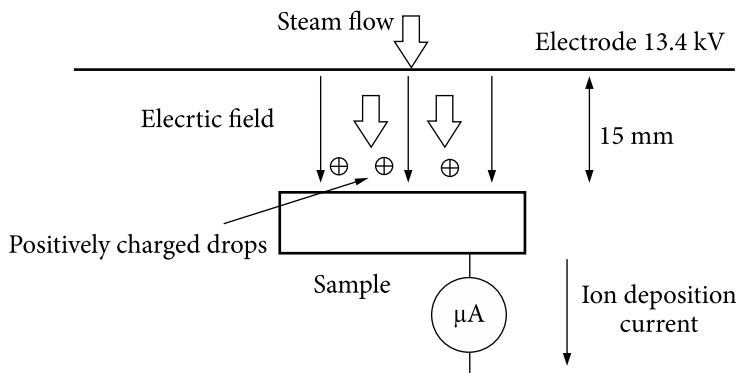


Fig. 2.6. Scheme of the effect of a steam flow and an electric field on the surface of a steel sample

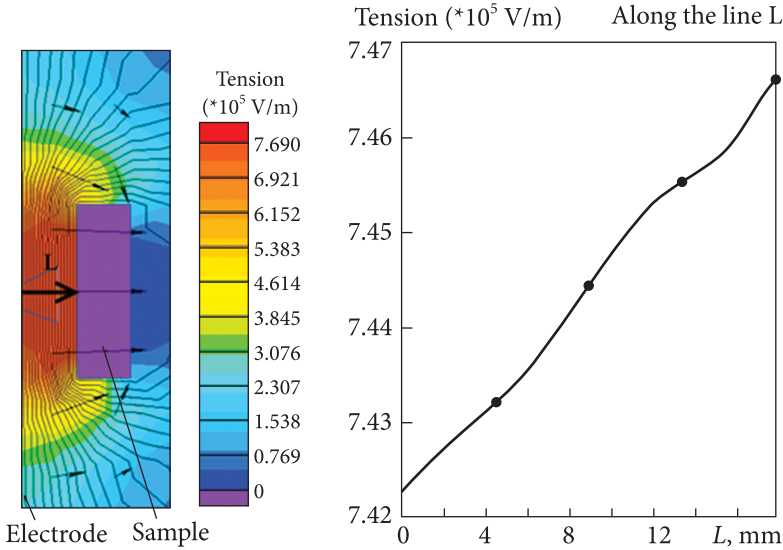


Fig. 2.7. Electric field strength between the grid electrode and the steel sample without taking into account the volumetric charge of the steam

processed area of the sample to ensure the uniformity of the field on the surface of the sample. The ionization of the steam flow was monitored using a dial micro ammeter. The voltage of the high-voltage source was raised to a level that allowed recording the current in the ground circuit. Under the experimental conditions, a grounding current of about $1 \mu\text{A}$ appeared at a voltage between the grid and the sample of 13.4 kV (Fig. 2.6).

Fig. 2.7 shows a two-dimensional image of the electric field distribution on the sample surface facing the grid electrode in the plane perpendicular to the electrode, as well as a graph of the electric field strength along the line connecting the center of the electrode and the center of the sample.

As can be seen from the calculation, the field strength on the sample surface is of about the same order of magnitude as the strength measured after the last stage of the turbine ($\sim 2 \cdot 10^5$ V/m) [1], the rotor blades of the last stage are in a similar field.

2.2.2. Experimental methodology

The impact of a charged wet steam flow on the turbine blades can initiate their damage due to the occurrence of erosion-corrosion processes. At the same time, at the initial stage of damage, there is an accumulation of structural changes in the material, and, accordingly, a change in the strength properties of the surface layer. The accumulation of damage by the surface layer of the material can be interpreted as a decrease in its continuity, i.e. the occur-

ce and increase in the number of structural defects having a hardness value different from the hardness of the base material, as well as microcracks.

Since in this experimental study, the planned duration of exposure to the steam-droplet flow is of the order of several hours, the expected value of material damage will be insufficient for external display of destruction, the expected surface structure defects will have geometric dimensions comparable to the grain sizes, and the material surface will be formed mainly by the matrix material. For an experimental study of such damage, a non-destructive testing method is required, which makes it possible to determine the strength properties of the surface layer of the material and the presence of structural inhomogeneities comparable in size to the size of metal grains. This method is durametry (determination of microhardness). Microhardness can be considered an integral characteristic of the strength of a local element of the surface layer of a material, since during indentation, as in any other type of mechanical tests, the material successively undergoes 3 stages of state change: elastic deformation, elastoplastic deformation, and destruction [33]. In this study, the Vickers method is used with surface indentation with a regular tetrahedral diamond pyramid [34].

On the mounted experimental installation, Fig. 2.4 conditions were created where a charged flow of condensing wet steam with a droplet size of approximately $120\ \mu\text{m}$, which did not create an impact load of droplets on the surface (speed less than $1\ \text{m/s}$), and an electric field with an intensity of sample surface $\sim 7.5\ \text{kV/cm}$ ($\sim 7.5 \cdot 10^5\ \text{V/m}$). The created conditions made it possible to investigate the electrochemical component of the surface damage with a minimal effect of the mechanical action on the steam flow.

The surface of a 20Kh13 steel sample in the form of a parallelepiped with dimensions of $56 \times 18 \times 17\ \text{mm}$ was used as a model of a fragment of the surface of the rotor blade.

The sample surface was prepared for microhardness measurements by the requirements of GOST 2789-73. On the prepared sample, an area for indentation was selected in the middle of the polished face.

In the selected area of the surface, indentation was carried out on a PMT-3 device so that the imprints covered the surface under study approximately evenly. As a result, various series of microhardness values of the surface area were obtained. The initial value of microhardness was determined at loads on the indenter — 10, 30, and 50 grams. After determining the initial microhardness, a ground wire was soldered to the sample surface, as shown in Fig. 2.8.

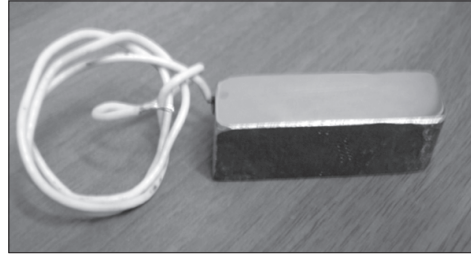


Fig. 2.8. Sample of steel 20X13 with a ground wire

The sample was installed on the dielectric site of the experimental installation and connected to the ground circuit. The steam generator was turned on, and with the appearance of a stream of condensing steam, a high voltage was applied to the grid electrode. A high voltage of positive polarity was applied smoothly until a current appeared in the ground circuit of the sample (approximately 1 μA). The sample was exposed to a charged steam stream for 1.5 hours, after which the installation was turned off, and the microhardness was measured.

The microhardness in the experiment was determined using a PMT-3 device according to the microhardness test method (GOST 9450-76). According to the passport data, the device provides measurement in units of HV hardness up to 200 gf with a relative error of $\pm 5\%$.

With a load on the indenter equal to $P = 10$ grams, measurements were made at 20 points. For loads of 30 and 50 grams, measurements were made at 10 points.

2.2.3. Experiment results

The results of measurements of the surface microhardness of the 20Kh13 steel sample under study in the initial state and after blowing with a wet steam flow are summarized and presented in Fig. 2.9 and Table 2.2. The charge of the fog droplets is positive.

The Table shows the following statistical characteristics of the variational data series:

- average value of microhardness HV, kg/mm^2 ;
- average indentation depth, microns;
- maximum value of microhardness HV, kg/mm^2 ;
- the minimum value of the microhardness HV, kg/mm^2 ;
- relative range of variation of several microhardness values, %;
- standard deviation σ ;
- dispersion S^2 ;
- coefficient of variation C_v ;
- the average value of the diagonal of the imprint, μm .

From the results of graphic processing of the experimental data presented in Fig. 2.10, it can be seen that in the initial state, the average value of the microhardness of the investigated surface area increases nonlinearly with increasing indentation depth.

Impact to charged steam significantly reduces the average value of microhardness to an indentation depth of up to 4 μm . The form of the dependence of the microhardness on the indentation depth is also linear, which means a change in the metal structure at a deeper level of the core. The boundary of structural changes in the surface layer in depth was not determined, since the indentation

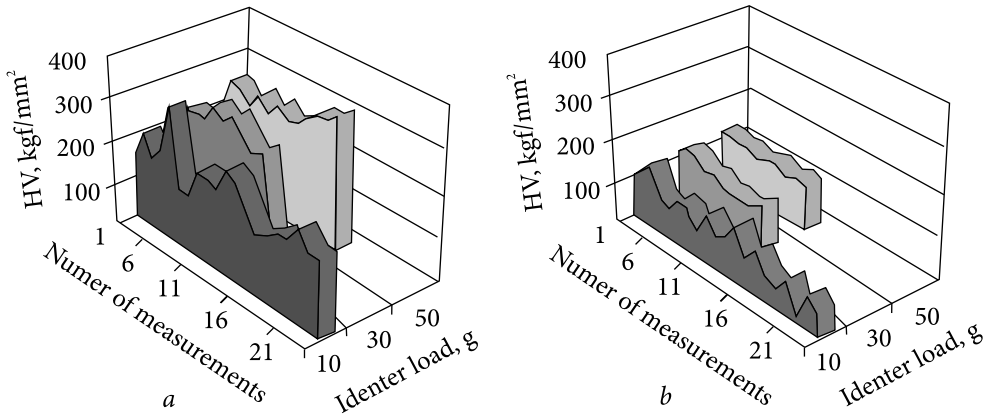


Fig. 2.9. Graphical presentation of the results obtained at loads on the indenter of 10 g, 30 g, 50 g: *a* — initial values of microhardness; *b* — values of microhardness after exposure

was carried out at a load of up to 50 g, as for the control measurements. The slope of the curve is not more than 10° , which means the homogeneity of the modified structure in depth is not less than $4\ \mu\text{m}$.

The nature of the inhomogeneity of microhardness by layers before exposure: the relative range of variation to a depth of $2\ \mu\text{m}$ was 93%, and the coefficient of variation was 0.22. This means the homogeneity of the upper part of the surface layer, with the presence of a small number of relatively large structural imperfections localized in a volume close to the volume of one imprint at a load

Table 2.2. Values of microhardness and statistical characteristics of experimental data before and after exposure to charged steam

Control			After exposure			Statistic characteristics
Load, g			Load, g			
10	30	50	10	30	50	
189	239	254	90	106	117	HV, kgf/mm ² , average
1.4	2.2	2.7	2.2	3.3	4.0	Wed depth, μm
309	274	308	153	135	126	HV, kgf/mm ² , maximum
134	214	197	19	84	106	HV, kgf/mm ² , minimum
175	59	111	134	51	20	The range of variation.
93	25	44	149	48	17	Rel. range var., %
41	21	30	31	17	7	σ , st.dev
1712.6	445.1	895.9	967.2	297.4	51.6	Disp.,
0.22	0.9	0.12	0.35	0.16	0.6	Coeff. variations
10	15	19	15	23	28	Wed diag. imprint, μm

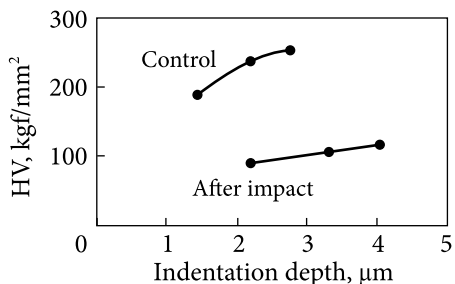
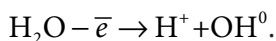


Fig. 2.10. Dependence of the microhardness of the surface layer under load (10 g, 30 g, 50 g) on the indentation

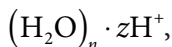
respectively. The coefficient of variation of microhardness values increases for these loads by 59% and 77%. This is due to the formation of structural defects at a depth of 3 μm or more. Defects of various sizes are formed in the surface layers. The number of structural defects increases significantly at a depth from 2 μm to 3.3 μm . At a load of 50 g, the values of the relative range of variation and the coefficient of variation are reduced. Which means the formation of smaller-scale structural defects at a depth of about 4 microns.

Based on the results of the experiment, it can be assumed that the main influence on the mechanical properties of the surface layer of a metal sample is exerted by the introduction of ions and hydrogen absorption of the surface upon contact with a charged steam-droplet flow.

The processes of electrization and discharge can be represented as: the mechanism of formation of a positively charged drop on the charging electrode (drop charge)

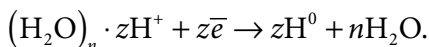


A water molecule from a drop gives an electron to a positively charged electrode (grid), as a result of which a positively charged hydrogen ion and a neutral hydroxyl group are formed OH^0 . The hydroxyl radical, being a strong oxidizing agent, interacts with the mesh material, and the drop flying away to the sample is charged positively, retaining the hydrogen ion (s). The expression for a charged drop can be written as

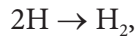


where z — is the number of ions captured by the droplet.

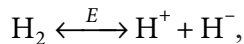
Mechanism of droplet discharge on a grounded electrode (cathode) with the formation of atomic hydrogen on the sample surface



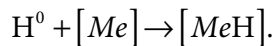
Atomic hydrogen is an active element and is then transformed either into the molecular form H_2



or it is absorbed by the surface of the metal. In turn, hydrogen molecules in a spark electric discharge, upon contact with a charged droplet with a grounded surface, can decompose into positive and negative hydrogen ions



which can also be absorbed by the surface or transformed into a molecular form. Atomic hydrogen can be in the metal structure either in a diffusion-mobile form, or react with metal atoms



However, this reaction requires an active metal surface without oxides. In this case, the surface is not subjected to intense mechanical stress, leading to damage to the oxide films, and the latter reaction is unlikely.

As a result of the experiments, it was found that the contact of a metal surface with a flow of a charged aerosol, even at low flow velocities, causes a noticeable change in the strength properties of the metal.

Comparison of the results of measuring the microhardness of the surface layer at different depths before and after exposure to steam and an electric field shows a significant decrease in the average values of the microhardness of the investigated surface layers of the metal by more than 50%.

The most probable cause for the degradation of the strength properties of the surface layer of the metal is structural changes in the crystal grid caused by the diffusion of hydrogen ions under the action of electrophysical processes on the surface of the sample, as well as electrochemical transformations on the surface and in the depth of the surface layer.

The consequence of the considered charge-discharge processes with chemical transformations on the surface of the blade steel should be an increase in the heterogeneity of the surface layer, which is confirmed by the obtained results of measuring the microhardness. However, given that the sample surface was processed in contact with atmospheric air, the increase in heterogeneity and a decrease in microhardness can be caused not only by hydrogen ions but also by other positively charged ions arising, for example, upon ionization of air, which complicates the interpretation of the results obtained.

In this regard, the contribution of charged wet steam (as a donor of hydrogen ions) in the experiment described above was investigated. For this,

a similar experiment was carried out where wet steam was replaced with a stream of compressed air.

2.2.4. Experimental determination of the influence of the physicochemical properties of the operational medium on the surface strength of blade steel

The experimental installation was reconstructed as follows: the boiler-steam generator was removed; instead, the steam tube inlet was connected to a miniature compressor, which gives an air stream at a speed corresponding to the stream speed of the previously used steam generator (Fig. 2.11). The exposure of the sample to the air stream was also 1.5 hours, after which the surface microhardness was investigated.

The surface of the sample was exposed to an electric field, but charged water droplets did not settle on it. The settling current of ions was not recorded by a microammeter, since it was significantly lower than the sensitivity of the device (Fig. 2.12).

The results of the experiment by blowing the surface of the sample with an air stream (steel sample 20X13) are presented in the Table. 2.3 and Fig. 2.13, 2.14.

It can be seen from the results presented that the nature of the change in the value of the microhardness of the surface of the test sample exposed to an air stream differs significantly from the effect of a charged steam-droplet flow. If

Table 2.3. Values of microhardness and statistical characteristics of experimental data before and after exposure to an air stream

Control			After exposure			ControlLoad, g
Load, g			Load, g			
10	30	10	30	10	30	
141	191	226	160	263	274	HV, kgf/mm ² , average
1.7	2.4	2.9	1.6	2.1	2.6	Middle club imprint, μm
166	225	268	212	568	292	HV, kgf/mm ² , maximum
100	163	182	114	202	259	HV, kgf/mm ² , minimum
66.61	61.92	85.94	98.2	365.89	32.96	The range of variation.
47	32	38	61	139	12	Rel. range of variation,%
21.53	19.46	28.04	33.13	109.1	10.39	σ, st. dev.
463.44	378.69	786.5	1097.78	11903.6	108.04	Disp.
15	10	12	21	41	4	C _v ,%
11.5	17.1	20.3	11	15	18	Average diag. imprint, μm

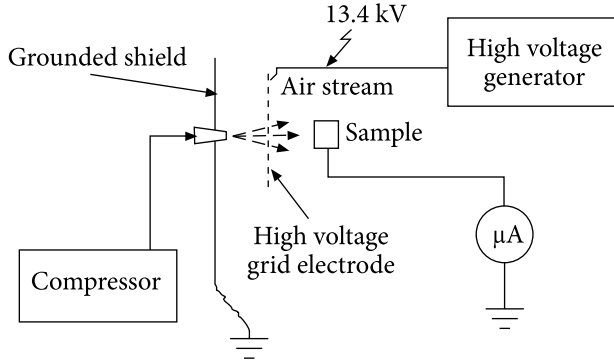


Fig. 2.11. Experimental installation schem

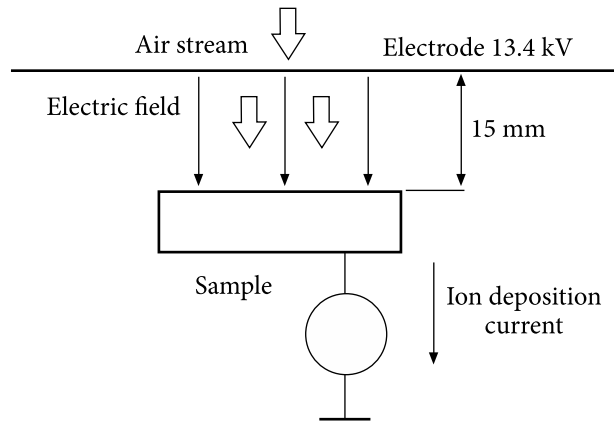


Fig. 2.12. Scheme of the processes in the experiment

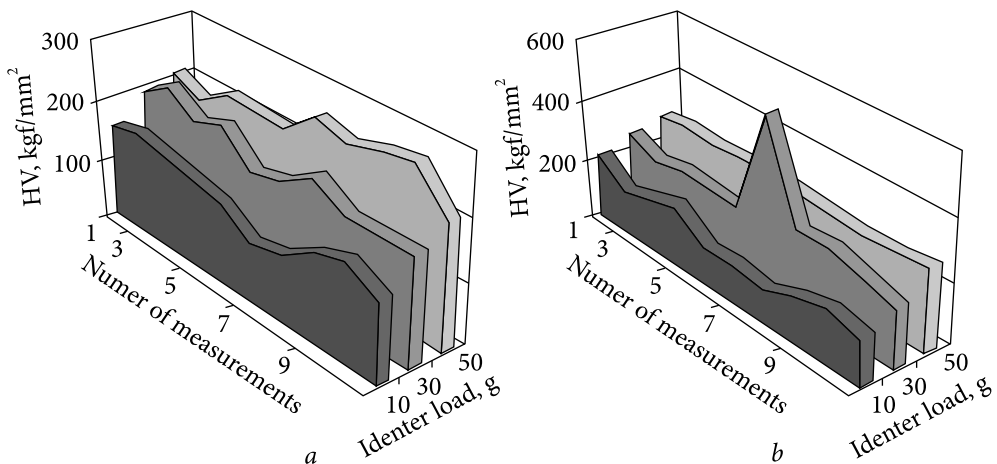


Fig. 2.13. Graphical introduction of the results obtained under loads on indenter 10 g, 30 g, 50 g: a — initial values of microhardness; b — values of microhardness after exposure

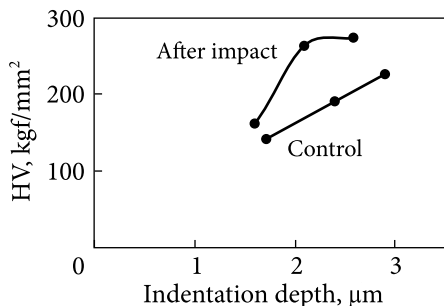


Fig. 2.14. Dependence of the microhardness of the surface layer under load (10 g, 30 g, 50 g) on the indentation depth

the action of steam with charged drops leads to a decrease in the microhardness of the surface, determined at all three investigated loads, by more than 50%, then the action of an air stream

and an electric field leads to an increase in the microhardness in the surface layer up to $\sim 1.5 \mu\text{m}$ in depth by 13% in a layer with a depth of 2 microns 37%, at a depth of over 2.5 microns by 21%.

The dependence of the microhardness on the indentation depth shows that at the depth of the surface layer from $2.2 \mu\text{m}$ and more, the process of formation of structural imperfections has reached saturation (see Fig. 2.13 *b*).

The range of variation of microhardness values after exposure to the test bench increases at all indentation depths, with a maximum increase of more than 4 times at an indentation depth of $\sim 2 \mu\text{m}$.

The obtained relations of microhardness show that the formation of structural imperfections in the surface layer of the metal, blown by an air flow without water steam, occurs according to a different mechanism than in the presence of water.

In the surface layer of the sample at a depth of $2 \mu\text{m}$, a hardened layer is formed due to the diffusion of positive ions from the air. The shallow depth of penetration of impurities is probably associated with the size of the ions, which are significantly larger than the hydrogen ions (prevailing when blowing with water steam) and, respectively, have a lower penetrating ability into the metal surface. Their interaction with the surface leads to the local formation of compounds in the form of monoatomic films (for example, nitrogenous, oxide, or others), which contribute to a heterogeneous increase in the microhardness of the metal.

A significant increase in both the relative range of variation and the coefficient of variation also indicates the appearance of a significant number of large structural inhomogeneities in the surface layer up to $2 \mu\text{m}$, which can be interpreted as the formation of a surface film by air ions in an electric field acting on the sample surface.

Thus, as a result of the presented studies (Section 2.2), the fact of a significant effect on the strength properties of the surface layer of blade steel of electrochemical processes arising in an electrochemical system with a dispersed electrolyte and an electric field acting on the surface of the sample has been established. The effect of an electric field and a stream of steam with

charged droplets is significantly different from the effect of an electric field and a stream of air.

The reason for the changes in the strength properties is associated with the processes occurring on the surface, as a result of which ions penetrate into the surface layer, leading to chemical and structural changes in the surface layers of the metal, as well as in the change in the surface energy of the metal in an electric field. The most probable mechanism for the damaging effect of a positively charged steam on the surface of blade steel is the hydrogenation of the metal.

As applied to turbine rotor blades, this means that the change as a result of electrization of the physicochemical properties of water steam as an operational medium in contact with the surface of the blades can significantly affect the strength properties of the surface layer. Changes in the properties of the working medium as a result of EPI can reduce or increase the surface resistance to mechanical loads, and in particular, increase the rate of accumulation of surface damage during a drop-shock effect on the surface of the blades. Based on the data obtained, a practically important conclusion can be drawn about the possibility of increasing the service life of the blades by controlling the chemical composition and electrical activity of the medium, including by selecting the chemistry.

2.3. Study of the effect of a high-speed stream of ionized wet steam on the kinetics of changes in surface strength and hydrogen content in blade steel

2.3.1. Stand for studying the effect of a high-speed stream of charged steam on a sample

At this stage of the study, in contrast to previous experiments, the problem was solved to study the effect of the complex mechano-electrochemical effect of a charged steam flow on hydrogen saturation of a blade steel sample at a supersonic flow rate and on the kinetics of changes in microhardness.

In a real turbine, the surfaces of the flow path are exposed to a high-speed flow of wet steam containing droplets of various sizes carrying an electric charge of both positive and negative signs. As a result, the flow has a mechanical drop-shock and electrochemical effect on the surface of the flow path. To simulate such a flow, an experimental installation was prepared, which makes it possible to obtain a supersonic stream of condensing steam flowing into the atmosphere (Fig. 2.15 and Fig. 2.16). In this case, it was possible to impart a positive or negative charge to the steam stream. In this case, the electric field

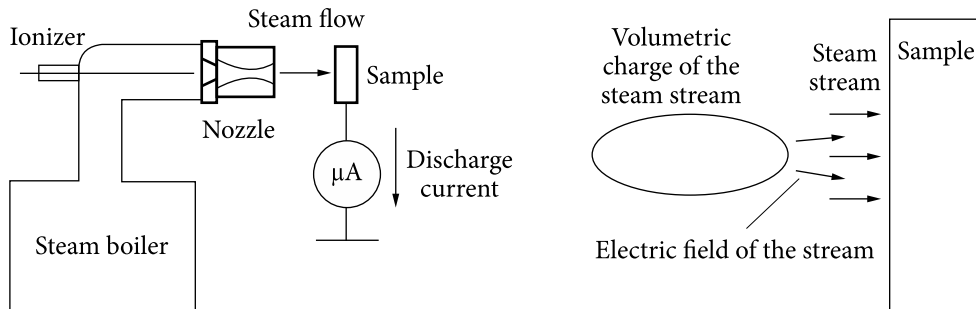


Fig. 2.15. Structural scheme of the processes in the experiment

Fig. 2.16. Scheme of exposure of the sample surface to a steam stream and its electric field

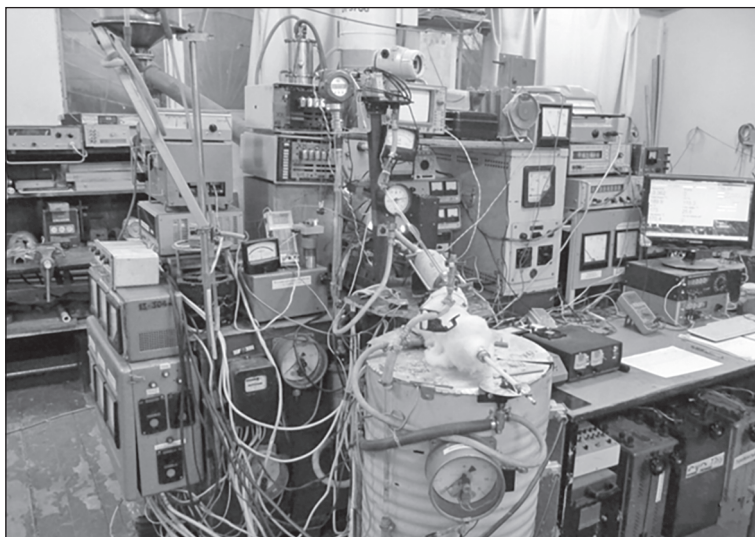


Fig. 2.17. General view of the installation

was not applied to the surface in a special way. The influence of the electric field was only from the stream of ionized steam, which corresponds to the conditions in the turbine with natural electrification of the steam flow.

To carry out tests under conditions similar to those existing in the flow path of the turbine, the installation was modernized, and designed to study the processes of flow of a supersonic ionized steam flow. The general view of the installation is shown in Fig. 2.17.

The main element of the installation is a steam boiler with an ionization chamber and a nozzle apparatus. The boiler steam chamber and internal parts were made of stainless steel. In the bottom part of the boiler, there were heating elements, feed and drainage pipes, and a sludge collector. In the side part, the pipes of the sensors of the monitoring and alarm system of the water level in

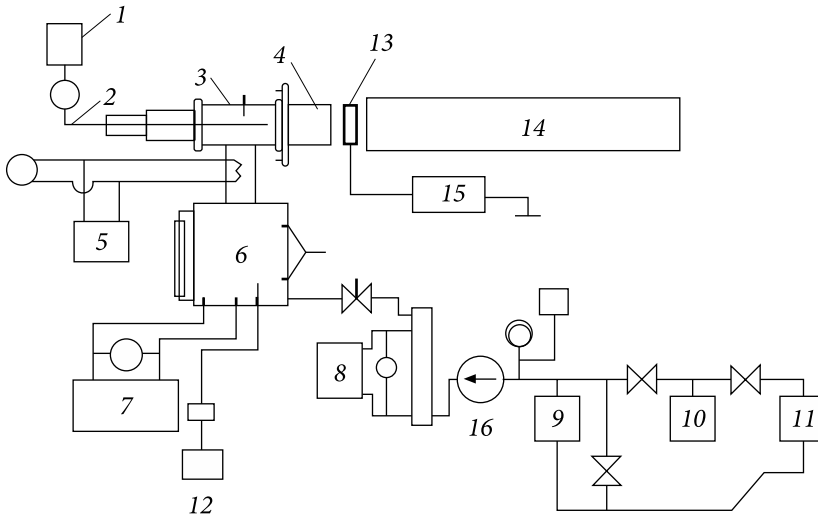


Fig. 2.18. Scheme of a steam plant with steam ionization by corona discharge: 1 — high voltage source; 2 — high-voltage input; 3 — ionization chamber of the boiler; 4 — nozzle part of the ionization chamber; 5 — superheater; 6 — boiler; 7 — boiler power supply; 8 — water preheating system; 9, 10, 11 — buffer tanks; 12 — temperature meter; 13 — blade steel sample; 14 — steam pipeline for venting steam into the atmosphere outside the laboratory; 15 — earth current recorder; 16 — feed pump

the boiler and the pipes of the glass water meter were cut in. To control the temperature, an electric-type superheater was installed in the upper part of the steam line. The outlet of the superheater was connected by an ionization chamber. A supersonic nozzle is located at the exit of the ionization chamber, behind which a unit for fastening bladed steel samples was installed.

The schematic scheme of the experimental installation is shown in Fig. 2.18.

The electric power of the boiler heaters was 6 kW, and controlled heating was provided by a group of LATRs controlled by an automatic voltage stabilization system with an electric drive. Tap water was used to power the boiler. At the stand, the operating mode was maintained with pressure in front of the nozzle $P \sim 176$ kPa, steam temperature $t \sim 126$ °C, steam flow $G \sim 2.3$ g/s, speed $v \sim 400$ m/s. Feed water temperature $108 \div 112$ °C, pressure $309 \div 310$ kPa.

The steam was ionized by a corona discharge in an ionization chamber. The design of the ionization chamber is shown in Fig. 2.19.

Inside the ionization chamber, at the outlet of the steam line, in front of the steam ionization nozzle, a corona electrode 7 is installed, connected to a high-voltage power supply of the VS-20-10 type. A kilovoltmeter was used to measure the voltage across the corona electrode 7. The registration of the current of charged particles deposited on the sample was carried out using a digital micro ammeter.

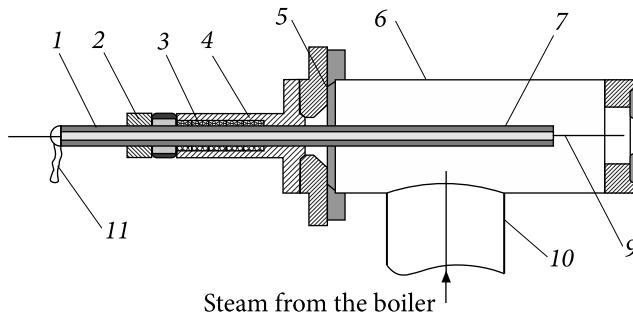


Fig. 2.19. Ionization chamber design: 1 — insulator; 2 — nut; 3 — rubber pad; 4 — electrode body; 5 — flange; 6 — steam inlet chamber; 7 — electrode; 9 — corona ionizer needle; 10 — superheater; 11 — cable from a high voltage source

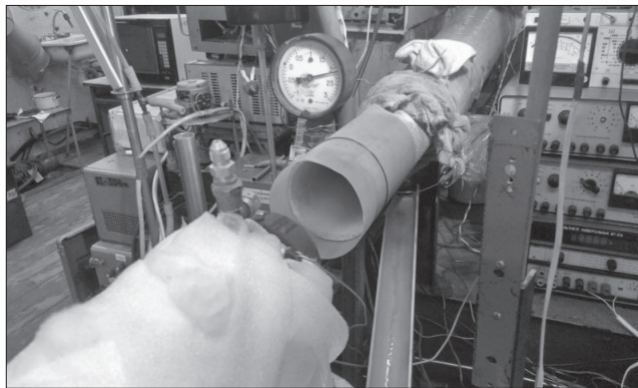


Fig. 2.20. Exhaust part of a steam generator with a supersonic stream entering the steam line of discharge into the atmosphere

The steam flow from the ionization chamber exited into the confuser-diffuser nozzle, which accelerated to a speed of about 400 m/s at a pressure drop of 50 kPa. Steam condensation began near the sample surface in the form of a stream of loose fog. The droplet size was visually assessed as not exceeding 120 μm . The stability of the boiler operation parameters was maintained by an automatic heating stabilization system. A blade steel sample was installed in the outgoing stream into the atmosphere in a dielectric attachment unit.

Fig. 2.20 shows a stream of condensing steam in the form of a mist plume.

Throughout the experiment, the stability of the boiler operation parameters was maintained by an automatic heating stabilization system based on the OWEN data collection and control system. The same system made it possible to write the recorded parameters of the stand operation into a file.

2.3.2. Technique and operating parameters of the experiment

For research, we used flat specimens with a size of 10×1 mm, cut from the feather of a turbine blade made of 15X11MΦIII steel. After mechanical treatment, the samples were subjected to heat treatment to relieve internal stresses. After heat treatment, the surface of the samples was ground and then polished by the requirements of GOST 9450-76 to determine the microhardness. On the prepared sample, the surface area for research was selected, and the PMT-3 device was used to measure the initial microhardness at two loads on the indenter — 10 and 50 grams. To place the sample in the steam flow, a dielectric fixture was made for its attachment, which was installed behind the nozzle at the entrance to the steam line. A conductor was attached to the studied sample, which made it possible to measure the potential induced on the sample by the steam flow, or the current flowing to the grounded sample from the charged steam flow. The impact on the samples was carried out in modes with positive and negative steam ionization.

The sign of the electric charge of the steam and the intensity of ionization could be controlled using a high-voltage source and switching devices.

When establishing the operating parameters of the electrical effect, it was taken into account that the steam flow in the LPC and at the exhaust of the turbine can have a positive, negative, or close to neutral electric charge. Most often, in a real turbine, large droplets are positively charged, and small ones are negatively charged.

In addition, the rotor blades, as a rule, have a certain electrical potential due to the final resistance of the grounding system. The value of this potential is minimal, on the order of several volts for the case of normal operation of the grounding system, however, in some cases, the potential can be significantly higher (for example, in the case of defects of the rotor grounding system).

Based on these options, a system of steam ionization modes was developed for processing steel samples (Table 2.4):

- zero superheated (0S) — superheated steam without ionization, the sample is grounded;
- zero wet (0W) — wet steam without ionization, the sample is grounded;

Table 2.4. Modes of processing samples with a steam flow

Mode No.	0S	0W	1W	2W	3W	4W	5W	6W
The polarity of the applied high voltage								
Steam (ionizer)	No	No	+	-	+	+	-	-
Sample	No	No	No	No	+	-	-	+

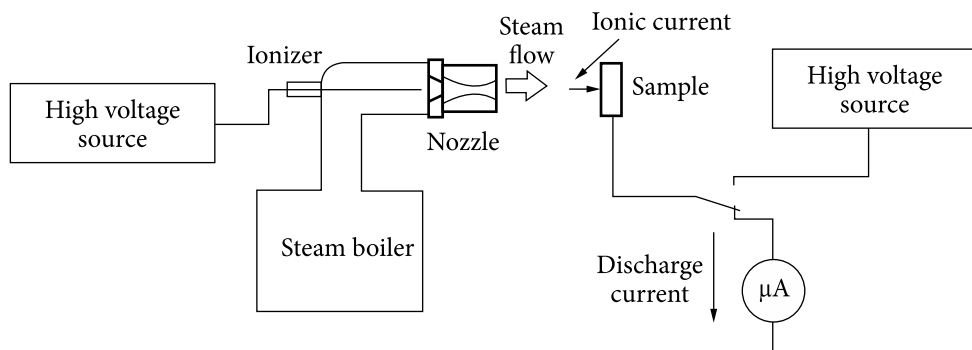


Fig. 2.21. Scheme of the electrical regimes of the experiment

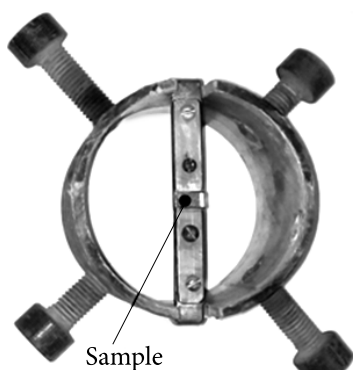


Fig. 2.22. Specimen fixing unit

- the first wet (1W) — the steam is positively charged, the sample is grounded;
- the second wet (2W) — the steam is negatively charged, the sample is grounded;
- the third wet (3W) — the steam is positively charged, the sample has a positive potential;
- the fourth wet (4W) — the steam is positively charged, the sample has a negative potential;
- the fifth wet (5W) — the steam is negatively charged, the sample has a negative potential.
- the sixth wet (6W) — the steam is negatively charged, the sample has a positive potential.

The electrical scheme of the experiment show in Fig. 2.21.

Depending on the mode of exposure, the sample was connected to the ground using an electrical switch (zero modes and 1W, 2W), or connected to a high-voltage source.

The samples were installed in the flow using the fixing unit (Fig. 2.22).

After steam treatment in various modes, the amount of hydrogen absorbed in the samples was measured at the «Skif» KIPT installation, and the microhardness was also determined.

2.3.3. Technique, results and analysis of the experiment on thermosorption of hydrogen

The determination of hydrogen dissolved in the samples was carried out by the method of thermal desorption spectroscopy. This method is one of the most important for studying the interaction of gases with metals. A detailed description of the installation is given in [35]. The scheme of the SKIF thermal desorption unit is shown in Fig. 2.23.

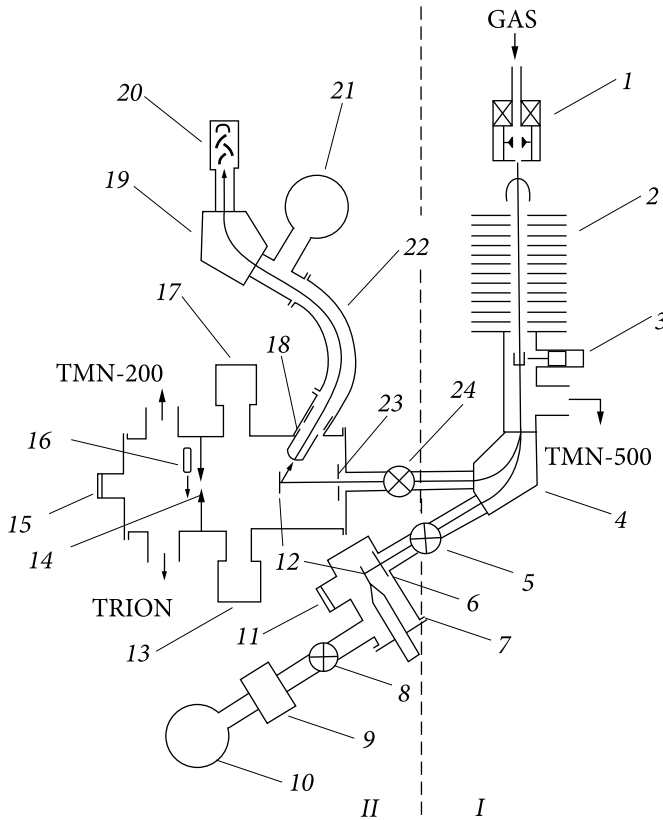


Fig. 2.23. Circuit scheme of the SKIF installation: *I* — accelerator section; *II* — section of output devices; 1 — source of ions; 2 — electrostatic accelerating tube; 3 — Faraday cylinder with electromagnetic drive; 4 — mass separator; 5 and 24 — valves; 6 — aperture; 7 — camera №2; 8 — valve DU-50; 9 — nitrogen trap; 10 and 21 — discharge pump NMD-0.025; 11 and 15 — windows; 12 — target; 13 — sensor of mass spectrometer APDM-1; 14 — iris diaphragm; 16 — quartz screen; 17 — sensor of the MX-7304 mass spectrometer; 18 — lens of the mass spectrometric analyzer of secondary ions; 19 — mass separator; 20 — wind turbine; 22 — energy analyzer; 23 — chamber No. 1

Experiments on the study of thermally activated gas release are carried out in the measuring chamber No. 1 of the installation. The investigated sample is heated according to an approximately linear law using an electric current in the temperature range 80 ... 1800 K, and in some cases (for control) — until the sample melts. The sample temperature is measured with a thermocouple. The partial pressure of gases in the analytical chamber is measured by monopole mass spectrometers APDM-1 and MX-7304 in dynamic mode. The registration of thermal desorption spectra is carried out in absolute values in two coordinate systems: pt and $p-T$ (where t and T are the time and heating temperature). At the same time, signals from the indicated two mass spectrometers, a vacuum

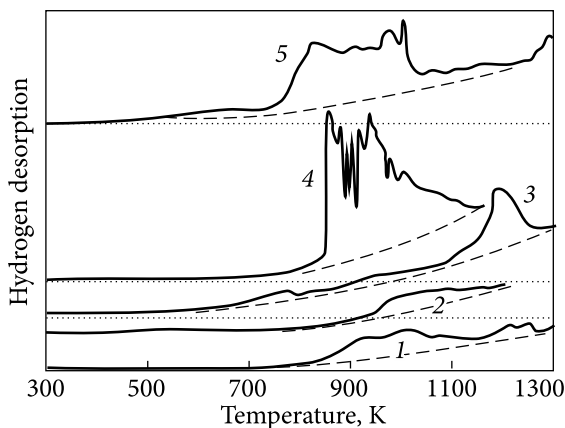
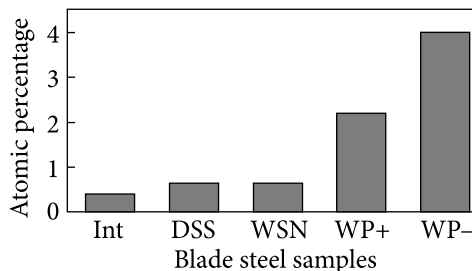


Fig. 2.24. Thermal desorption spectra of hydrogen for different modes of exposure: 1 — spectrum of the sample not treated with steam; 2 — spectrum after exposure to superheated dry steam; 3 — spectrum after exposure to wet neutral steam; 4 — spectrum after exposure to negatively electrified steam; 5 — spectrum after exposure to positively electrified steam

Fig. 2.25. Saturation of samples with hydrogen depending on the mode of exposure: Int— not treated with steam; DSS — dry superheated steam; WSN — wet neutral; WP+ — wet positively charged; WP- — wet negatively charged



gauge, and a thermocouple are recorded using an analog-to-digital converter WAD-AIK-BUS (4-channel analog input module with galvanic isolation per channel to the USB bus. The input voltage range is ± 60 mV. The signals are recorded on a computer in the form of a file with the «dat» extension. The temperature measurement error is ± 5 K. time.

The main results of the study are shown in Fig. 2.24 and 2.25.

Fig. 2.25 shows the results of the experiments carried out in the form of a histogram of the hydrogen content in steel samples with the greatest change after exposure to a steam flow.

Analysis of the results of the hydrogen content in the metal showed that after exposure to steam, the smallest value of 0.4 at.% corresponds to neutral dry superheated and wet steam. The maximum value of hydrogen is 4.0 at.% For a sample treated with negatively ionized steam. The lower value of 2.2 at.% of dissolved hydrogen in the sample treated with positively ionized steam, but still 5 times more than neutral.

Attention is drawn to the fact that the highest hydrogen concentration was found in the sample treated with negatively charged steam. In this regard, the results of the study presented in article [36] are of interest, and should be paid attention to. The authors provide data that hydrogen in various active forms H^+

and H^- has a different effect on the static tension of 08KII steel. Hydrogen in the proton state decreases the fluidity stress, and the length of the fluidity area, and decreases the elongation at break. At the same time, hydrogen particles, which have a negative electric charge, like hydrogen in the atomic and molecular state, do not have a noticeable effect on the mechanical parameters of steel.

Further studies to determine the microhardness of a metal under the influence of a charged flow with different polarity both in this experiment and in subsequent ones confirmed the results obtained.

2.3.4. Study of surface strength of the sample and the kinetics of changes in microhardness under the action of a high-speed charged steam flow

Further research was devoted mainly to the kinetics of changes in the microhardness of metals under the influence of a charged flow. For this, a stand was used (Fig. 2.17), where contact with atmospheric air was not excluded.

The results of the experiment are presented in Fig. 2.26 and 2.27. From Fig. 2.26 it can be seen that exposure to positively ionized steam produces a softening effect on the surface of the blade steel. The greatest softening (more than 50%) occurs up to a depth of about 2 microns, at a depth of 2 to 3.5 microns, the decrease in microhardness is almost 2 times less.

Under the action of a high-speed negatively charged flow (Fig. 2.27), metal hardening is first observed by 50% at a depth of 2 μm and by 30% at 3.5 μm , which can be caused both by the implantation of nitrogen ions and the formation of an oxide film, and in further, after 2—10 hours of treatment, weakening of the metal is observed by 10% and 20%, respectively, caused by saturation of hydrogen.

Unfortunately, in the experiments carried out, an unambiguous dependence of the microhardness on the concentration of absorbed hydrogen was not revealed, although a certain regularity can be traced in this case (a positively charged flow always more significantly reduces the strength of a metal in comparison with a negative one).

These studies were also carried out to determine the rational time factor of the impact of the charged flow on the surface strength of the metal to minimize the energy and time spent on the experiment.

From Fig. 2.26 and 2.27, it can be seen that structural and chemical transformations on the surface of blade steel most actively occur in the first 4—5 hours of exposure to a charged steam flow. Therefore, in further studies, this exposure time interval was taken as a basis.

In the process of analyzing the numerous results obtained in this experiment, it was found that some of the results are contradictory and ambiguous (Fig. 2.27). The most likely reason for this was the influence of atmospheric air,

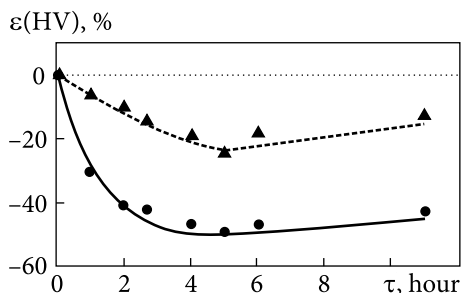


Fig. 2.26. The relative change in the microhardness of the sample of steel 1X11MΦIII under the influence of positively ionized steam: 1 — load on the indenter 10; 2 — load on indenter 50g

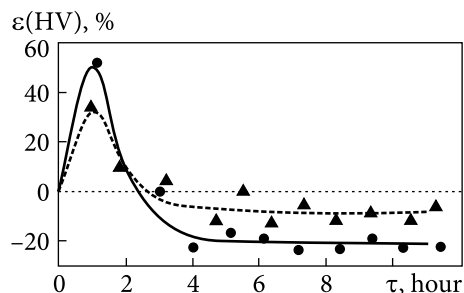


Fig. 2.27. Relative change in the microhardness of the sample when exposed to negatively ionized steam: 1 — load on the indicator 10 g, 2 — load on the indicator 50 g

and as a result, during the first hours of treatment, films of oxides and other chemical compounds could form on the surface due to contact with atmospheric gases, as well as various chemical impurities in the steam. This was the reason for conducting studies that would exclude these factors as much as possible.

2.4. Study of strength properties of blade steel in a vacuum system under the action of a high-speed ionized flow of steam of different polarization

2.4.1. Modernized stand and research methodology

To make the conditions of the influence of the steam flow at the experimental installation to the conditions in the turbine, its modernization was carried out.

To reduce impurities in the steam, the pipeline and shut-off fittings were, where possible, replaced by stainless steel. The boiler drum was re-made from stainless steel. The automated monitoring and control system for the installation (Fig. 2.28 b) has been improved. The boiler power supply switched to distilled water. A vacuumed flow path with a hermetic fastening of the processed samples was made. A steam condenser and a condensate recirculation system were manufactured and installed (Fig. 2.28 a). The stationary operating mode of the installation was provided by an automatic boiler heating stabilization system. Steam from the steam generator was accelerated in the converging-diffuser nozzle used in previous experiments. A processed sample was installed behind the nozzle exit.

The scheme of the experimental installation is shown in Fig 2.29.

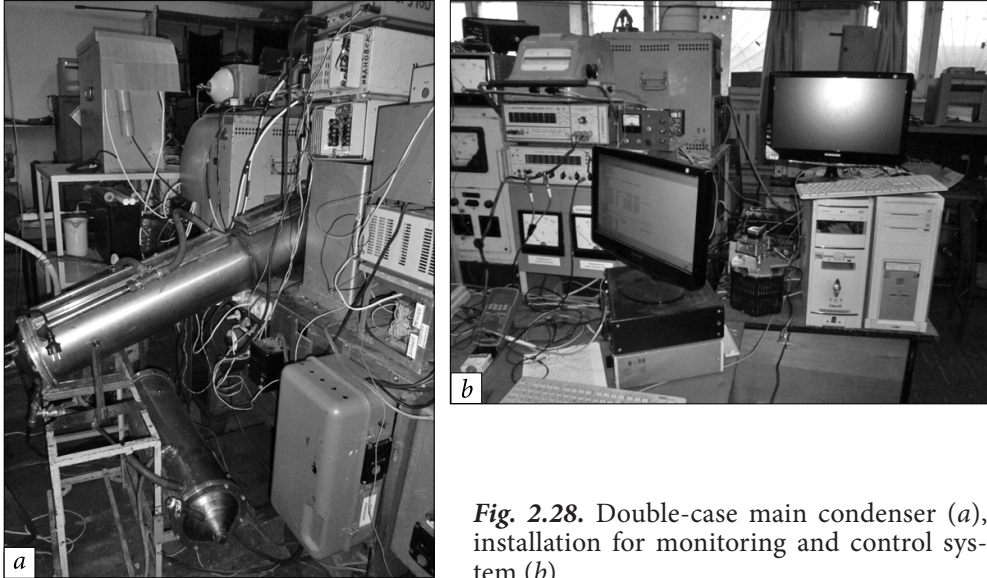


Fig. 2.28. Double-case main condenser (a), installation for monitoring and control system (b)

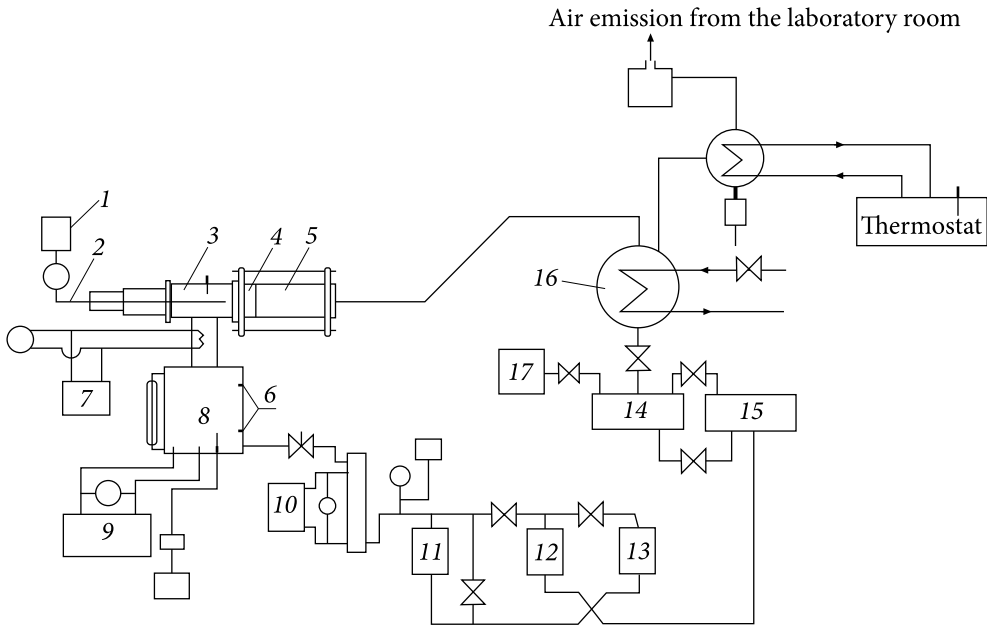


Fig. 2.29. Scheme of a modernized steam installation with a corona discharge: 1 — high voltage source; 2 — high-voltage input; 3 — ionization chamber of the boiler; 4 — module for fastening a sample of blade steel; 5 — processing chamber; 6 — water level sensors; 7 — superheater; 8 — boiler; 9 — power supply for heating elements; 10 — feed water heater; 11 — feed pump; 12 and 13 buffer tanks; 14 and 15 — condensate accumulators; 16 — capacitor; 17 — vacuum pump

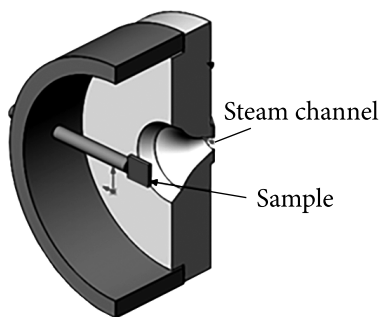


Fig. 2.30. Scheme of installation of samples in a steam flow

The main objectives of the study on the modernized steam installation were: to study the processes of hydrogen absorption of blade steel under the action of a flow of ionized steam of different polarity; study the effect of steam on the microhardness of the steel surface in the presence of an electric potential on the sample or when it is grounded. Based on previous studies (Fig. 2.26 and 2.27), a processing time of 4 hours was chosen.

The system for registering the parameters of the installation made it possible to control the following parameters: boiler supply water temperature, boiler water temperature, boiler water level, boiler steam temperature, boiler pressure, nozzle inlet temperature, ionizer voltage, and current, condenser inlet temperature, temperature at the inlet and outlet of the heat exchanger of the main condenser. The electrization potential of the sample, or the short-circuit current from the sample, were also recorded. When the calculated pressure drop of 50 kPa in the nozzle section was reached, the steam velocity at the nozzle exit was supersonic. A foggy plume of condensing steam was visually observed behind the nozzle in the glass flow path. The required parameters of the steam installation were maintained at the same level throughout the experiment by the stabilization system.

The working section of the stand was a split pipeline with a unit for fastening bladed steel samples (Fig. 2.30). Steam entered the test section through a supersonic nozzle, at the outlet of which a steel sample under study was installed. The design of the pipeline made it possible to quickly replace the test samples through flange connections.

The attachment point made it possible to register the electrization of the sample or to ground it to the body of the installation using a conductor attached to the clamp. In the course of the experiments, all variants of the possible polarity of the flow charges and the blade surface in a real turbine were simulated. In addition, since it was found in earlier bench experiments that artificial ionization of steam in a quasineutral mode increases the efficiency of the expansion of supercooled steam by 2.5%, it was decided to investigate also the effect of exposure and a barrier discharge on the strength properties of the surface layer of the sample. To treat the sample with quasi-neutral steam, a tubular barrier discharge module was developed and manufactured (Fig. 2.31).

In terms of geometric characteristics, the module was identical to the tubular working section used in experiments with corona ionization of the flow

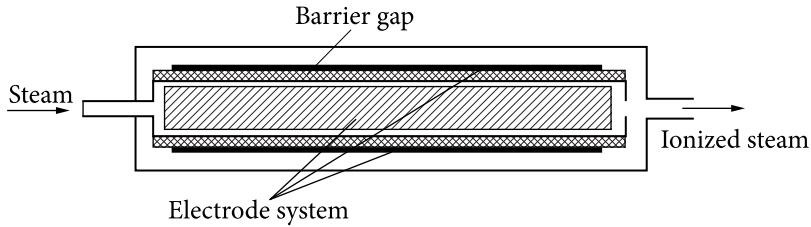


Fig. 2.31. Scheme of the discharge chamber of the barrier discharge module

and was installed in the same way as the previous working section between the steam generator and the condenser.

As a material for experiments, a fragment was cut out from the tail part of the working blade of the low-pressure cylinder of a turbine (steel 15X11MΦ). Samples with dimensions $10 \times 4 \times 1.2$ mm were cut from this piece of steel. The surfaces of the samples were polished per the requirements for conducting microhardness studies, and the initial microhardness value was measured. The samples were processed in the following modes:

Sample No. 1 is treated with neutral wet steam. Sample No. 2 was treated with negatively charged steam. Sample No. 3 was treated with positively charged steam. Sample No. 4 was treated with a quasi-neutral steam flow.

2.4.2. Results of the experiment with a high-speed stream in a vacuumed system

The influence of various modes of electrization of the steam flow on the change in the hydrogen content in the metal and the value of microhardness after 4 hours of exposure to the surface of the blade steel samples were studied.

Table 2.5. Modes of processing samples isolated from the ground

Sample no.	Charged steam polarity	Ionizer		Sample	
		Voltage, kV	Corona discharge current, mA	Flux-induced voltage, V	Short-circuit current to ground, μ A
6	No	No	No	No	No
1	negative	- 7	75	7 ... 12	0.2
VI	positive	+8.6	100	14.7 ... 15.1	0.2
4	quasi-neutral (barrier discharge)	Alternating voltage 3.2 — 3.4 kV, frequency 7.8 kHz, discharge current 15 mA		~24	0.1

The results of the experiment to determine the microhardness of the samples are presented in Table. 2.5—2.7 and at Fig. 2.32 —2.36.

The samples were processed for 4 hours in the modes presented in Table 2.5.

Fig. 2.32—2.36 presents the resulting and summary graphs on the change in microhardness after exposure to neutral, positive, negative, and quasi-neutral steam.

From the presented summary graph of the experimental results (Fig. 2.36) it is seen that the most aggressive from the point of view of metal degradation is a wet steam flow with positive polarity.

Table 2.6. Results of exposure to neutral and charged steam

Sample No. 1 — neutral steam treatment			
Indenter load, g	The initial state	After processing	Relative change %
	HV, kgf/mm ²	HV, kgf/mm ²	
10	160	158.4	-1
30	198.7	180.6	-9.1
50	194.8	189.9	-2.5
100	212.5	197.5	-7.1
Sample No. 2 — negative steam treatment			
10	181.4	192	5.8
30	214.3	212	-1.1
50	211.9	205.1	-3.2
100	215.2	210	-2.4
Sample No. 3 — treatment with positively charged steam			
10	250	150	-40.0
30	251	200	-20.3
50	249	230	-7.6
100	249	247	-0.8

Table 2.7. Results of exposure to quasi-neutral steam

Sample No. 4 — treatment with quasi-neutral steam			
Indenter load, g	The initial state	After processing	Relative change %
	HV, kgf/mm ²	HV, kgf/mm ²	
10	148.6	146.5	-1.4
30	174.5	167.9	-3.8
50	185.3	179.7	-3.0
100	191.1	185.2	-3.1

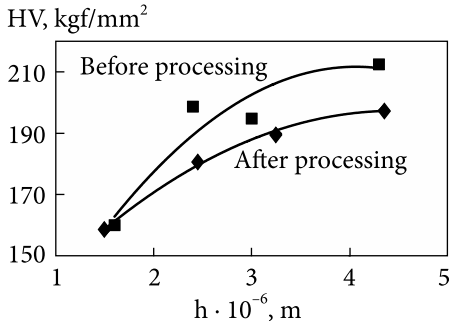


Fig. 2.32. Relative changes in microhardness in depth after treatment with neutral steam

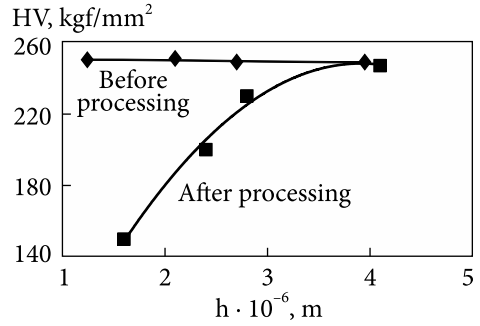


Fig. 2.33. Relative changes in microhardness in depth after treatment with positively electrified steam

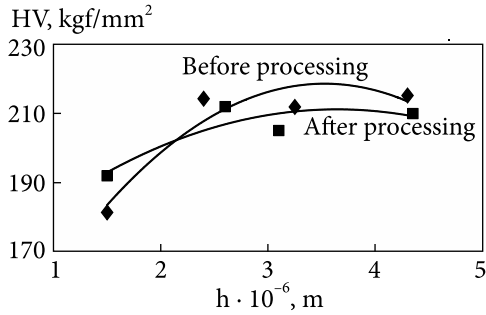


Fig. 2.34. Relative changes in microhardness in depth after treatment with negative electrified steam

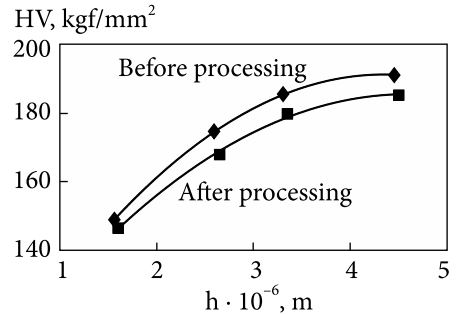
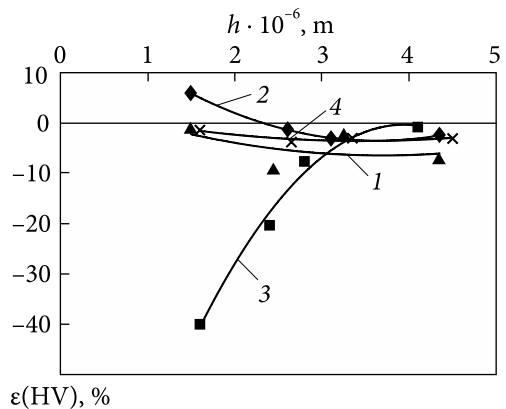


Fig. 2.35. Relative changes in microhardness in depth after treatment with quasi-neutral steam

Fig. 2.36. A summary graph of the relative change in microhardness over the depth of the surface of the samples processed in wet steam in the following modes: 1 — neutral wet steam; 2 — negatively charged wet steam; 3 — positively charged wet steam; 4 — quasi-neutral steam (electrization in a barrier discharge)



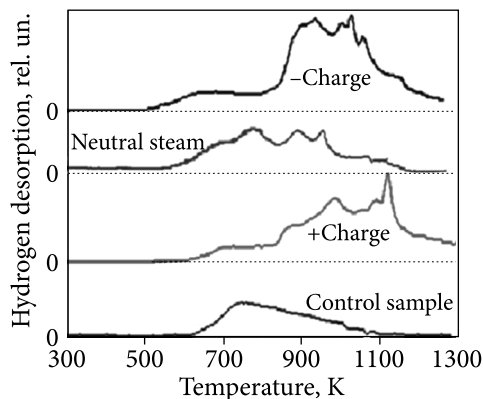


Fig. 2.37. Thermal desorption spectra of samples

After determining the microhardness, the steel samples were examined for hydrogen content. The thermal desorption spectra of the control and processed samples are shown in Fig 2.37. As can be seen in the graph, the thermal desorption spectra have a significant difference. The spectrum of the control sample, not exposed to steam, is in the temperature range of $600 \div 1100$ K. The spectra of all samples treated with steam (both neutral and electrified) have a wider temperature range. The spectra of electrified steam have the largest temperature range. The nature of the spectral curves of the samples treated with electrolyzed steam is similar and has specific differences from the spectra of the control sample and treated with neutral steam. The values of the area under the curves of thermal desorption for samples exposed to negative and positively electrolyzed steam are close in magnitude, but the area under the curve for negatively electrolyzed steam is somewhat larger. This means that the hydrogenation of a blade steel sample after exposure to negatively electrolyzed steam is greater than after exposure to positively electrolyzed, i.e. in principle, the trend confirms the results presented in the previous experiment (see Fig. 2.24).

As a result of the experiments performed and their comparison (Fig. 23 b), we can conclude that four hours of treatment with negatively ionized steam did not lead to a noticeable change in the strength properties of the surface layer of the steel sample (Fig. 2.34).

Exposure to positively ionized steam significantly (by 30—50%) reduced the microhardness of the surface layer. Dry neutral and quasineutral steam also reduced the microhardness but by a small amount (less than 10%).

Since in this experiment, there was an insignificant influence of air, the main reason for the changes in surface properties can be considered the effect of charged water droplets of different polarities, the electric field of the steam stream, and ions — the products of water dissociation.

From the experiments carried out, it could be seen that there is no direct relationship between the total hydrogen saturation and the change in strength properties. This is explained by the fact that in this experiment the fraction of diffusion-mobile hydrogen, which makes the main contribution to softening, was not determined [36]. Taking into account that the effect of ion currents under certain modes of ionization of the steam flow has a significant effect on

the strength properties of the surface layer of steel, it can be assumed that in these modes the fraction of hydrogen introduced into the surface in a diffusion-mobile state increases.

The sign of the charge, as discussed in the analysis of the previous experiment, probably influenced not only the total concentration of hydrogen absorbed in the surface layer but also the fraction of absorbed hydrogen in a diffusion-mobile form. The basis for this conclusion is the fact that in all the experiments carried out, the hydrogen concentration when exposed to negatively electrified steam is higher than when exposed to positively electrified, and the effect on the surface strength is much less. It is especially necessary to pay attention to the fact that, as shown by numerous field studies, in the zone of the last stages, the steam polarity, as a rule, has a positive sign, and therefore has the greatest degradation feature [37].

2.5. Study of the influence of constant and alternating electric field on the microhardness of the surface layer of the blade steel

2.5.1. Experimental installation and selection of parameters for electric field exposure to a steel sample

The presence of a volumetric charge in the working body of the wet steam turbine causes the appearance in the space of the flow part of both constant and alternating electric fields. Such fields were registered during experiments at Eshar CHP [1]. These fields can initiate various electric currents, and also directly affect the surface of metal parts. It is known that the effect of an electric field on the metal surface can change the strength properties of the surface layer [38, 39]. So, the task of experimental verification of the possibility of the influence of electric fields on the strength properties of blade steel is relevant.

To select the value of the field strength on the surface of the blade steel sample, an approximate estimate of the field strength in the turbine LPC between the working and guide blades was made in the experiment. As shown above, the range of changes in the volumetric charge density in the steam flow in the turbine is from $\sim 10^{-10}$ C/m³ in the phase transition zone and up to $\sim 10^{-3}$ C/m³ in the turbine exhaust. Taking into account previous studies at various thermal power plants and combined heat and power plants, a volume value close to the average value was chosen for the calculation.

Calculation of the field strength in the interblade space in the wet steam zone according to the two-dimensional model for a volumetric charge density

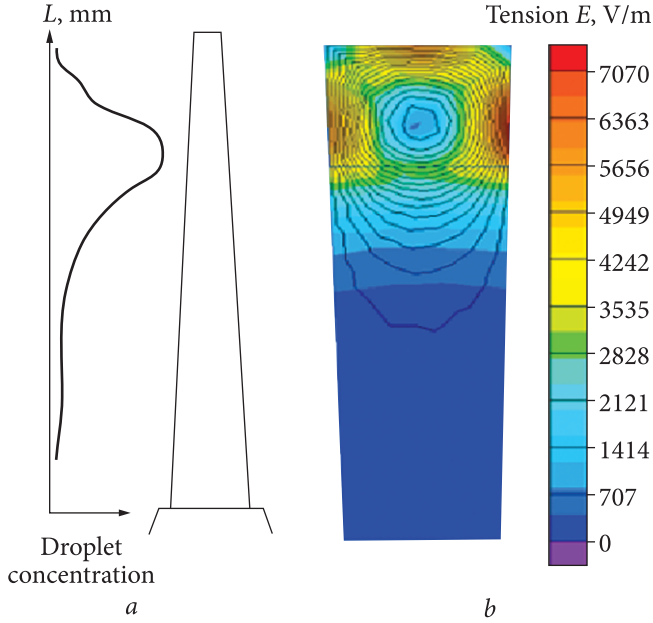


Fig. 2.38. Distribution of coarse charged moisture on the height of the blade: *a*) and the field strength V/m between the guides and the working blades (*b*)

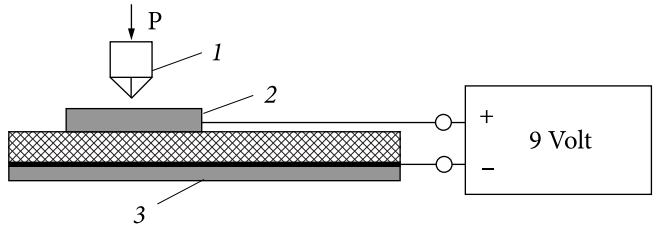


Fig. 2.39. Electric field indentation system: *1* — indenter; *2* — sample; *3* — dielectric base

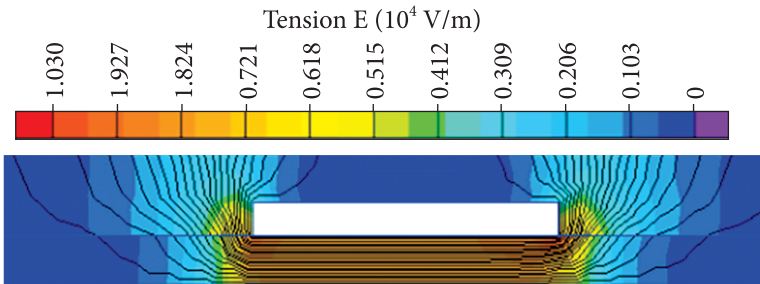


Fig. 2.40. Field strength diagram on the surface of the blade steel sample

of 10^{-6} C/m^3 , the distance between the blades 170 mm and the blade height 960 mm gives the following picture (Fig. 2.38):

As can be seen from the diagram, the maximum field strength on the blade surface is of the order of 7000 V/m.

To experiment to study the effect of an electric field on the mechanical properties of the blade steel surface, a test device based on the PMT-3 was assembled. The scheme of the indentation system in an electric field with a sample is shown in Fig. 2.39.

Installation design: a plate of foiled fiberglass, foil to the dielectric was attached to the dielectric base. The test sample was fixed on top of the fiberglass plate. Conductor difference conductors are soldered to the foil and sample. The source of the potential difference was a stabilized laboratory power supply.

At a sample potential of 9 V, the distribution of the field strength on the sample is shown in Fig. 2.40.

The numerical value of the surface tension is of the order of 8000 V/m, which is comparable to the value of the stress estimate in the flow part of the CND obtained above.

2.5.2. Methods and results of the experiment

For the experiment, samples of steel 15X11MΦ with a size of 10x5x1 mm were taken. The steel sample was attached to the surface of the plate made of single-sided foil fiberglass 85x20 mm, 1.5 mm thick on the non-foil side with plasticine. To insulate the entire system from the body of the device PMT-3 strip of foil fiberglass side with foil was glued to the vinyl plate — the base 110x25 mm 2 mm thick. The second conductor was soldered to the foil. A positive potential was applied to the sample and a negative potential to the foil. The potential difference was 9 V. The scheme of mechano-electric action on the sample in the experiment is shown in Fig. 2.41.

Indentation was performed under the direct influence of an electric field, in contrast to previous studies, where the effect of ionized steam flow on the mechanical properties of the surface after its exposure was investigated.

The results of the impact on the sample of the electric potential of 10 V of different signs are given in Table 2.8.

From the results shown in Table 2.8, it is seen that the electric field affects the microhardness of the surface of the studied samples of 15X11MΦ steel and the nature of this effect depends on the polarity of the electric voltage applied to the sample. For example, with positive polarization, the microhardness decreases by 11—12%, and with negative polarization, the reverse process occurs, and the microhardness HV 0.01 increases by 9.6%. This effect of the polarizing voltage on the microhardness of the surface can be explained by the

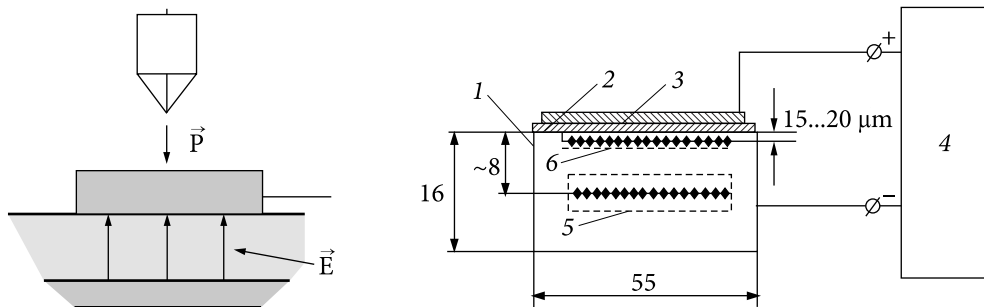


Fig. 2.41. Scheme of field overlay and indenter impact

Fig. 2.42. Conditional scheme for measuring the microhardness of the surface of the sample, to the side surface of which is applied a polarizing constant electric field: 1 — sample; 2 — dielectric gasket; 3 — copper electrode; 4 — voltage source; 5, 6 — places of identification

Table 2.8. Influence of the electric field on the microhardness of the surface of studied samples

Indicator	Value		Relative change $\epsilon(\text{HV})$	Value		Relative change $\epsilon(\text{HV})$
	Initial	Under voltage + 10V		Initial	Under voltage -10V	
HV 0.01	157.9	140.5	-11.0%	128.7	141.1	9.6%
HV 0.02	172.2	150.7	-12.5%	154.5	156.8	1.5%

change in the specific surface energy due to the change in the surface density of the electron distribution.

To examine this assumption, the effect of the electric polarization voltage, regulated in the range from 0.2V to 12V, and the location of identification (Fig. 2.42, positions 5 and 6) on the change in surface microhardness was studied. A 20X13 steel sample with dimensions of $50 \times 18 \times 12$ mm was used as the sample under study.

The results of the relative change in the microhardness measured in zone 5 (in the center of the sample surface) are shown in the form of graphs in Fig. 2.43.

Fig. 2.43 shows that the nature and degree of dependence of the change in the microhardness of the surface measured in the central part of the sample (Fig. 2.42, section 5) on the polarization voltage of the side face surface is complex polyextreme. In this case, the amplitude of oscillations depends on both the load on the indenter and the magnitude of the polarization voltage. Moreover, the largest fluctuations are observed when the polarization voltages change in the range from 0.2 to 3 V. With step by step increase in the load on the indenter from 20 g to 200 g, the degree of influence of the polarization vol-

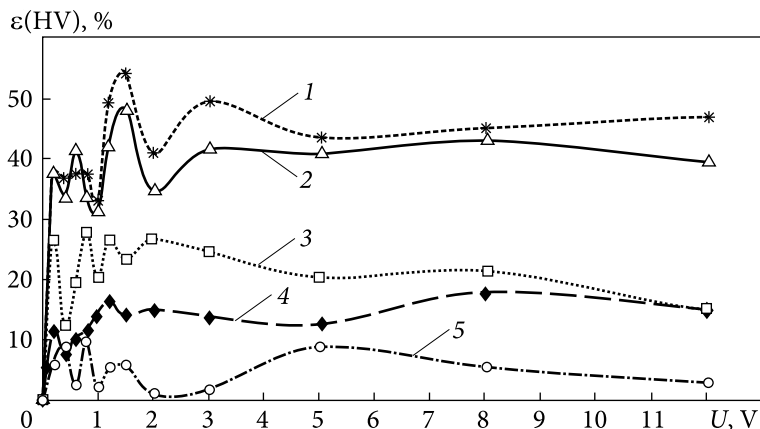


Fig. 2.43. The relative change in the microhardness of the sample surface made of 20X13 steel, determined by the central part at indenter loads of 20, 50, 70, 100 and 200 gf, depending on the electric field voltage between the sample and the electrode: 1 — $\varepsilon(\text{HV } 0,02)$; 2 — $\varepsilon(\text{HV } 0,05)$; 3 — $\varepsilon(\text{HV } 0,07)$; 4 — $\varepsilon(\text{HV } 0,1)$; 5 — $\varepsilon(\text{HV } 0,2)$; the potential of the sample is positive

tage on the relative change in surface microhardness decreases 5 times. For example, at a voltage of 1.5 V and an indenter load of 20 g, the relative change in microhardness $\varepsilon(\text{HV})$ with increasing polarization voltage ranges from 34% at $U = 1\text{ V}$ to 54% at $U = 1.5\text{ V}$, and at a further increase in voltage, the amplitude of oscillations decreases and the relative change in microhardness remains in the range of 43... 47%. As the load on the indenter increases, the degree of influence of the polarization voltage on the relative change in surface microhardness $\varepsilon(\text{HV})$ decreases sharply and at $P = 200\text{ g}$ the relative change ranges from 2% to 10% in the range of polarization voltage from 0.2 to 5 V, and with a gradual increase to 12 V, the microhardness of the surface smoothly tends to the initial value.

It can be assumed that such a complex polyextreme change in microhardness from the polarization voltage is caused by several reasons. These include the course of several competing processes that oppose the process of plastic deformation of the metal during indentation (generation of dislocations, their movement, fusion, and possible annihilation). In addition, due to the deterministic change in the energy state (or distribution density) of surface electrons, the specific surface energy of the metal also changes, on which both the generation of dislocations and the energy of new surface formation depend. And since with increasing depth of penetration with increasing load on the indenter, the degree of influence of specific surface energy on the overall work of plastic deformation of the metal surface layer decreases sharply (inversely proportional to the depth of the impression), its influence on the relative change in microhardness decreases.

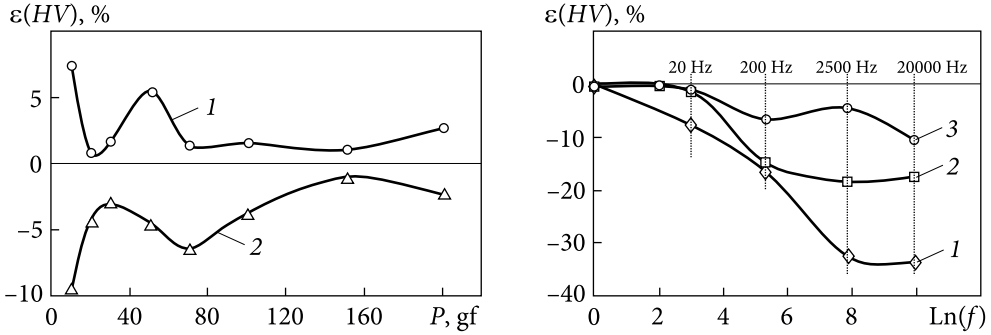


Fig. 2.44. The relative change in the microhardness of the surface with negative and positive polarization of the sample of steel 20X13, measured at loads on the indenter 10, 20, 30, 50, 70, 100, 150, and 200 gf: 1 — voltage $U = -1.5 B$; 2 — voltage $U = +1.5 B$

Fig. 2.45. Relative change in the microhardness of the surface of a sample made of steel 15X11MΦ depending on the frequency of an alternating electric field with voltage 10 V, 1 — $\varepsilon(HV 0,01)$; 2 — $\varepsilon(HV 0,02)$; 3 — $\varepsilon(HV 0,1)$

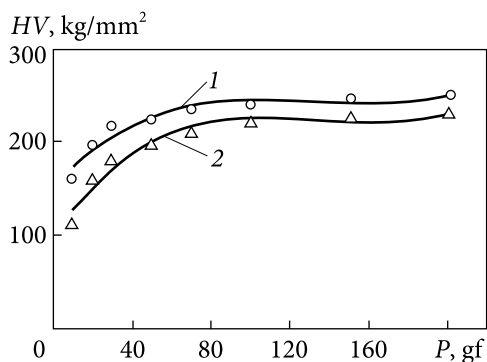
To test the assumption of the influence of the sign of the polarizing stress on the nature of the change in the microhardness of the surface (Fig. 2.45), an experiment was performed. The microhardness of the surface was measured at a distance of 15... 20 μm from the edge of the side face (Fig. 2.42, zone 6) at positive and negative stress values. The voltage value was selected from the graph of Fig. 2.43 from the condition of its maximum effect on microhardness, which was $\pm 1.5 V$. The results of measurements in the form of graphs are presented in Fig. 2.44.

The graphs show that the sign of the relative change in the microhardness of the surface is inverse to the sign of the polarity of the stress on the sample. The nature of the relative change in microhardness from the load on the indenter is polyextreme.

In our opinion, this is caused by the complex evolution of the relationship between such competing phenomena as the generation, movement, and interaction of dislocations and their clusters against the background of the influence of the energy state of the surface (Fermi energy). At negative voltage on the sample, the surface density of electrons, and with it the specific surface energy increases, which leads to an increase in surface microhardness compared to its initial value (Fig. 2.44, curve 1), with positive polarization, the opposite happens — when microhardness decreases (Fig. 2.44, curve 2). Thus, we obtained indirect confirmation of our assumptions about the correlation of the change in the surface density of electrons with the change in the microhardness of the metal surface.

Earlier, during research at Eshar CHP [1], it was found that alternating electromagnetic fields in a wide range of frequencies appear in the CND in

Fig. 2.46. Influence of a magnetic field on change of microhardness of a surface of a sample from steel 20X13 measured at various loadings on an indenter: 1 — without a magnetic field; 2 — in a magnetic field



the wet steam electrization zone (Fig. 1.17). In this regard, the effect of alternating electric fields with frequencies of 20, 200, 2500, and 20,000 Hz

and a voltage of 10 V on the microhardness of the surface of a prismatic sample of 15X11MΦ steel was studied. Microhardness was determined at three different indenter loads: 10, 20, and 100 gf. The results of measurements in the form of graphs are presented in Fig. 2.45.

The graphs show that variable electric fields in the range from 200 Hz to 20,000 Hz have a significant effect on the plastic deformation of the surface layer of the 15X11MΦ blade steel. The greatest relative decrease in microhardness is observed at an indenter load of 10 g (HV 0.01) up to 30% and at an indenter load of 20 g (HV 0.02) up to 18%. When the load on the indenter increases to 100 g, the relative decrease in the microhardness of the surface is in the range of 5—10%. The obtained results show that electromagnetic fields also harm the resistance of the metal.

Because the currents generated in the flow part create magnetic fields and magnetize the turbine parts, a study of the effect of a constant magnetic field on microhardness when identifying a blade steel sample was carried out. The change in the microhardness of the sample surface under the conditions of exposure to the side face of a permanent magnet with a magnetic induction of 0.31 T was observed. The results of measurements in the form of graphs are presented in Fig. 2.46.

The data shown in the figure indicate that the constant magnetic field weakens the resistance of the blade steel 20X13 to plastic deformation during micro indentation in the entire studied range of loads (in grams) on the indenter ($P \in 10; 20; 30; 50; 70; 100; 150; 200$). In this case, the magnetic field has the maximum effect on the plastic deformation of thin surface layers (up to 2.5 μm). For example, the relative decrease in surface microhardness in a magnetic field, measured at indenter loads of 10 g (insertion depth $h = 1.8$ μm) and 50 g (insertion depth $h = 3.1$ μm), was 30 and 12%, respectively. (2.46). With a further increase in the penetration depth by increasing the load on the indenter from 100 g to 200 g, the relative decrease in the surface microhardness due to the magnetic field does not exceed 7... 8%. Based on the obtained data,

it can be concluded that the magnetization of the blade material can affect the resistance of the surface to mechanical stress. However, this change is observed at a significant level of magnetic induction, which exceeds the values of the magnetic field generated in the flowing part. And this impact requires more detailed research.

Analysis of the results presented in this subsection. 2.5 allows us to make the following conclusions:

- the electric field, both constant and variable, acting on the surface of the blade steel sample changes the microhardness within plastic deformation;
- the maximum reduction of microhardness in a thin surface layer of steel can reach the value of about 30%. As a result, when the impact of erosion-hazardous droplets and an electric field are combined, the damage may be higher than in the case of neutral droplets.

Conclusion and main outputs in section 2

Experiments on the influence of steam flow on the surface of the blade steel showed that the charged dispersed medium is an additional factor that intensifies the degradation of the blade steel surface. The nature of the effect of charged steam flow depends on the speed of contact of the flow with the steel surface, the sign of the charge, the physicochemical properties of the working environment in which the interaction takes place, the initial state of the metal surface, and its electrical potential. In conditions close to the existing processes in the flow part of the turbine (in the vacuum system), the positively charged flow has the greatest strengthening effect on the metal surface.

An important feature of the effect of steam flow on the metal surface is the general hydrogenation, which is shown in almost all modes of blowing the surface flow. In the above studies, it was shown that the highest amount of absorbed hydrogen was in grounded samples exposed to both positively and, to a greater extent, negatively charged steam.

It has been experimentally approved that there is no direct relationship between the hydrogen concentration and the change in strength properties. This is because in these experiments the proportion of diffusion-mobile hydrogen, which makes the main contribution to the softening, was not determined. Given that the effect of ionic currents under certain modes of ionization of the steam flow has a significant effect on the strength properties of the steel surface layer, we can assume that these modes increase the proportion of hydrogen introduced into its surface in the diffusion-mobile state, in our case H^+ .

In addition, the presence of charged droplets in the steam flow causes a volumetric charge, which generates an electric field of the flow, thereby having an additional effect on the strength properties of the surface layer of the blade

material. An important factor is the polarity of the electric field potential, which depends on the nature and degree of change in the surface energy of the metal.

Summarizing the obtained data, we can conclude that the change in the properties of the working fluid as a functional erosion medium as a result of electrization causes a significant increase (relative to neutral wet steam) in electrochemical processes. This changes the kinetics of the accumulation of damage to the surface layer of the metal due to the joint course of several negative processes: drip-shock action; electrochemical processes due to mechanical and structural-chemical inhomogeneity of the surface; hydrogen absorption; changes in mechanical properties under the action of an electric field. Moreover, the greatest contribution to changes in mechanical properties is made by the absorption of hydrogen. According to preliminary estimates, the complex negative drip shock and electrophysical influence on the metal surface reduces the incubation period and intensifies the erosion-corrosion process by about 2 times.

Indirect confirmation of this conclusion is in the research conducted by Doctor of Technical Sciences O.L. Shubenko and presented in [25].

The basis for the study were experimental data on the development of erosion zones of the last stage of the turbine TK-200 (Poland) in two sections 0.784 and 0.588 length of the working blade of the last stage. Fig. 2.47 shows the kinetic curves obtained by the author of this work by approximating the experimental data of field tests (curves 1 and 2) and calculation by a universal mathematical model of erosion, taking into account all major factors of metal degradation (except electrophysical) from the mechanical action of drops (curves 1' and 2').

As can be seen from Fig. 2.47, curve 1 differs significantly from curve 1', and curve 2 differs from 2' to a lesser extent. These features of the kinetic curves are interpreted as follows. It is known from field experiments on turbines that the degree of electrization of the steam flow and, accordingly, the electrophysical impact on the blade is greatest in the peripheral region. Namely, here the greatest discrepancy between approximating curve 1 and universal curve 2 (almost 2 times) is observed.

In the middle section of the blade, where the electrization of the flow is insignificant, the divergence of curves 2 and 2' is minimal.

The divergence of curves 1 and 1' by almost 2 times in the peripheral part is an additional factor explaining the effect of electrophysical phenomena on the degradation of the blade surface, which was not previously taken into account in the modeling of these processes.

The above ideas define a general approach to solve the problem of reducing the damaging effects of charged droplets on the surface of metal parts: it is necessary to neutralize the ion flux before contact with metal surfaces, or radically reduce droplet moisture in contact with the surfaces of the flowing part.

The main conclusions for section 2.

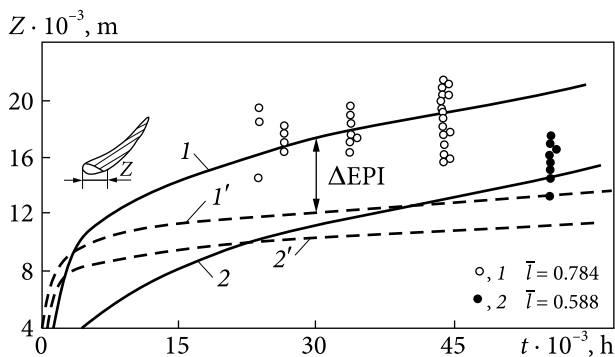


Fig. 2.47. Width of the zone of erosion damages of an entrance edge of a working blade of the turbine of 200 MW: I and 2 — verification with the use of correction factors; I' and $2'$ — theoretical calculation by a universal mathematical model [25]

The solution to this problem allowed obtaining the following important scientific and practical results:

- it has been experimentally identified that when blade steels come into contact with the flow of wet steam, the concentration of hydrogen in the metal increases, regardless of whether the steam is charged or neutral. However, in the case of contact with charged steam, the concentration of sorbed hydrogen is the highest (in the experiments increased by 5—10 times or more);

- it has been identified that the impact of a positively charged flow reduces the strength properties of the surface layer of the blade material by 30—50%;

- the effect of a negatively charged flow has little influence on the strength and may not have a destructive effect and even, as some results have shown, somewhat strengthens the surface;

- it is established that the working fluid as a functional medium, its chemical composition significantly affects the resistance of the surface layer of the blade material to mechanical impact;

- it has been identified that the microhardness of the surface layer of the blade material changes when exposed to an electric field. Depending on the magnitude and sign of the electric potential on the metal surface, the microhardness can increase or decrease up to 12%;

- at the uneven distribution of the charged droplet moisture in a flowing part, and also at its accelerated movement there is a variable electric field with a frequency of 20 kHz. It is established that the influence of a variable electric field in a given frequency range leads to a change in the microhardness of the surface layer of the blade material, and the magnitude of the effect depends on the frequency. The maximum reduction of microhardness in the surface layer up to $2 \mu\text{m}$ thick can reach 35% in the frequency range $f = 2.5\text{—}20$ kHz.

The presented results can be useful for improving the physical modeling and methodology of bench tests for the strength and reliability of blade materials by taking into account previously unknown electrophysical factors identified in the course of this study.

**THERMAL ELECTROPHYSICAL STUDIES
OF THE INFLUENCE OF ARTIFICIAL IONIZATION
ON THE EFFICIENCY OF EXPANSION
OF A WET STEAM FLOW IN A TURBINE**

**3.1. Features of the thermodynamic
process of expansion of the supercooled
steam flow in the turbine**

The process of steam expansion in the flow path of the turbine from the saturation line to the Wilson zone differs notably from the expansion of superheated steam. The expansion of superheated steam is similar to the expansion of an ideal gas since it occurs without any phase transformations. In the region below the saturation line, the expansion process can proceed either without condensation or with condensation. In the case of expansion with condensation, the change in the parameters of the steam differs significantly from the change in the parameters of the ideal gas. Due to the release of the heat of condensation, the decrease in temperature slows down, and part of the steam turns into a liquid state, which leads to a decrease in the mass of the steam component, the isentropic index changes, and, accordingly, the work of expansion.

Real processes of steam expansion in the two-phase region are always of a nonequilibrium nature. Due to the deficit of condensation nuclei, the actual moisture of the steam turns out to be below the diagrammatic one and the steam is to a greater or lesser extent supercooled. It is known that in a Wilson chamber, pure water steam, free of dust and air, can undergo a reversible adiabatic expansion (increase in volume) by 25% before liquid is formed [40]. With this expansion, the temperature of the steam turns out to be lower than the saturation temperature t_s by the value Δt , which is called the supercooling value. Supercooled steam is in a metastable (unstable) state, in which it cannot remain for an arbitrarily long time. After some time, condensation will begin and the steam will enter an equilibrium state. In the flow path of the turbine from

the moment of reaching the saturation state to the entrance to the condenser, steam is no more than $\sim 10^{-2}$ s. This time is not enough for its transition to an equilibrium state without a sufficient concentration of condensation nuclei. In addition, in contrast to the Wilson chamber, the expansion process does not stop in the flow path of the turbine, which makes it impossible for the steam to reach an equilibrium state before entering the condenser. Subcooling 10–15 °C, which can persist even after the last stage of the turbine at both increased and reduced pressure in the condenser [41], is accompanied by a change in the thermodynamic parameters of steam and leads to a decrease in the generated power.

In power heat equipment, phase transitions are preceded by a metastable state of the working fluid. The evaporation of water in steam generators operating at subcritical pressures is preceded by overheating, the magnitude of which can vary from fractions of a degree to tens of degrees. Condensation of steam in the flow path of the turbines is preceded by subcooling, the magnitude of which, as a rule, reaches tens of degrees. Depending on the concentration of condensation nuclei in the steam flow, the transition from the metastable to the equilibrium state can occur gradually or abruptly. As the supercooling increases in the steam flow, a certain amount of moisture is formed, however, the heat released in this case is not enough to heat the steam to the saturation temperature. As a rule, during expansion in the turbine flow path, until spontaneous condensation occurs, the steam moisture remains close to zero [42]. When spontaneous condensation occurs, the steam moisture increases abruptly but never reaches the diagrammatic value. Since the process of expansion of steam in the flow path of the turbine continues until the exit from the last stage, some supercooling persists even after spontaneous condensation. The amount of hypothermia is determined by the dependence

$$\Delta t_M = \frac{(x_M - x_p) \cdot r}{c_{pM}''}$$

where x_M is the actual degree of dryness of the steam; x_p — equilibrium (diagrammatic) degree of steam dryness; c_{pM}'' — average heat capacity of steam in the temperature range $t_s - t_M$, where t_M is the temperature of the supercooled steam.

Since the heat of the phase transition is very high (2300–2400 kJ/kg), even a slight deviation of the actual degree of dryness from the diagrammatic one leads to a noticeable supercooling of the steam.

When designing the expansion process in a turbine stage, steam parameters in the two-phase region are traditionally determined from the equilibrium h , S -diagram without taking into account supercooling and enthalpy changes,

which, strictly speaking, is not permissible. Not taking into account the supercooling of steam in a stage operating in a two-phase region can lead to a large error in determining both the available heat drop and in determining the efficiency of the stage.

When designing the expansion process in the h, S -diagram in the two-phase region of wet steam, it should be mentioned that since the enthalpy of supercooled steam $h_{1\text{sc}}$ is greater than the enthalpy of steam in the equilibrium state $h_{1\text{eql}}$, the available heat drop $H_{0\text{per}}$ of the non-equilibrium process turns out to be less, than the equilibrium process $H_{0\text{is equal}}$.

If the supercooling in the turbine stage reaches 32—35 °C, then the available heat drop, found from the equilibrium h, S -diagram, turns out to be overestimated by 10—12 kJ/kg. With a heat drop of ~ 140 kJ/kg typical for a wet-steam stage, this will amount to 7—8%. In the next stages, where supercooling can reach 10—12 °C, the available heat drop decreases in comparison with the one determined by the equilibrium h, S -diagram by 3.5—4 J/kg, which can be from 2 to 3 % of the heat drop per stage.

At the expansion rates existing in the turbine stages, the supercooling of steam can reach 32—35 °C [42—44]. With such supercooling, the specific volume of steam decreases in comparison with the equilibrium volume by 8—9%, which leads to a corresponding decrease in the volumetric steam flow through the stage and a decrease in the power generated by the stage. When spontaneous condensation occurs, the moisture and temperature of the steam increase abruptly. In contrast to the Wilson chamber, the process of steam expansion in the flow path of the turbine does not stop until it enters the condenser. Therefore, after spontaneous condensation, the state of the steam remains to a greater or lesser extent non-equilibrium.

Until recently, the lack of real methods of controlling the process of volumetric condensation of steam was a constraining factor in the development of this direction. Unfortunately, the attempts made to control the process of steam condensation in the phase transition zone have not yet found industrial application. The use of chemical additives in feed water to create condensation nuclei is costly due to the need for continuous reagent addition. In addition, decomposition products of chemical reagents can negatively affect the reliability of the turbine plant. Charged particles (ions and electrons) can serve as nuclei of condensation. However, too few such charges are generated in the phase transition zone due to natural electrization. It is known [1] that such a charge density in the phase transition zone is 10^{-11} — 10^{-8} C/m³, moreover, the charges are concentrated in a relatively small number of drops of film primary moisture. A charge density sufficient to influence the volumetric condensation process is reached only after the last stage of the turbine, where the steam expansion process has already been completed. The most suitable for practical

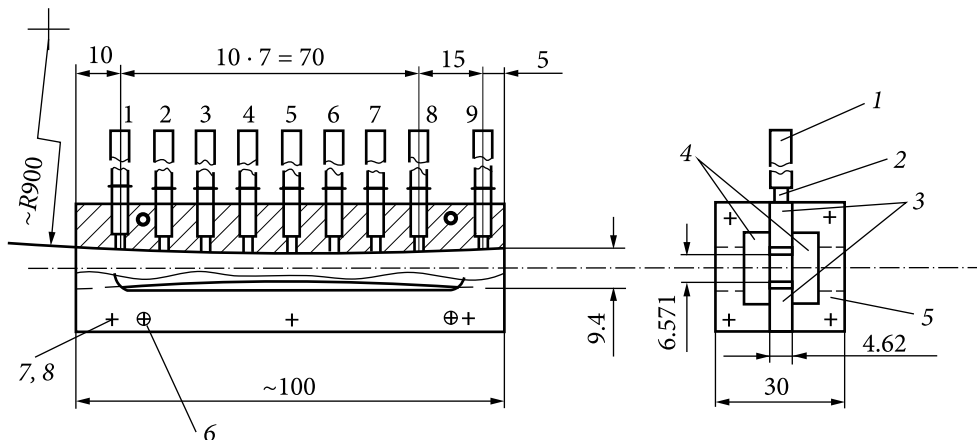


Fig. 3.1. Nozzle: 1 — tube $\varnothing 4$ mm; 2 — tube $\varnothing 3$ mm; 3 — profile plates; 4 — flat plates; 5 — case; 6 — pin; 7 — screw; 8 — nut

use is the method of creating condensation nuclei due to artificial ionization of the steam flow in front of the phase transition zone [45].

3.2. Experimental studies on artificial ionization of steam flow

To carry out experimental studies in this direction, a thermodynamic stand was created at the IPMash NAS of Ukraine, the schematic diagram of which is shown earlier in Fig. 2.29.

Let us remind you that the stand consists of the following independent interconnected systems, which include the constituent elements indicated on the stand diagram: steam, circulation, vacuum, condensate, boiler feed, steam ionization, and measurement system.

One of the main elements of the experimental stand is a flat embarrassing diffuser supersonic nozzle (Fig. 3.1). The nozzle channel is formed by two profile (3) and two flat (4) glass plates. Holes with a diameter of 1.5 mm are made in the upper profile plate of the nozzle for pressure measurement. In Fig. 3.1 the indicated holes are noted by numbers 1, 2, 3 ... 9. They indicate the numbers of the pressure measuring points.

It is known that a decrease in supercooling and prevention of a condensation jump in steam can be achieved due to additional heterogeneous condensation nuclei. In this experiment, a corona-type ionizer was used to create heterogeneous condensation nuclei. The principle of operation of the ionizer is as follows. Steam, flowing through the high-voltage electric discharge zone located between the tip of the electrode needle and the inlet plane of the nozzle, is ionized, and the amount of heterogeneous condensation nuclei (electric

charges) created in this way is controlled by the amount of current passed through the ionizer (see Fig. 2.19).

When carrying out studies to determine the effectiveness of the effect of ionization on the steam expansion process, it was important to know the polarity of the voltage supplied by the electric discharge device.

To assess the influence of the polarity of the voltage applied to the electrode on the flow parameters, a special experiment was carried out. One of the main methodological conditions for experimenting was to carry out all tests at a constant mass flow rate of steam $G_s = \text{const}$.

In the regime with the initial steam temperature equal to the saturation temperature t_s , positive or negative voltages of different magnitudes were applied to the electrode. For each value of the magnitude and polarity of the voltage, measurements were made of the current in the ionizer circuit, as well as the pressures at 7 and 8 points of the supersonic part of the nozzle ($j = 0.7$ and $j = 0.8$), in which the greatest influence of ionization was observed. The pressures at the same points were also measured without applying a voltage to the electrode. Fig. 3.2 shows the dependences of the change in pressure Δp at the indicated points on the current in the ionizer circuit at different voltage polarities.

Comparison of the change in pressures Δp_7 and Δp_8 at points 7 and 8 of the supersonic part of the nozzle at the same current values showed that the effect of ionization at a negative voltage is 1.4—1.5 times greater than at a positive one. On this basis, subsequent tests, in which the corona ionizer was used, were carried out with negative charges, including the experiment presented below. During the experiment to determine the effect of ionization on the efficiency of the expansion process, a corona electric discharge device was used in compliance with the following main characteristics of the nozzle and steam parameters:

- steam consumption through the nozzle $G_0 = 0.00115 \text{ kg/s}$;
- the area of the outlet section of the nozzle $F = 1.418 \cdot 10^{-5} \text{ m}^2$;
- steam pressure in front of the nozzle $p_0 = 59 \text{ kPa}$;
- pressure in the zone of sudden expansion $p_k = 5.99 \text{ kPa}$;
- the heat of steamization in the zone of sudden expansion $\chi = 2415.3 \text{ kJ/kg}$;
- the specific current of the corona discharge in the experiment is $J = 3.2 \cdot 10^{-3} \text{ A/(kg/s)}$.

Studies of the steam expansion process in an axisymmetric nozzle have shown that the nature of the pressure changes significantly in the process of steam ionization. In this case, charged particles are formed from neutral steam molecules under the action of an electric discharge device.

The change in the relative value of the steam pressure along the nozzle is shown in Fig. 3.3.

As the neutral steam expands behind the nozzle throat, a decrease in the pressure gradient is observed, which is caused by spontaneous condensation. When

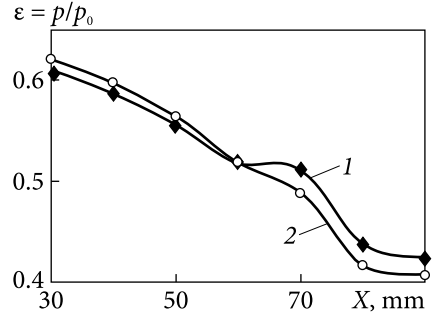
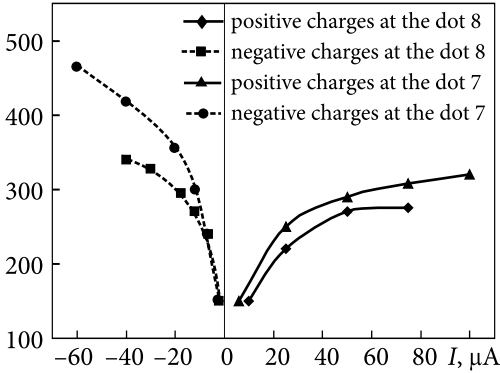


Fig. 3.2. Dependences of the pressure change at points 7 and 8 of the nozzle flow path on the current in the corona ionizer circuit

Fig. 3.3. Distribution of relative pressure along the length of an axisymmetric nozzle: 1 — neutral steam; 2 — charged steam

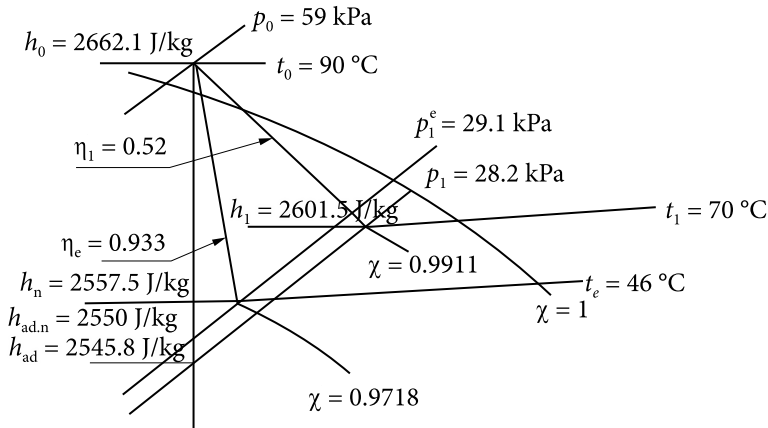


Fig. 3.4. Steam expansion process in h, S -diagram (the subscript «e» denotes the process during steam ionization)

the ionized steam expands, the pressure decreases uniformly along the entire length of the nozzle (Fig. 3.3, curve 2) and the process approaches equilibrium.

When the steam flow is ionized, the degree of steam dryness at the nozzle exit decreases from 0.991 to 0.9718, and the enthalpy decreases from 2601.5 to 2557.5 kJ/kg (Fig. 3.4). As a result, the amount of phase transition heat used in the nozzle increases by 44 kJ/kg, which increases the efficiency of the expansion process from 0.52 to 0.933. The maximum moisture of neutral steam at the outlet from the nozzle does not exceed 1.5% (with adiabatic — 3.5%). In ionized steam, the moisture can reach 3.4%, which is very close to adiabatic, i.e. the process is approaching equilibrium. The positive effect is achieved due to the

action of the ionizer, which forms in the volume of steam numerous hydrated ions (additional nuclei of heterogeneous condensation), which are a complex of an ion and associated electrostatic forces of water molecules. They are «frozen in» into the steam flow and, getting into the volume of saturated and supersaturated steam, intensify the condensation process, thereby reducing the level of supercooling of the process.

It should be noted that such a process and an increase in efficiency correspond only to this nozzle. Nevertheless, it can be argued that due to the more complete use of the heat of condensation during the ionization of steam, the tendency to increase efficiency should remain for any process of steam expansion, including in real turbines.

3.3. Determination of a rational zone of thermodynamic parameters for artificial ionization of a wet steam flow

For the practical implementation of this approach, it is very important to determine the thermo-gas-dynamic parameters of steam at which hydrated ions are stable (tenacious) and do not collapse both in the zone of temperatures of slight overheating (the zone before the phase transition) and in the zone of low pressure, i.e. it is necessary to determine the boundaries of the thermodynamic parameters of steam expansion at which the ionization process will be effective.

It is especially important to know the maximum values of steam pressures and temperatures at which the action of the ionizer initiates and intensifies the beginning of the steam condensation process.

These values can be identified through numerous experiments on the bench, which makes it possible to determine the efficiency of the steam expansion process with and without ionization. However, in addition to the difficulties of this approach, it should be noted that determining the steam parameters corresponding to the beginning of condensation is quite difficult too. The change in pressure and temperature in the nozzle, the values of which are fixed in the experiment, in this case ambiguously determine the point of condensation beginning, since the process is influenced by such factors as losses arising in the nozzle and at its exit, which are difficult to take into account when carrying out experiments. In addition, the result is affected by the measurement accuracy.

Therefore, another quite simple and original approach to solve this problem was proposed using both a barrier ionizer (BI) and a corona discharge (CD).

For these purposes, optical probes were used, which perceive in the visible part of the light spectrum changes in the optical density of the steam flow depending on the moisture according to the values of the output current of the

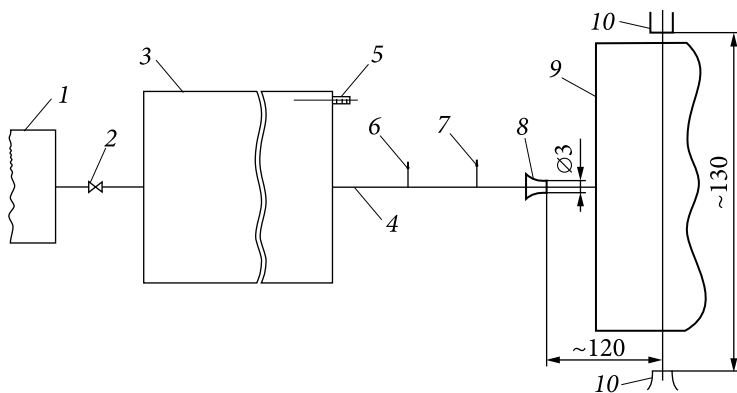


Fig. 3.5. Scheme of the working section of the steam stand with a barrier ionizer and optical probe: 1 — steam inlet chamber; 2 — valve; 3 — barrier ionizer; 4 — steam line; 5 — outlets of the BI heater winding; 6 — pressure sensor; 7 — thermocouple; 8 — nozzle; 9 — outlet pipe; 10 — optical probe

probe. The value of the difference between the values of the current of the optical probe in the neutral and the charged flux in these experiments was used to estimate the ionization efficiency. The greater the difference in the values of the indicated currents (the greater the fog density), the higher the ionization efficiency.

For these studies, a thermodynamic steam test bench was taken as a basis (Fig. 2.29). The diagram of the modernized section of the stand with the BI and the optical probe is shown in Fig. 3.5.

A similar modernization of the stand was also carried out for the corona discharge device. At this stage of the research, it was planned to evaluate the boundary parameters of temperatures and pressures at which ionization is effective, as well as to determine and compare the performance of the barrier and corona electric dischargers.

During the experiments in all operating modes of the stand, the values of the current of the optical probe of the neutral and charged steam flows were recorded at different values of the initial temperature of the steam in front of the nozzle.

For performance tests, a number of pressure values were adopted, typical for a number of wet-steam stages of the LPC turbines, p_0 : 112.8; 127.5; 142.2; 156.9; 176.5 kPa. At the highest value of p_0 , a near-critical pressure drop across the subsonic nozzle was ensured, as well as reliable operation of the stand elements. The values of the initial temperatures and the ranges of their change were determined during the experiments.

In Fig. 3.6—3.8 as an example, the study results obtained in some operating modes of the stand are given.

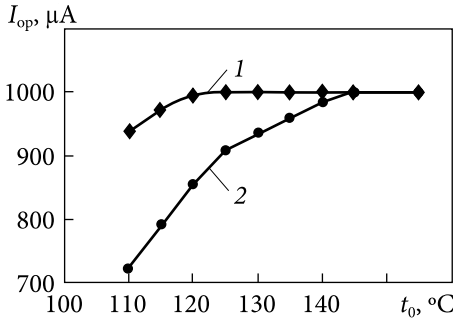


Fig. 3.6. Dependences of the optical probe current in the visible part of the light spectrum in a neutral and charged BI flow of steam on its initial temperature at an initial pressure of 112.8 kPa: 1 — neutral steam; 2 — charged steam

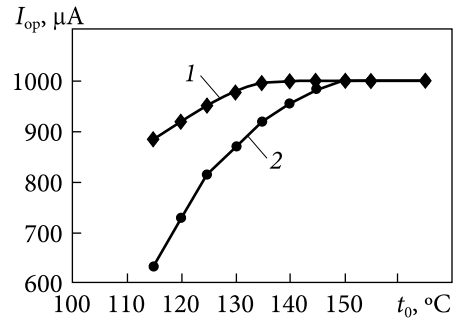
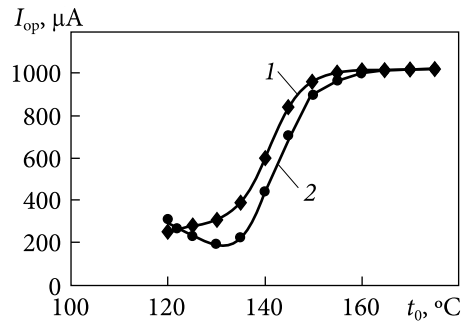


Fig. 3.7. Dependences of the optical probe current in the visible part of the light spectrum in a neutral and charged BI flow of steam on its initial temperature at an initial pressure of 142.2 kPa: 1 — neutral steam; 2 — charged steam

Fig. 3.8. Dependences of the optical probe current in the visible part of the light spectrum in a neutral and charged BI flow of steam on its initial temperature at an initial pressure of 176.5 kPa: 1 — neutral steam; 2 — charged steam



As seen from Fig. 3.6—3.8, for each value of the initial pressure p_0 there is a range of initial temperatures in which the effect of ionization on the state of the steam flow behind the nozzle is observed. This is evidenced by the change in the probe current in the visible part of the light spectrum in the flow of non-ionized (neutral) and ionized (charged) steam at the same initial temperature. As the initial temperature t_0 rises, the ionization efficiency decreases. This is explained as follows.

In a charged steam flow, as mentioned above, hydrated ions arise, which, when the steam expands and its temperature decreases to the saturation temperature or close to it, are additional centers of condensation. The higher the concentration of such ions, the more steam condenses and the greater the moisture density due to the greater amount of moisture in the flow. Therefore, its transparency decreases, and the probe current decreases. With an increase in the initial steam temperature t_0 , i.e. with an increase in steam superheat, the kinetic energy of water steam molecules increases, the number of steam mole-

cules deposited on charged particles decreases, and the mass of hydrated ions and their number also decreases. In this case, the amount of condensed steam decreases, and the transparency of the flow increases. Consequently, the difference between the values of the optical probe current in the neutral and charged flux decreases. With a further increase in the initial steam temperature, the kinetic energy of water steam molecules becomes so large that they are not retained on charged particles in the zone of the barrier or corona discharge of the ionizer. In this case, hydrated ions are simply not formed and condensation nuclei are absent. Therefore, it is inappropriate to speak about the «survivability» of hydrated ions in this case. In this case, steam condensation does not occur. The transparency of the flow does not change; therefore, the current of the neutral steam probe, which has the greatest value, is equal to the current of the charged steam probe. The higher the initial pressures, the higher the initial temperature t_0 , and the equality of the probe current of neutral and charged steam occurs, i.e. $I_{oz}^n = I_{oz}^z$. So, for example, in the mode with $p_0 = 112.8$ kPa, the equality of the probe current of the neutral and charged steam occurs at $t_0 \approx 145$ °C, and in the mode with $p_0 = 176.5$ kPa – at $t_0 \approx 160$ °C (see Fig. 6 and 8). Thus, in the investigated range of initial pressures in front of the nozzle $p_0 112.8 \div 176.9$ kPa, the maximum values of the initial temperatures t_{0max} , at which the effect of steam ionization by the barrier ionizer is no longer observed, are in the range of $\approx 150 \div 160$ °C.

The results of the study of the influence of ionization of the BI steam on the parameters of the steam flow made it possible to determine the maximum values of the initial temperatures t_{0max} in all studied modes, in which the influence of ionization is no longer observed, and the current of the optical probe of the neutral steam is equal to the current of the charged steam (Fig. 3.6—3.8). Naturally, the use of steam ionization at temperatures equal to or greater than t_{0max} does not make sense.

In this case, with increasing pressure p_0 in front of the nozzle, t_{0max} increases, and the ionization efficiency decreases. The same will be observed with a decrease in the temperature of the expanding steam in the flow path of the wet steam stages of the turbine.

As a result of the research, lines of equal level were obtained (Fig. 3.9), which reflect the degree of efficiency of steam ionization with a change in pressure and temperature, and their boundary values were determined.

It follows from what has been said before that, in the investigated range of initial pressures, the effect of vapor ionization is most effective at a temperature close to the saturation temperature and its effect is practically absent when t_0 increases to t_{0max} .

Similar studies, with the same regime parameters of the steam as the experiments with BI, were carried out with a corona ionizer (CI). Based on the test

Fig. 3.9. Steam ionization efficiency depending on changes in pressure and temperature: 1 — $\Delta I_{oz} = 50 \mu\text{A}$; 2 — $\Delta I_{oz} = 100 \mu\text{A}$; 3 — $\Delta I_{oz} = 150 \mu\text{A}$; 4 — $\Delta I_{oz} = 200 \mu\text{A}$; 5 — $\Delta I_{oz} = 250 \mu\text{A}$

results for all modes, the dependences of the optical probe current in the visible part of the light spectrum in a neutral and charged KI steam flow on its initial temperature at the selected pressure were obtained.

The upper limits of the maximum temperature and steam pressure for experiments with IC at the same steam parameters at the nozzle inlet as in experiments with BI were found.

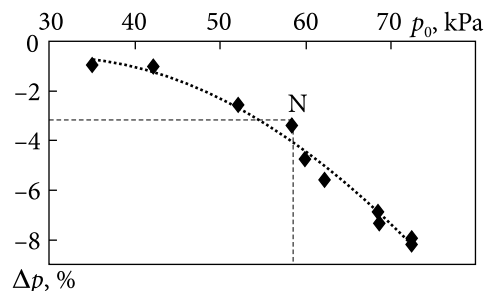
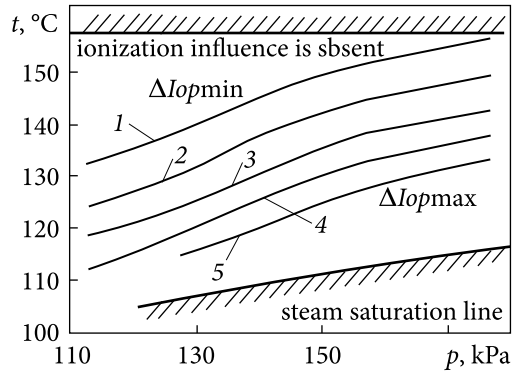
To determine the lower limit of the effect of steam ionization on the flow parameters in the flow path of the nozzle, it was sufficient to use the previously obtained results of studies carried out on the above stand, which were carried out at various minimum possible values of the initial pressure in front of the nozzle. The ionization efficiency was determined in these experiments by the magnitude of the decrease in the relative pressure in the nozzle outlet. In this case, the initial temperature of the steam was chosen so that the superheating of the steam was maintained for all the accepted values of the pressure in front of the nozzle in the range of 30–72 kPa. The research results are shown in Fig. 3.10 in the form of the dependence of the relative change in pressure on the steam pressure in front of the nozzle during ionization. At a maximum pressure of $p_0 = 72 \text{ kPa}$, the change in Δp is 8–8.2%, and at a pressure of $p_0 = 30 \text{ kPa}$, the effect of ionization is practically absent.

The result of the previously presented experiment at $p_0 = 59 \text{ kPa}$ (Fig. 3.2) is also plotted in Fig. 3.10 and is in the zone of effective steam ionization (point N).

Thus, when the turbine stages operate in wet steam, where the steam density is low (pressure $p_0 \leq 30 \text{ kPa}$), the use of an ionizer to reduce losses from supercooling of steam may be ineffective.

The studies carried out made it possible to determine the area of the most effective steam ionization in the

Fig. 3.10. Relative pressure change at the nozzle outlet on the initial pressure during ionization



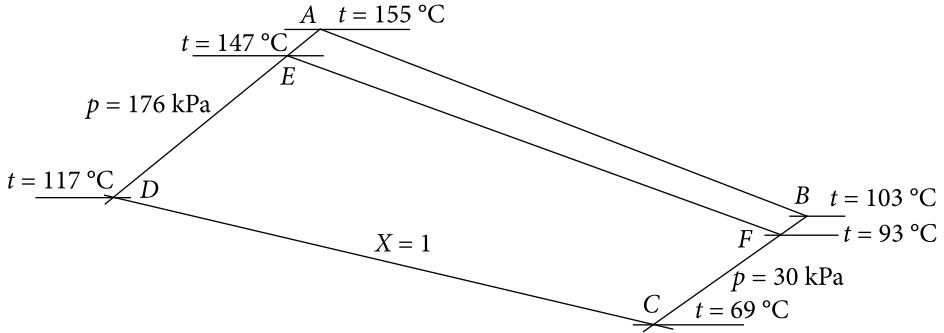


Fig. 3.11. The area in the h, S -diagram of water steam, including the parameters at which steam ionization is most effective: $ABCD$ — during BI ionization; $EFCF$ — with ionization CI

h, S -diagram (Fig. 3.11), which is especially important for the practical implementation of this method.

As a result of the studies carried out, it was shown that ionization of steam based on BI and CI is effective in the zone of the found rational flow parameters.

It was found that if ionization occurs in the field of a barrier discharge, a quasi-neutral wet steam is formed. This and previous experiments give grounds to believe that such a discharge will not have a significant effect on electro-corrosive processes in the flow path. At the same time, the effectiveness of influencing the parameters of the flow of wet steam often exceeds the indicators obtained with a corona discharge.

However, the practical application of such a discharge device is accompanied by great difficulties, and therefore the author prefers the corona ionizer since it is easy to manufacture and practical to operate. In addition, as shown by special studies presented in Section 2, with a negative polarity of the flow, ionization practically does not have a significant effect on the deterioration of the surface strength of the metal, which means that such a (corona) current ionizer is effective both in terms of efficiency and reliability.

3.4. Determination of the dispersion of an artificially ionized flow

For the practical implementation of the considered approach, it is no less important to have information about the flow dispersion resulting from steam ionization, since it is known that the presence of large droplets in the flow leads to a decrease in the efficiency and reliability indicators.

In more detail, we will be focused on determining the dispersion of the flow.

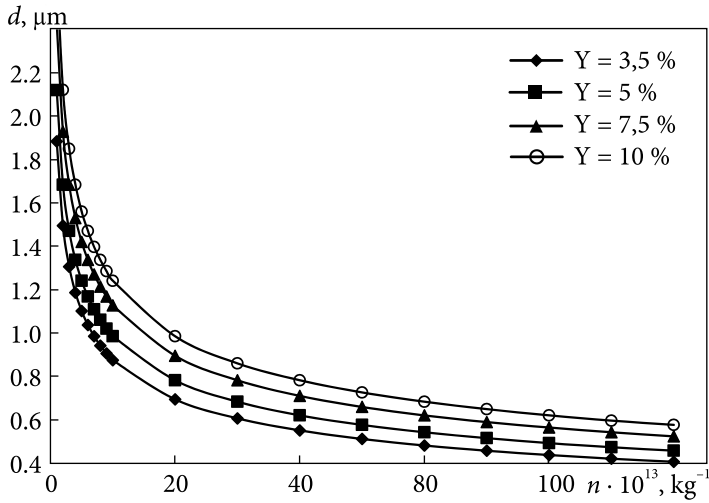


Fig. 3.12. Changing the diameter of droplets in a wet steam flow

It is known that the sizes of the drops formed during condensation depend on the concentration of nuclei and diagrammatic moisture at the end of the expansion process

$$r_k = \sqrt[3]{\frac{3G \cdot Y}{4\pi \cdot n \cdot \rho}},$$

where r_k is the radius of the drops, m; G — steam consumption through the channel, kg/s; Y — diagrammatic steam moisture; n is the number of drops formed in the steam flow per second, 1/s; ρ is the steam density, kg/m³.

Since each nucleus can contain no more than one elementary charge [46], the number of drops at the end of the expansion process is equal to the number of condensation nuclei and can be determined by the magnitude of the electric current carried by the steam flow,

$$n_e = \frac{I}{e},$$

where n_e is the number of condensation nuclei carried by the steam flow, s⁻¹; I is the current carried by the steam flow, A; e — elementary electric charge ($1.6 \cdot 10^{-19}$ C).

By changing the concentration of condensation nuclei in front of the phase transition zone due to a change in the current value, it is possible to change the droplet size at the end of the expansion process. Fig 3.12 shows the dependence of the droplet diameter at the end of the expansion process

on the concentration of condensation nuclei achieved by ionization and on the degree of steam moisture.

Concerning the conditions of our experiment (Fig. 3.4), for example, when a corona discharge was used to create condensation nuclei in a steam flow, at a moisture of 3.5% and a concentration of condensation nuclei (charges) of $10^{14} - 10^{15} \text{ kg}^{-1}$, necessary for an equilibrium expansion [47], the droplet size is $\sim 0.4-0.8$ microns (Fig. 3.12). The value of the corona discharge current $I_{\text{c.d.}}$ to provide the desired concentration of condensation nuclei depends on the flow rate of steam flowing through the corona discharge field G and the specific corona discharge current J .

$$I_{\text{c.d.}} = J \cdot G,$$

where

$$J = \frac{(n_e \cdot e)}{G}.$$

Since some of the charged particles arising in the corona discharge zone settle on grounded surfaces, when determining the required value of the corona discharge current, one should take into account the utilization factor of the corona discharge $\eta_{\text{c.d.}}$.

$$I_0 = \frac{(J \cdot G)}{\zeta_{\text{c.d.}}}, \quad \eta_{\text{c.d.}} = \frac{I_s}{I_{\text{c.d.}}},$$

where I_s is the value of the current carried by the steam flow.

The results of laboratory studies have shown that the efficiency of using the corona discharge current can be $\eta_{\text{c.d.}} \geq 0.01$. With this value of $\eta_{\text{c.d.}}$ the specific current of the corona discharge should be $\sim 3.2 \cdot 10^{-3} \text{ A}/(\text{kg}/\text{s})$, which coincides with the value of the specific current, which was used in our experiment (Fig. 3.4).

Thus, during the ionization of steam with a specific current providing a charge concentration of $10^{14} - 10^{15} \text{ kg}^{-1}$ for conditions close to the equilibrium state, the droplet size should not exceed 1 micron.

It is important to note that the energy consumption for steam ionization, as shown by numerous experiments, is 0.03—0.15% of the energy released during condensation on ions.

The obtained theoretical results of the formation of finely dispersed moisture when exposed to a flow by a corona discharge were also confirmed in the process of specially carried out field tests.

In these experiments, an optical probe developed at MPEI-CKTI (Fig. 3.13 *a*) was used to measure the moisture content and droplet size, with the help of

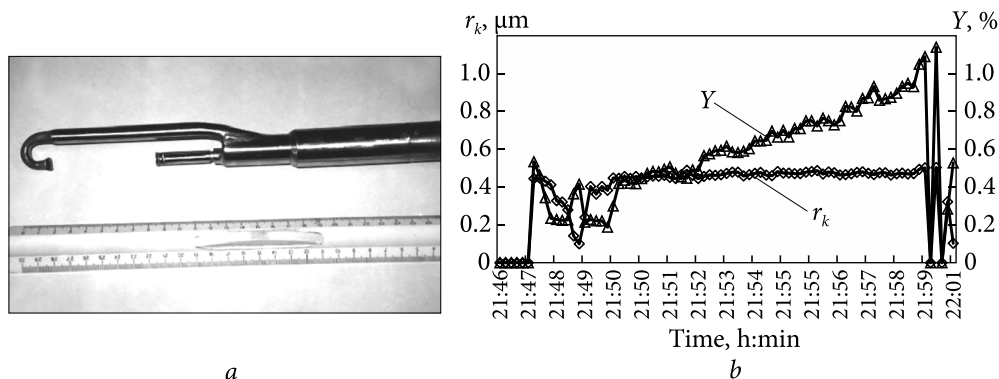


Fig. 3.13. Traversing the flow downstream of the last stage with an optical probe: *a* — optical probe for measuring moisture and droplet size «MPEI-CKTI»; *b* — change in dispersity and moisture on time-based approach depending on changes in the charge of the flow

which the corresponding measurements of the flow dispersion were made directly in the turbine operation mode, using a specialized vacuum chamber. Changes in the dispersion and moisture content of the flow with time under the influence of a corona discharge are shown in Fig. 3.13 *b*. The zone of switching on the corona electrodes from 21 h 46 min to 22 h 00 min.

From Fig. 3.13 *b*, it can be seen that artificial ionization initially leads to an increase in moisture and droplet size (up to a certain limit $d = 0.8 \mu\text{m}$), with the subsequent stabilization of the dispersion. A further increase in moisture occurs due to an increase in the number of condensation centers with a fixed droplet size.

3.5. «Vitality» of condensation nuclei formed during steam ionization

It is not always possible to place a device for ionizing a steam flow directly in the phase transition zone and has to be installed at some distance from this zone. In this case, it is necessary to know how «tenacious» the nuclei of condensation are. To answer this question, special studies have been carried out. A barrier discharge was used to ionize the steam (see Fig. 3.14).

From the steam boiler 1, dry saturated or superheated steam was supplied to the barrier discharge chamber 2, then through the steam line 3 to the nozzle 4, and then the free stream 5 was diverted through the pipe 6 outside the laboratory window. When a stream of steam escapes into the atmosphere, its temperature rapidly decreases, reaching the saturation temperature. An insignificant part of the steam condenses on the solid particles and ions contained in the air, as a result of which a transparent, barely perceptible fog is formed

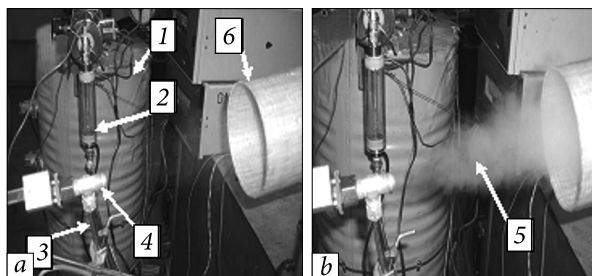


Fig. 3.14. Outflow of a stream of water steam into the atmosphere: 1 — steam boiler; 2 — barrier discharge chamber; 3 — steam line; 4 — nozzle; 5 — steam stream; 6 — pipe for removing steam; *a* — outflow of neutral steam; *b* — the outflow of ionized steam

(Fig. 3.14 *a*). When steam is ionized (Fig. 3.14 *b*), a dense fog is formed. In this experiment, a copper tube with an inner diameter of 8 mm and a length of 1 to 2 meters was used as a steam line. Even though the steam line was grounded, the nuclei of condensation in the steam flow persisted not only when dry saturated steam was supplied from the boiler, but even steam superheated by several degrees. Under the action of a barrier discharge, positive and negative hydrated ions with almost the same concentration are formed in the steam volume, i.e. the steam flow remains quasi-neutral. Since the mobility of hydrated ions is much less than molecules, they are «frozen in» in the steam flow and, as its temperature decreases, increase in size due to condensation. The formed hydrated ions are very stable and are not destroyed even with some overheating of the steam. When the steam temperature drops below the saturation line, steam begins to condense on them.

Thus, as a result of the experiment, it was found that the ionization of steam can be carried out at a certain distance from the condensation zone, which allows the electric discharger of the steam flow to be placed outside the flow path of the turbine. In this case, it is recommended to use a barrier discharge.

3.6. Evaluation of the effectiveness of artificial ionization of the steam flow in the LPC

To begin with, let's consider the known method of dosing chemical additives such as octadecylamine (ODA) in feed water, which allows, by reducing the surface tension of the liquid phase, to intensify the crushing of drops. In this case, initially on ODA molecules, heterogeneous condensation develops, and then the effect of active fragmentation of droplets into additional centers occurs, which integrally, due to the intensification of condensation, gives the effect of reducing hypothermia. Full-scale tests with the use of ODA were carried out on turbines with a capacity of 12 MW, TPP «Georgiy Dimitrov» and KA-70-30 in Reinsberg. A short-term increase in efficiency of more than 2% was found [48]. However, this technology has not

become widespread, since it turned out to be expensive due to the need for continuous use of the reagent. In addition, with long-term use of ODA, the reagent products have a negative effect on the reliability and efficiency of the turbine: there is a hydrophobization of the heat exchange surfaces of the entire boiler-turbine path, which reduces the intensity of heat exchange; impulse tubes of control and protection devices are clogged; when cleaning surfaces, hidden fistulas appear, etc.

We are proposed, an equivalent approach, where ionized steam rather than chemical additives are used to intensify the condensation process. In this case, in contrast to ODA, the activation of the process of heterogeneous condensation occurs on ions and the fragmentation of large droplets in the flow into small ones — under the action of an electric field. Considering that positive effects during steam ionization, such as a decrease in losses from hypothermia, droplet size, etc., are comparable to the use of ODA, and in some cases even exceed these indicators, then when using ionization, the same can be expected (at least 2%) increasing the efficiency of the turbine unit.

3.7. Field studies of the efficiency of ionization of supercooled steam

Based on the results presented above, it can be argued that an artificial increase in the charge density in the flow path of the turbine could reduce the amount of supercooling of the steam and increase the efficiency of the wet-steam stages. Unfortunately, it was not possible to carry out direct full-scale tests on steam ionization directly in the flow path of the turbine. However, to answer the question a full-scale experiment described below was carried out.

In the course of the experiment, the temperature distribution in the steam flow downstream of the last stage of the T-250 / 300-240 turbine (TPP-5, Kharkiv) and the effect of the space charge on the steam temperature were investigated. A universal probe was used to measure charges, temperature, and total and static pressure of the steam flow (Fig 3.15).

To control the flow charge, a space charge neutralizer was used, installed on high-voltage insulators along the entire perimeter of the diffuser at a distance of 500 mm from the outlet edges of the rotor blades (Fig 3.16).

The design of the neutralizer (see details in Section 5.2) allows it to be used not only for neutralizing the space charge in passive (neutralizer is grounded) and active (high voltage is applied to the neutralizer) modes but also in controlling the charge formation process on the working blades of the last stage turbines due to changes in the electric field strength directly behind the impeller.

During the research, it was found that in the flow zone with coordinates $X = 500$ mm, where the flow rate for this mode did not affect the thermocouple

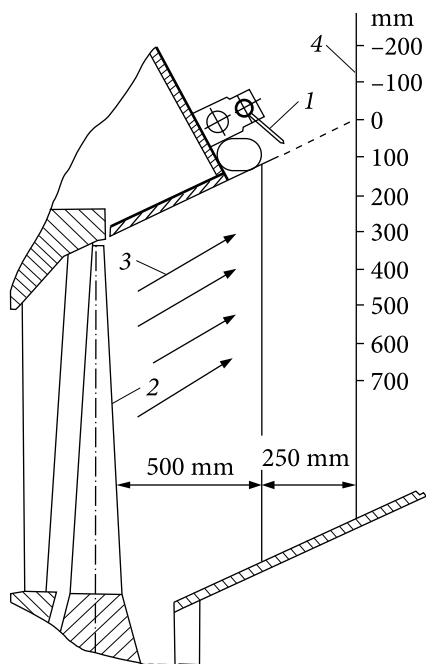


Fig. 3.15. Combined probe

= 300 mm, and the temperature distribution on the probe surface was measured. Then the neutralizer was grounded and the measurements were repeated.

Grounding the neutralizer led to an increase in temperature behind the last stage along the entire perimeter of the probe surface. At the same time, the temperature at the frontal point increased from 42 to 42.6 °C, i.e. by 0.6 °C. This is because the neutralizer grounding causes a natural intensification of the formation of charges on the impeller and the charge density between the blades and insulators increases.

readings since it was close to zero, the steam temperature remained practically constant and it was below the saturation temperature by the entire surface of the probe at 5–8 °C. This indicates the presence of supercooling of the steam flow.

If there is indeed steam supercooling at the turbine exhaust, then by changing the concentration of condensation nuclei in the steam flow, the supercooling value can be changed. Since charged droplets or particles can serve as condensation nuclei, changing the density of charges in the steam flow can affect the volumetric condensation process, and hence the amount of supercooling and the static temperature of the steam.

To determine the effect of the space charge on the flow temperature at a steady-state turbine operation, the thermal probe was installed in the coordinates $X = 0$; $X =$

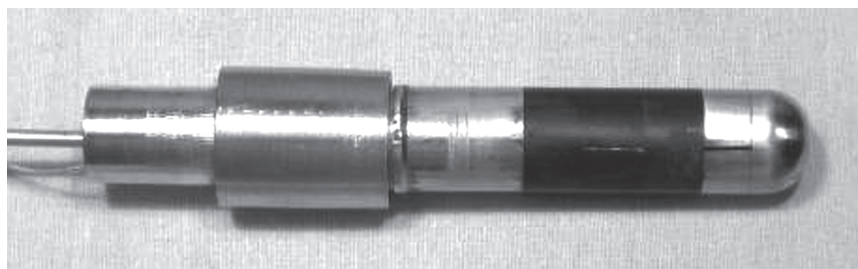


Fig. 3.16. The layout of the neutralizer and probe behind the last stage of the T-250/300-240 turbine: 1 — space charge neutralizer; 2 — working blade of the last stage; 3 — direction of steam flow; 4 — axis of the probe

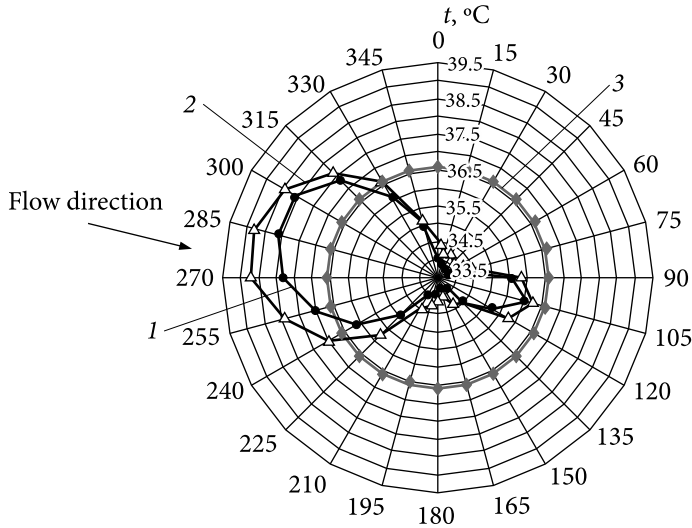


Fig. 3.17. Temperature distribution on the probe surface in the $X = 300$ mm coordinate: 1 — initial mode; 2 — voltage across the neutralizer (-4.6 kV); 3 — saturation temperature in the condenser

The same picture is observed when the neutralizer is turned on in active mode (Fig 3.17). When a voltage of -4.6 kV is applied to the neutralizer, the temperature rises along the entire perimeter of the probe.

Fig 3.17 shows that when voltage was applied to the neutralizer, the temperature increased from 38 to 39 °C, i.e. by ~ 1 °C. In this case, the intensification of condensation and an increase in temperature were caused by the active forced ionization of steam by charges flowing from the neutralizer.

Thus, the conducted full-scale experiment shows the possibility, by increasing the charge density, to reduce the value of steam supercooling, which means that it justifies the prospects of this approach for increasing the efficiency of a turbine plant.

Conclusions

- the developed approach allows: to intensify of the process of steam condensation in the form of fine moisture (the droplet size does not exceed 0.4 — 1 microns); to reduce film condensation and the concentration of coarse moisture; to reduce the level of hypothermia and condensation unsteadiness in the flow path;

- various options for the use of discharge devices in a turbine were considered and presented and it was found that the most preferable in terms of production and operational parameters is a corona electric spark gap that repro-

duces negative charges, a barrier source is more difficult to manufacture but can be effectively used if installed outside the turbine housing;

- the range of parameters at which steam ionization is most effective is determined, which is especially important for the practical implementation of this method;

- the concentration of condensation nuclei, at which the steam expansion process tends to equilibrium, is $10^{14} - 10^{15} \text{ kg}^{-1}$, and the energy consumption for ionization is 0.03—0.015% of the energy released during condensation on ions.

A set of scientific studies has shown that steam ionization can be used to increase the efficiency of turbine stages operating in a two-phase region. Preliminary estimates based on the analysis and comparison with methods similar in purpose (for example, using chemical additives) showed the possibility of increasing the efficiency of a turbine plant by 1.5—2%.

INFLUENCE OF WATER-CHEMICAL REGIME (WCR) ON ELECTRIZATION OF WET STEAM FLOW WITHIN CHANGING PH, INDICATORS OF RELIABILITY AND ECONOMIC EFFICIENCY OF THE TURBO UNIT

4.1. Influence of water chemistry on electrization of the steam flow

The main task of the chemistry of each TPP and CHP is to ensure the operation of heat-power equipment without damage and decrease in efficiency, which can be caused by the following reasons:

- formation of sedimentations on the heating surface of boilers, in the flow path of the turbine, in the condenser;
- formation of sludge accumulation in the boiler water, feed water path;
- corrosion of the internal surfaces of heat and power equipment.

Normalized indicators for sodium, silicic acid, electrical conductivity, total hardness, iron, and copper content are currently the main requirements for the formation of water chemistry for TPP and CHP, the implementation of which ensures the minimization of the above negative consequences.

The determination of the fact of presence in the flow of various densities charges (from 10^{-11} to 10^{-3} C/m³) in the flow path and behind the last stage and the significant influence of this phenomenon on the erosion-corrosion processes of degradation of blades of low-pressure pump turbines served as the basis for study the relationship between electro physical phenomenon and various WCR, their influence on the indicators of reliability and efficiency. Such studies introduce the need for additional standardization of the water chemistry parameters that affect the charge formation of wet steam.

One of the main parameters of water chemistry is pH, therefore, in this study, the task was to determine the effect of

pH on the performance and reliability of the turbine. The study of the electrization of the wet steam flow and the dependence of these processes on the chemical composition of the working medium was started by the author in the 80s of the last century, and in 1992 the natural experiments were carried out directly at CHP (Eskhar) [1]. During these studies, the first attempt was made to determine the change in turbine efficiency depending on various pH values (8.2—9.5). However, it was not possible to determine any influence of pH on the efficiency of the turbine in these experiments but for the first time important results on the electrization of the flow were obtained during the experiment in natural conditions. The technical literature contains very scanty information on works in this direction. So, for example, in [8], which was discussed in Section 1, it was suggested that the electrization of the flow, which depends on the parameters and properties of the steam medium, has an insignificant effect on reducing the efficiency of the turbine plant and requires additional research in this direction. Deserves attention to the work [49], in which the author investigated the processes of electrization of pure steam with the addition of ammonia on an experimental stand. Despite the inconsistency and ambiguity of the results obtained in real conditions, he determined the fact of some influence of ammonia on the rate of charge formation: the addition of ammonia led to a decrease in the intensity of charges in a flow with negative polarity. Unfortunately, the work did not establish any regularity in the process of charge formation from different pH values. At the same time, the authors do not propose any explanations for these phenomena based on the results obtained. There is also no information in the literature on field studies in this direction. All of the mentioned above require a more thorough and concrete analysis of these issues.

Comprehensive studies were carried out in this direction in IPMash NAS of Ukraine, including experimental ones described earlier in Sec. 1 on the electrization, of the air-droplet flow depending on the pH in the range from 8.0 to 9.6, where it was found that increasing pH from 8.0 to 9.0 the electrization current gradually decreased to zero and with further increasing pH to 9.2, the current reversed its polarity and then increased. In our opinion, the mechanism for the formation of charges on water droplets in air and steam flows remains practically the same. This allows us to assume a similar pattern of the considered phenomena in airborne droplets and steam flows. A clear confirmation of this conclusion is the results of studies carried out on full-scale objects. To clarify the possibility of controlling the charge formation process in the flow path of a steam turbine by changing the pH value of the feed water, special studies were carried out at an 800 MW turbine at the Navajo station (Arizona, USA). The experiment was carried out in collaboration with Sonoma Research Company on behalf of the US EPRI.

During the experiment, to obtain the required pH value of the feed water, the required amount of ammonia was added to the feed water. To determine the volumetric density of charges in the steam flow of the turbine, an electric probe similar to that described in Sec. 1.2. The research results are shown in Fig 4.1.

It can be seen that an increase in pH from 8.2 to 8.8 units causes a decrease in the probe current to zero, and with a further increase in pH to 9.2, the probe current reverses its polarity and sharply increases.

The pH of the condensate formed in the flow part of the turbine has not been measured, but [50] shows that the pH of the condensed moisture moves downward, i.e., into the acidic region. Based on the results of the experiments, it can be concluded that by changing the pH of the feed water, it is possible to control the process of charge formation in the turbine's wet steam flow.

Thus, under natural conditions, the determining influence of pH on the electrization of the steam flow has been convincingly shown.

If in the previous experiment, the process of charge formation in a zone of already sufficiently high moisture was considered, then at the second stage of research it was no less important to study the process of formation and accumulation of charges in the steam flow at the beginning of the phase transition zone and the effect of different water-chemical regimes on the value of the generated charges. The studies were carried out jointly with the MPEI staff at the ET-12 stand at the MPEI. Stand ET-12 is a specially equipped turbine with 750 kW [19]. Determination of the bulk density of charges in a wet-steam flow was carried out under various water-chemical regimes, including ammonia (AWR): pH = 9.3, $C(O_2) < 10 \mu\text{g/kg}$; neutral (NWR): pH = 8.2, $C(O_2) < 10 \mu\text{g/kg}$; oxygen (OWR): pH = 8.2, $C(O_2) = 150\text{--}450 \mu\text{g/kg}$.

During the experiments, the dispersion of the droplets and the degree of steam moisture behind the last stage of the turbine were constantly monitored by an optical probe.

At the regimes with steam moisture of 0.1, 1.0, and 1.7%, steam humidification occurred naturally — due to the triggering of a heat drop in a two-row speed stage, while the proportion of the formed secondary (coarse) moisture is small, less than one percent. Modes with moisture $Y_0 = 3.0$ and 4.0 % were achieved due to the operation of the upstream stage and additional injection of feed water into the receiver located in front of the turbine.

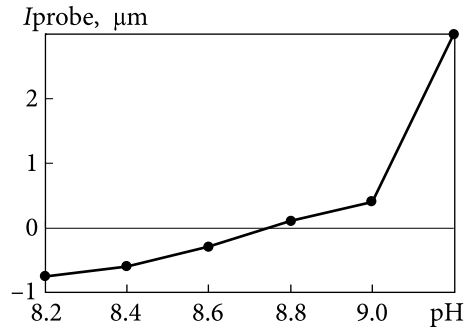


Fig. 4.1. Dependence of the probe current on the pH of the feed water (800 MW turbine)

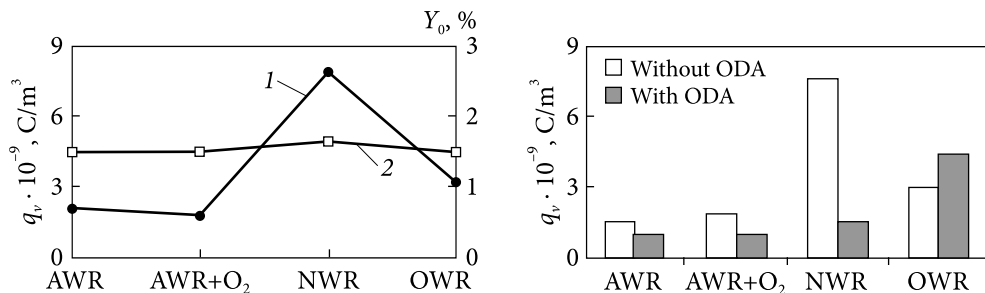


Fig. 4.2. The change in the volumetric charge density depending on the water chemistry, at $Y_o \sim 1.5\%$: 1 — volume charge density; 2 — mass steam moisture

Fig. 4.3. Changes in the volumetric charge density when dosed into ODA steam at different chemistries

At all WCRs, the volumetric charge density was determined with the following steam parameters in the measurement zone: overcooling $\Delta T = 2-3$ K; moisture $Y \sim 0.7\%$ and $\sim 1.5\%$.

The main results obtained with the electric probe are shown in Fig. 4.2.

As seen from Fig. 4.2, a decrease in the concentration of ammonia leads to a significant increase in the volumetric density of the measured charge, from initial values to $20.8 \cdot 10^{-10} C/m^3$ with positive charge polarity on the AWR, to $79 \cdot 10^{-10} C/m^3$ with negative charge polarity on NWR. At the same time, the moisture degree did not change.

During the experiment, it was found that an increase in steam moisture from 1.5% to 4% is accompanied by a sharp increase in the bulk density of charges, approximately 2 times.

Interesting results were also obtained in the course of studies on the change in the volumetric charge density upon the introduction of ODA into the steam path in front of the experimental turbine. During the experiments, the concentration of octadecylamine in the primary droplets formed in the flow of condensing steam, in liquid films taken from the surface of the channel under study, and in the steam in front of the turbine was monitored.

In the course of the experiment, the following study was carried out: wet steam with $pH = 9.3$ flows around the sensor on $AWR + O_2$, ODA is introduced into the steam, which leads to a decrease in the volume charge density by 1.9 times (see Fig. 4.3). Further, the transition to NWR with $pH = 8.0$ is carried out, while dosing into ODA steam leads to a decrease in the charge by 4.9 times. From the above experiment, it follows that with a decrease in the pH value of the steam, the influence of ODA on the charge value increases, which means that ODA can be used as a factor that reduces the charge density in the flow.

Analysis of the results obtained in the course of laboratory and natural experiments showed the following:

- in the range of pH values from 7.0 to 9.6, which are currently implemented in water chemistry at operating CHP and TPP, the processes of electrization of wet steam occur in different ways, both in magnitude and in polarity;
- with an increase in pH from 7.0, the electrization current has a negative potential, decreases to zero (in the pH zone 8.8—9.0)^[1], and with a further increase in pH, the concentration of charges increases with positive polarity;
- in the considered water-chemical regimes, both positive and negative charges are present in the wet steam flow in the phase transition zone;
- in condensing steam with a finely dispersed structure of the liquid phase at the beginning of the phase transition zone, there are electric charges on all the considered WCRs, their bulk density at steam moisture $Y_0 = 1.7\%$ is about $-7 \cdot 10^{-9} \text{ C/m}^3$;
- an increase in the degree of steam moisture from $\sim 1.5\%$ to 4% (the appearance of coarse moisture) leads to a sharp increase in the bulk density of charges, by about two orders of magnitude;
- the introduction of ODA into steam in all the considered water-chemical regimes leads to a significant (2—4 times) decrease in the bulk density of charges, which is very important, if necessary, to control the processes of charge formation.

4.2. Thermal electrophysical studies of the influence of water chemistry (pH) of feed water on the efficiency of the steam expansion process in the flow path of a supersonic nozzle

To study the effect of water chemistry on the possibility of changing the flow characteristics, a thermodynamic stand was used, designed to study electrophysical phenomena in the flow path of a supersonic nozzle and presented in detail in Sec. 2 (see Fig. 2.28 and Fig. 2.29).

On this stand, experiments were carried out to determine the influence of the pH of the feed water on the absolute pressure in the nozzle and on the efficiency of steam ionization. The design of the stand allows to use of pure water with the addition of ammonia and ionized steam for research. Different pH values of feed water were obtained by adding a dosed amount of ammonia to the distillate, and ionized steam — using a special discharge device. The main idea of this experiment was as follows: since the pH of the flow, as shown by the earlier studies, can contribute to natural electrization, it is necessary to check whether the additional condensation nuclei formed in this case are sufficient to reduce the level of supercooling and increase the efficiency of the expansion process in a supersonic nozzle. The experiments were conducted at constant steam pressure upstream of the nozzle, and the initial temperature was changed in a range from the saturation temperature of 89.5 to 100 °C. During

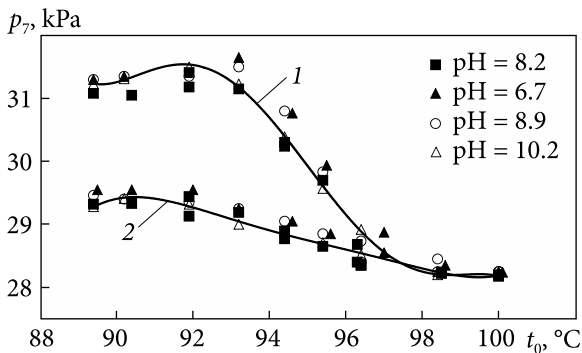


Fig. 4.4. Change in pressure at point 7 of the nozzle in regimes with different pH values of feed water without ionization and with ionization depending on the initial temperature of the steam: 1 — without ionization; 2 — with ionization

experiments with different pH values feedwater pressure measurements were performed at several points in the flow part of the nozzle at neutral and charged steam. Fig. 4.4 shows the dependences of the absolute values of the pressures of neutral and charged steam at point 7 in the outlet zone of the flow path of the nozzle, in which the greatest influence of ionization was observed, obtained at different pH values of the feed water depending on the initial temperature of the steam in front of the nozzle.

As seen from Fig. 4.4, the absolute pressures of neutral and artificially charged steam practically do not change at all studied pH values of the feed water and mainly depend only on the initial steam temperature. Although a slight decrease in the pressure of the initial neutral steam is noted at pH = 8.2, it is incomparable with the effect of using ionization.

This experiment once again convincingly confirmed the effectiveness of artificial ionization, which makes it possible to organize a sufficient number of condensation nuclei to achieve an almost equilibrium process of steam expansion and showed that the pH of the feed water practically does not affect the absolute values of the pressures in the flow path of the supersonic nozzle during natural electrization (Fig. 4.4, curve 1), nor to an increase in the efficiency of artificial ionization of steam (Fig. 4.4, curve 2), and hence, in general, to the efficiency of the expansion process.

As for the effect of pH on the efficiency of a real turbine itself, taking into account that pH can affect the rate of charge formation and the fact that a steam flow with a high charge density in its entire volume can have a noticeable effect on the efficiency of a turbine as was in tests on turbine T-37/50-8.9 [1] (neutralization of charges in the flow in this experiment made it possible to reduce the pressure downstream of the last stage by 150 Pa and increase the power by 140 kW), then, despite the results obtained in laboratory conditions, it was necessary for cogency to conduct tests on full-scale objects as well. Such tests were carried out on an 800 MW turbine unit in the USA at the Navajo CHP. The studies were carried out in a wide range of pH changes (7.0—9.6),

which made it possible to change the concentration and polarity of charges in the flow (Fig. 4.1). In the course of these tests, it was found that the changes made in the water-chemical regime during operation do not significantly affect the change in the power value. For the sake of fairness, it is necessary to say about some inaccuracy of these studies, carried out on our instructions by American specialists, since changes in the pH value did not record changes in other (except for power) parameters, for example, steam consumption. Under conditions of automatic maintenance of the set power, the flow rate could decrease, which may indicate an increase in efficiency.

The absence of the expected effects is explained by the following circumstances: in the initial zones of the phase transition, where, as a rule, there is a high level of supercooling, the number of condensation nuclei naturally created by the flow is visibly insufficient (several orders of magnitude less than necessary) for a tangible effect on the thermodynamic process. At the same time, a high density of native charges, as noted earlier, takes place in the zone of the last stage. But at this point, the level of overcooling of the flow is already minimal and the possible achievable effect due to the polarization of the droplets is neutralized by the loss of electrostatic forces directed against the flow at the exhaust.

Based on the research carried out by the author and other works in this area, it should be stated that a change in pH during the formation of water chemistry does not lead to any noticeable increases in the efficiency of the turbine.

4.3. Influence of water chemistry on the reliability indicators of turbine blades

The movement of a charged stream of wet steam where the volumetric charge density and velocity of charged particles are changed, the phenomena of fragmentation, merging, and corona of charged droplets take place, it is accompanied by the induction of secondary charges and currents in parts of the flow path, as well as by the appearance of electromagnetic radiation in the zone of the last stages and the exhaust pipe.

As shown earlier in Sec. 2, all these phenomena can have a significant effect on the state of the surface strength of the blades and be a complementary factor to the mechanical (drop-impact) degradation of the metal, as well as the electrical erosion of the rotor bearings.

Let us recall the main results of research in this direction:

- the impact of a positively charged flow softens the surface layer of the blade (reduces the resistance of the metal) by 30—50%, the flow with negative polarity minimize the destruction effect;
- the microhardness of the metal can increase or decrease up to 12% depending on the magnitude and sign of the constant electric field, and the effect

of an alternating electric field with a frequency in the range from 2.5 kHz to 20 kHz (close to real conditions) leads to a decrease in microhardness by 35%;

- All the above results and conclusions on the strength characteristics of the elements of the turbine unit are directly interconnected with WCR for the preparation of feed water, since, depending on the amine content, both intensification (or minimization) of natural processes of charge formation and a change in their polarity occur. Consequently, taking into account the above circumstances, it is necessary, in our opinion, to supplement the requirements for choosing such pH values that would allow minimizing the conditions that accelerate the degradation of the blade and bearing metal into the main indicators of water chemistry regulation, taking into account the above circumstances. According to our results of field studies, the pH values should be in the range of 8.8—9.1 [51]. At the same time, it should be understood that for each turbine unit, these operational indicators of the working environment will be determined individually using appropriate measurements of the charge density and approved only if they do not contradict more significant technological standards. The proposed standardization of water chemistry for charge formation in a wet steam flow will extend the service life of the LPC blades and reduce the likelihood of electroerosive destruction of bearings.

**DIAGNOSTIC METHODS AND MEANS
OF INCREASING RELIABILITY
AND EFFICIENCY INDICATORS
DEVELOPED BASED ON ELECTROPHYSICAL
PHENOMENA IN A TURBINE**

**5.1. Diagnostics of the concentration
of erosive moisture**

Large and small drops have one very significant difference. Drops formed in the course of volumetric condensation are always electrically neutral, while large (erosion-hazardous) droplets formed upon stripping from the surfaces of the flow path carry a surplus electric charge. This difference can be used to control the presence and change in the concentration of large dispersed moisture in the steam flow of the turbine, which is extremely important for predicting the erosional destruction of the rotor blades. The diagram of the formation of charges on drops when moisture strips off the edges of the working surfaces is shown in Fig 5.1.

The main mechanism of droplet electrization is associated with the rupture of the electric double layer when the droplet is detached from the blade edge (guide or working) or from another surface.

This circumstance allows for determining the distribution and changes in the concentration of large dispersed moisture in the steam flow by measuring only the probe current. The design of the electric probe and the measurement technique are described in detail in [1, 19]. Even though the electric probe does not allow measuring the total moisture content of the steam and the dispersion of moisture in the steam flow it can be used (due to its extremely high reliability and simplicity) to continuously monitor the distribution and relative change in the concentration of erosive moisture along the turbine stage height.

The electric probe used in the research consists of an insulated metal sphere with a diameter of 10 mm, a holder, and a rod for installing and moving it in the steam flow of the

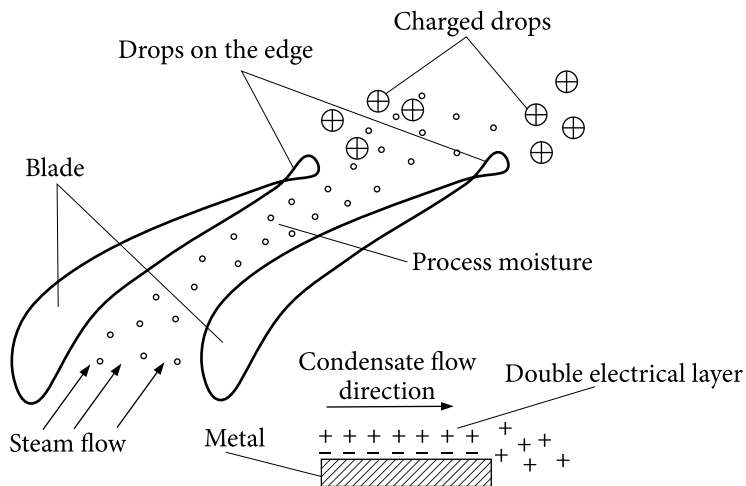


Fig. 5.1. Charge formation diagram in steam flow

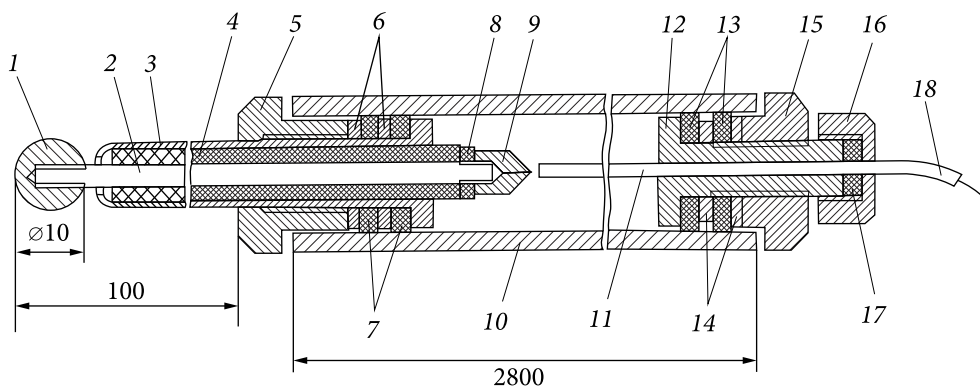


Fig. 5.2. Electric probe: 1 — receiver element (sphere); 2 — electrode; 3 — framework; 4 — insulator; 5 — puck; 6 — washer; 7 — rubber ring; 8 — puck; 9 — puck; 10 — bar; 11 — cable; 12 — sleeve; 13 — rubber ring; 14 — washer; 15 — puck; 16 — puck; 17 — rubber ring; 18 — electrode output

turbine. The design of the probe is shown in Fig 5.2. Such a probe allows monitoring of the change in large dispersed moisture when changing the operating mode of the turbine.

A sluice device is used to install an electric probe into the steam stream and extract it from the steam stream without stopping the turbine. The installation diagram of the sluice device in the turbine exhaust pipe is shown in Fig 5.3.

To install the sluice device during the shutdown of the turbine, holes were coaxially cut in the wall of the exhaust pipe and in the visor of the exhaust diffuser. The guide tube of the sluice device is installed and welded into these holes.

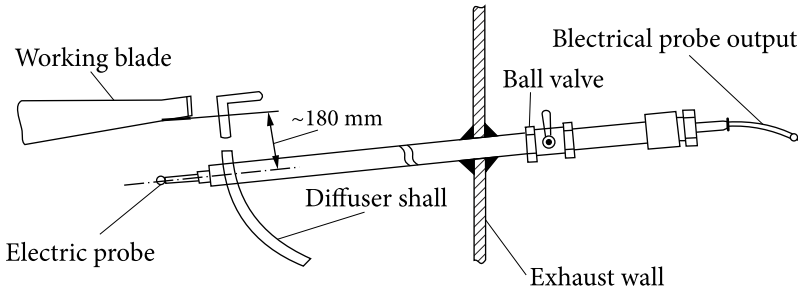


Fig. 5.3. Installation diagram of the sluice device in the turbine exhaust pipe K-325-23.5

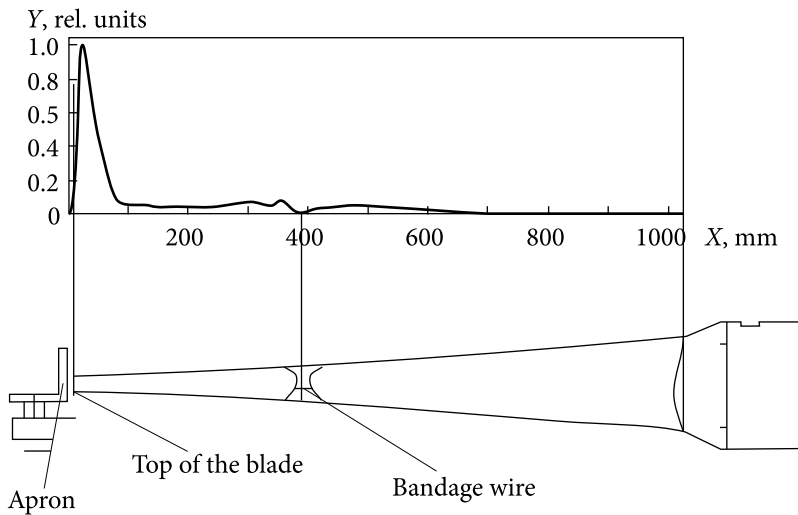


Fig. 5.4. Distribution of large dispersed moisture along the height of the blade of the last stage K-325-23.5

To obtain information about the distribution of large dispersed moisture along the stage height at various operating modes of the turbine unit, the electric probe was moved along the radius using a coordinate device. When the turbine was operating at nominal power, the electric probe current was measured in various coordinates along the stage height. The change in the probe current is proportional to the relative change in the concentration of large dispersed moisture in the steam flow.

The distribution of large dispersed moisture obtained at the nominal operating mode of the turbine is further used as a basis for comparing the results of measurements with other modes.

Fig. 5.4 shows the distribution of large dispersed moisture along the blade height of the last stage blade K-325-23,5 ($N_e = 300$ MW, $t_{i0} = 545$ °C).

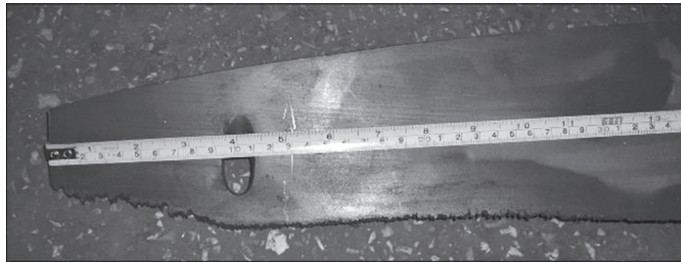


Fig. 5.5. Erosion of the working blade of the last stage of the LPC turbine K-300-23.5 after 87,000 hours of operation

Fig 5.4 shows that the maximum amount of large dispersed moisture is concentrated at the tip of the blade in the region of 30—100 mm, and then it decreases. At a distance of 385 mm from the top of the blade, a shroud wire is installed, in the area of which the concentration of large dispersed moisture is reduced, practically, to zero. In the root zone, a decrease in the amount of large dispersed moisture is also observed. Based on this, it can be concluded that the most intense erosive wear occurs at the tip of the rotor blades.

This conclusion is confirmed by the practice of operating the K-300-23.5 turbines.

The blades of the last stages of the K-300-23.5 turbine have maximum erosion wear in the range of 0—90 mm from the top (Fig. 5.5).

Thus, to predict the intensity of erosive wear of the rotor blades using a stationary electric probe, it is sufficient to place it behind the last stage opposite the tip of the blades at a distance of 20—50 mm.

5.2. Neutralizer of the volumetric charge of the steam flow in the turbine

In the case when it is impossible to prevent the formation of charges in the steam flow of the turbine by changing the chemical composition of the feed water or by suppressing the process of charge formation, the volume charge in the steam flow can be reduced using neutralizers. Both active and passive neutralizers can be used to neutralize the space charge. To neutralize the space charge, it is necessary either to increase the conductivity of the medium or add charges of equal quantity and opposite sign to the bulk. In the first case (the method of increasing the conductivity of the medium), the volumetric charge decreases due to the flow of charges from the bulk to the «ground». In the second case (compensation method), there is a mutual neutralization of the charges of the same sign in the bulk and the added charges of the opposite sign. The method for increasing the conductivity of the medium is simpler. The compensation method is more effective, but it requires a high

accuracy of supply of compensating charges to the bulk, otherwise either incomplete compensation or overcompensation occurs and a charge of the opposite sign is formed in the bulk.

Structurally, the neutralizer can be made in the form of two half-ring electrodes (Fig. 5.6), installed, for example, on support insulators on the outer wall of the exhaust diffuser.

The electrodes are made of a steel bar with a diameter of 16 mm. Sharp pins 5 mm in diameter and 160 mm in length are installed on the electrodes with a pitch of 100 mm between the support insulators.

Due to the fact that the electrodes of the neutralizers are installed on support insulators it allows to use the neutralizer in both passive and active modes. Each neutralizer electrode has its own high-voltage terminal, which can be used for independently grounding or supplying voltage to each neutralizer electrode.

To determine the efficiency of the neutralizers, a special lock chamber was installed in exhaust zone, through which, during the experiment, either gas-dynamic or electric probes were inserted. The probes were moved using a coordinate device along the radius of the impeller allowing us to measure the distribution of charges in the flow and its gas-dynamic characteristics.

Fig. 5.7 shows the results of testing the neutralizer.

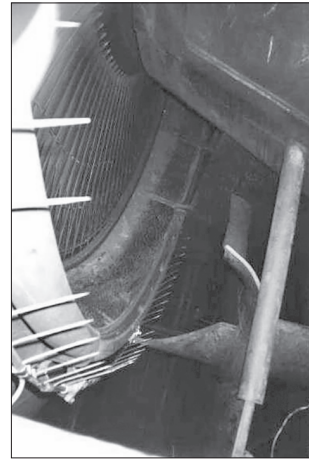


Fig. 5.6. General view of the turbine exhaust converter

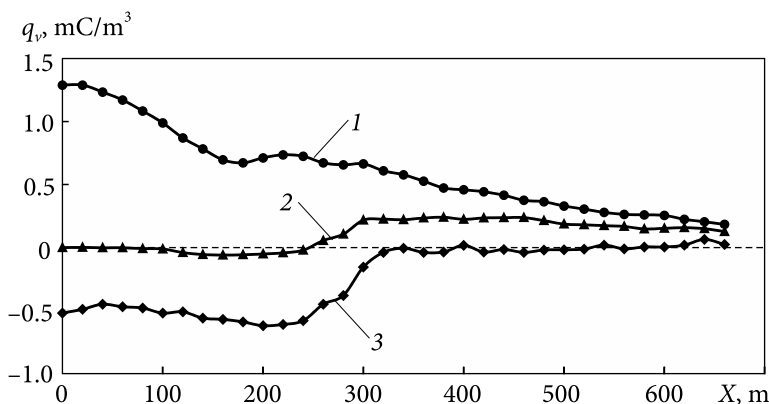


Fig. 5.7. Change in the volumetric density of charges in the steam flow along the radius of the last stage in three modes of the neutralizer (coordinate $X = 0$ corresponds to the top of the rotor blade): 1 — initial mode (neutralizer is off); 2 — passive mode (neutralizer is grounded); 3 — active mode (voltage -7 kV applied to the neutralizer)

It can be seen that when neutralizing electrodes are grounded (passive mode) in the region from the top of the stage at a distance of ~ 250 mm, almost complete neutralization of the space charge occurs. In the range from 250 to 650 mm, the density of charges in the steam flow decreases approximately two times. In the active mode, when a voltage of -7 kV is applied to the electrodes of the neutralizers, almost complete neutralization of charges in the region from 300 to 650 mm from the top of the stage is ensured, but overcompensation is observed near the top, as a result of which the charge in the flow changes its sign to the opposite. By changing the voltage on the neutralizer the degree of neutralization of the steam flow can be changed as well.

Studies have shown that a passive neutralizer is simpler and more reliable than an active neutralizer does not require maintenance during operation and has a fairly high efficiency. Therefore, to neutralize the volumetric charge after the last stage of the turbine, it is suggested to use a passive neutralizer.

The result of neutralizing the flow downstream of the last stage, as previously shown in the subsection. 1.5 reduces back pressure and reduces flow pulsations arising from electrostatic processes, thereby increasing the efficiency of the turbine unit.

5.3. Methods for reducing erosion-corrosion processes from the effects of electrized large dispersed moisture

5.3.1. Estimative method for removing moisture from the channels of the guide apparatus of the last stage of a wet steam turbine

In the case of electrization of wet steam, a flow-through system of ion transport occurs in the steam flow of the turbine with accompanying electrophysical phenomena, see Fig. 5.8.

Parts of the surface of the flow path with moisture films dispersed on them act as electrodes — ion emitters. The result of the flow of ion current and electrophysical phenomena in the flow path is electrochemical degradation of the surfaces of the flow path. The most dangerous, from the point of view of hydrogen saturation, as it was previously established, is the positive ion current carried by large dispersed moisture. In this case, in addition to the mechanical effect of moisture, erosive moisture has an additional negative factor affecting the metal as the effect of electrically charged drops. Considering this, the most effective method of dealing with the damaging effect of charged erosive-dangerous moisture is to minimize its contact with the surfaces of the rotor blades. A promising method for solving this problem is the method of removal of estimative moisture. In the technical literature on these issues,

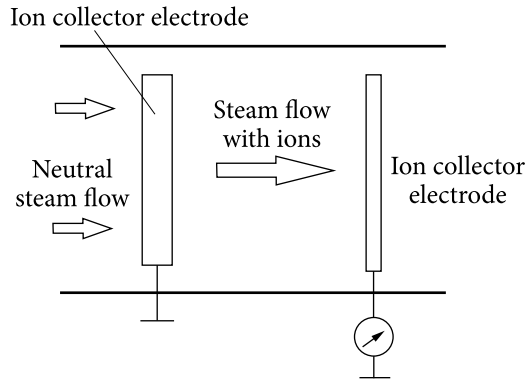


Fig. 5.8. Ion transport system in the flow path

several patent solutions are presented by such companies as Rateau (heating with hot water through channels along the guide blades), Siemens AG (electric heating of blades), CEM company (heating steam is supplied to the hollow blade through a tube that is lowered almost to its root, and then sucked into the condenser through a hole in the periphery) and many other authors.

In 1996, CKTI developed a heating system for hollow guide blades, which ensures complete condensation of the heating steam during heat exchange. This technical solution was patented by a team of authors from CKTI and Turboatom [52]. However, the proposed method has many disadvantages: uncontrolled heating of the blades, which does not allow the blades to be heated to the optimum temperature; different operating modes of the turbine are not taken into account, at which the optimal temperature for heating the blades is different. There is no diagnostic device for determining the presence or absence of large dispersed moisture escaping from the guide blades. There are turbine operating modes in which the wet steam stage operates in superheated steam or with low moisture. In these cases, it is either unnecessary to heat the blades or the heating must be reduced so as not to reduce the efficiency of the turbine.

Unlike the CKTI patent, the authors of IPMash proposed an improved version of estimative moisture removal, taking into account the electrization of moisture in the flow [53], based on a (electric) probe that monitors the presence of large dispersed moisture in the last stage. The design of such a probe is presented in detail in Sec. 5.1, its functioning is based on the processes of formation of large dispersed moisture in the last stages of the LPC.

The developed method for preventing the formation of large dispersed moisture in a wet steam turbine stage includes controlled utilizing a thermocouple installed on the outer surface of one of the blades, heating of all blades of the stage guide vane to the optimum temperature, depending on the operating

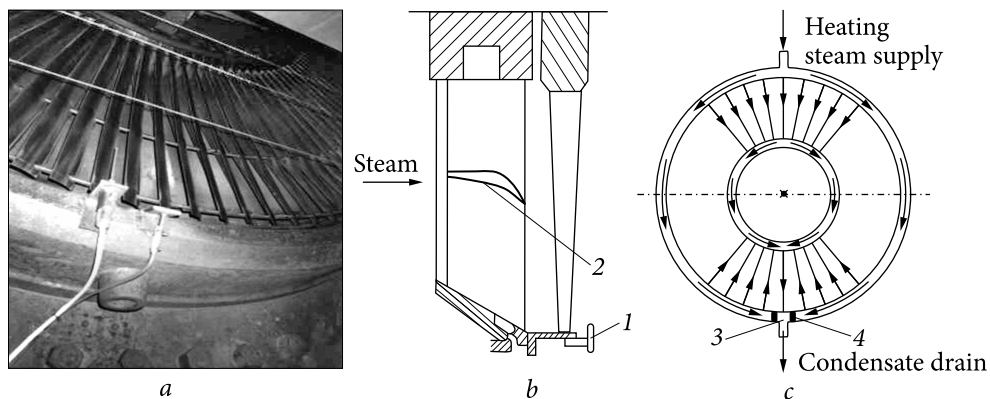


Fig. 5.9. Estimative method for removing moisture from the channels of the guide blades: *a* — an electric probe behind the turbine impeller; *b* — longitudinal section of the turbine stage and the cross-section of the guide blades; *c* — diagram of the flow of heating steam in the guide vane of the stage and the place of installation of the plugs separating the drainage holes from the rest of the cavity in the rim of the guide vane

mode of the turbine and determined by the minimum content of large dispersed moisture in the steam flow acting on working blades of the stage, measured with an electric probe. The blades are heated by steam taken from one of the previous wet-steam stages directed into the inner cavities of the hollow blades of the guide blades, and then steam in the form of condensate or steam-water mixture is discharged through the drain holes into the turbine condenser. The regulation of the steam consumption for heating the guide blades according to the feedback signal from the electric probe makes it possible to exclude inefficient use of steam and significantly increase the efficiency of the moisture removal system. The electric probe is a stick electrode installed downstream of the last stage of the turbine (Fig. 5.9 *a*). Erosive droplets are electrically charged and, when hitting the probe, cause an electric current. The intensity of the current signal depends on the amount of erosive moisture and makes it possible to organize a feedback system to control the heating of the blades.

Below are the Figures from the patent of Ukraine No. 113131 [53], illustrating the technical solution.

In Fig. 5.9 *b*, position 1 is an electric probe that records the charge of the steam flow; 2 — temperature control thermocouple. In Fig. 5.9 *c* 3 — the drain hole on the left and right is separated from the cavity in the rim of the guide vane by plug 4, which made it possible to pass the same amount of heating steam into the blades, heat all blades to the same temperature, and also to exclude perforating flow of a part of the heating steam past the blades into the capacitor.

High efficiency of moisture removal is achieved due to the controlled heating of the guide blades to the optimum temperature, measured by a thermo-

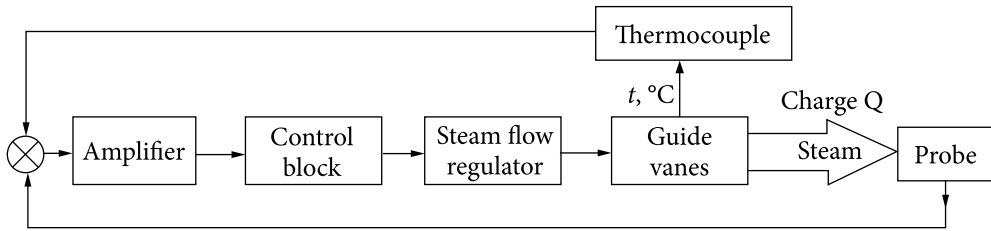


Fig. 5.10. Block diagram of the guide vane temperature control system

couple mounted on the outer surface of the blade. The optimum temperature of the sensor depends on the operating mode of the turbine, the steam consumption for heating the blades and is determined by the minimum amount of large dispersed moisture in the steam flow behind the rotor blades of the stage, measured with an electric probe.

For the technical implementation of blade heating, an Automated Control System ACS (120) can be used, the block diagram of which is shown in Fig. 5.10:

The technical implementation of such a system is associated with the solution of the problem of creating an appropriate design for a compact steam supply regulator, which can be used in conjunction with a modernized diaphragm of the last stage.

5.3.2. Method of reducing the flow charge by correcting the water-chemical regime and material properties (coatings)

Experimental studies of the process of formation and accumulation of the space charge of the steam flow from the water-chemical regime carried out on the 750 kW turbine of the MPEI ET-12 stand and on the 800 MW turbine, showed that the water-chemical regime affects both the intensity of steam electrization and the electric polarity [1]. In our opinion, this may be due to the following reasons.

A change in the water-chemical regime, which leads to a change in the pH of the working fluid, can be accompanied by a change in the surface tension forces of water condensate. It is logical to assume that the nature and intensity of the destruction of the water condensate film, and hence the double electric layer, largely depends on the forces of its surface tension. Therefore, a change in the forces of surface tension of the condensate caused by a change in the pH of the working fluid can and should be accompanied by both a change in the dispersion of drops towards a decrease or increase in their size, and the nature and degree of their electrization. What we see in the graphs shown in Fig. 1.11 and Fig. 4.1.

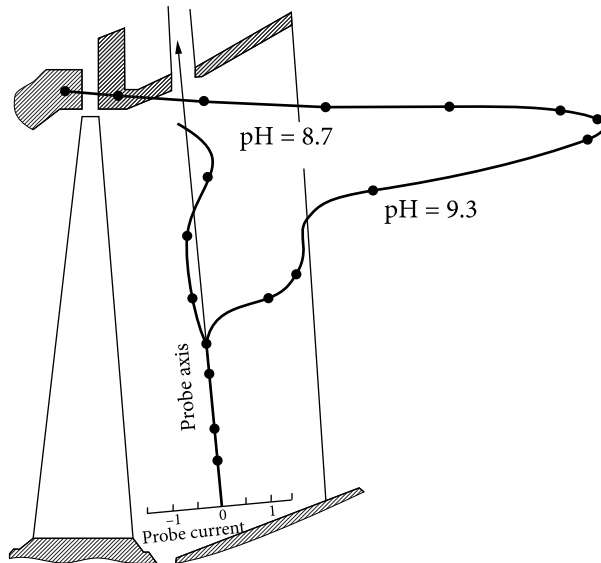


Fig. 5.11. Results of measurements of charges after the last stage of the turbine

The studies presented in Sec. 2, also showed that the most dangerous, from the point of view of metal surface degradation from charged droplets, is a flow with a positive polarity, while droplets with negative and neutral signs have a minimal effect. In addition, it was shown earlier that it is possible to change the polarity and intensity of charge formation by changing the pH of the medium. From all that has been said as already noted in the subsection 4.3 it means that a rational choice of pH can minimize the negative effect of electrization on the surface strength of the blade by imparting a neutral or negative potential to the flow, as, for example, was achieved on an 800 MW turbine (see Fig. 5.11).

The technical implementation of the electrization suppression system by the WCR correction can be performed based on an automated system using a steam flow electrization sensor.

The solution that minimizes the unipolar space charge in the flow of the working fluid in the LPC can be both special methods of neutralizing charges [1], and the use of various metals and coverings of guide blades, consisting of materials that give a negative or quasineutral sign of the electrostatic charge of moisture dispersed from them, which, as shown earlier, minimizes the degrading effect from electrophysical influences. In this case, the electrochemical damaging ability of the working fluid is similar to neutral steam, i.e. minimal. In this direction, as a confirmation factor of such possibilities to control the polarity of the flow, one can cite the studies previously presented in the subsection 1.2, in which, as a result of experiments, it was found that the polarity of

the flow depends on the material of the sample (stainless steel gives a positive sign, and black steel and brass — a negative sign).

Research in this direction should be continued and a technology for coating materials should be developed to minimize the process of charge formation.

5.4. Improving the efficiency of the turbine due to artificial ionization of the steam flow of the LPC

In the previously presented results of experiments carried out on laboratory and full-scale installations, it was convincingly shown that it is possible to reduce the loss of flow energy from overcooling and to increase the efficiency of the steam expansion process due to artificial ionization of the working fluid. In the course of these studies, the necessary elements of devices and structures were developed and tested in operational conditions, ensuring reliable and safe operation of the ionizing steam system. These are a high-voltage unit supplying the system of ionizing electrodes, providing stabilization, switching off the current in case of deviations from the specified electrical parameters in emergency modes; designing of bushing (current lead into the turbine) and suspended (for installing electrodes) high-voltage insulators; electrodes and their fastening elements, etc. The operation of this system during tests for the ionization of steam in a turbine at various TPPs and CHPs has shown high efficiency and reliability. Below it is proposed to consider possible options for the implementation of artificial ionization of a wet steam flow in a turbine.

The greatest effect with the use of corona or barrier discharge ionizers can be achieved if, at the stage of design and construction of turbines, the location of the ionizing device is taken into account, which depends on the thermodynamic parameters of the process, which determine the initial phase transition zone in the flow path and take into account the most rational parameters steam for ionization.

When determining the possibility of introducing the results of ionization of steam at operating power units, problems of a constructive nature arise, since such a technology was not envisaged in the design. One of these problems is the choice of the location for the installation of the ionizing device in the flow path of the operating turbine. So, for example, in K-300-23.5 turbines operating at many power plants in Ukraine, it is most expedient for all recommended parameters to ionize steam before the third stage of the LPC, i.e. before the phase transition zone (Fig. 5.12). At the same time, it is very difficult to carry out a reliable design of the ionizing device in the indicated place of the existing flow path of the turbine and this requires serious additional design and technological improvements.

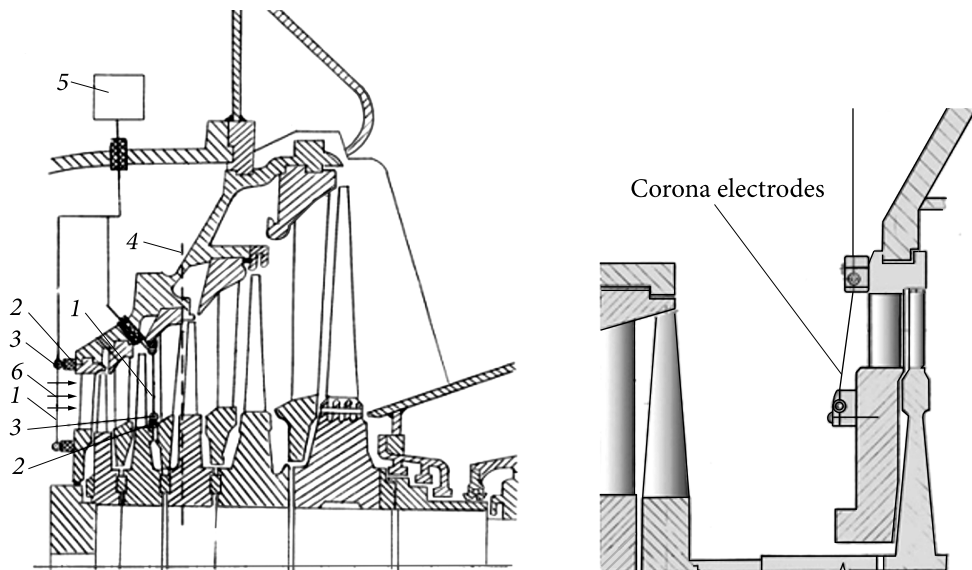


Fig. 5.12. Placement of discharge electrodes for ionization of the steam flow in the flow path of the turbine: 1 — discharge electrodes; 2 — insulators; 3 — collector; 4 — zone of the beginning of condensation; 5 — high-voltage source; 6 — steam flow

Fig. 5.13. Placement of steam flow ionizers in the flow path of the turbine in front of the first stage of the LPC

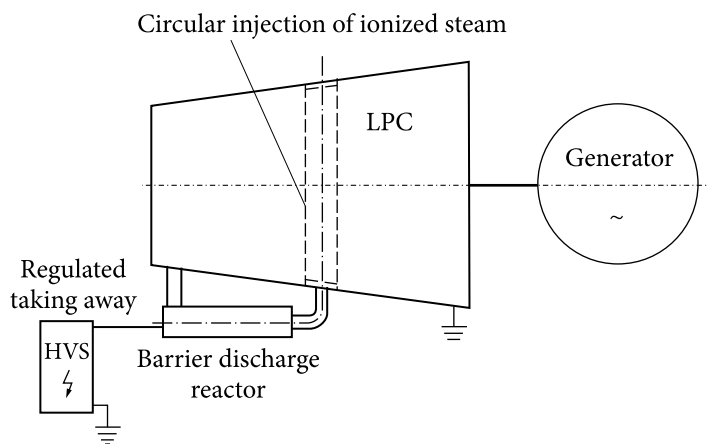


Fig. 5.14. Scheme of external supply of ionized steam to the flow path

The most suitable place for steam ionization in such turbines is the chamber behind the flow path of the medium-pressure cylinder of the K-300-23.5 turbine (Fig. 5.13). From this chamber, steam enters all three streams of the LPC. However, concerning this turbine, the steam temperature before the first

stage is ~ 200 °C. The ionization of steam at this temperature, based on previous studies, becomes problematic, and more research is required.

Considering already presented in subsection 3.5 studies on the «survivability» of ionized steam particles when using a barrier discharge, the arrangement of devices schematically shown in Fig. 5.14 can be considered promising. In this case, the generation of steam charges is carried out outside the flow path.

Taking into account the research carried out on the selection of rational thermodynamic parameters at which steam ionization is effective, this technology can be successfully implemented in geothermal installations for turbines with the following steam parameters: inlet temperature 80—150 °C and pressure 180—200 kPa.

The considered options for the possible practical implementation of the ionization of the steam flow, of course, require careful design studies and tests on model and full-scale installations. Such work will increase the efficiency of the turbine plant by 2% or more, which is a stimulating factor for manufacturers of wet steam turbines.

5.5. Study of the possibility of using physical fields (magnetic and electromagnetic) to increase the efficiency of a turbine unit

Improving the efficiency of modern steam turbine installations has been and remains one of the most urgent tasks in the economy sustainable development. Most of these plants operate on the Rankine cycle with intermediate superheating of steam and regenerative feed water heating.

Traditional methods of increasing the efficiency of the Rankine cycle, such as increasing the initial parameters of the steam, lowering the final pressure are almost over exhausted.

Some new ways for increasing unit capacities and efficiency of power plants have been started quite long ago and developed: steam-gas cycles [54]; the use of multicomponent low-boiling mixtures with a variable temperature of vaporization as a working fluid; the choice of optimal, in the thermodynamic sense, new working fluids [55, 56].

However, among a few substances with known thermodynamic behavior, water is still the most preferred working fluid for steam power plants.

A characteristic feature of the presence of phase transitions is a sudden change at the transition point in the values of the functions of the thermodynamic state of the working fluid: heat capacity, entropy, enthalpy, isobaric-isothermal potential, and others.

In the case of the second-order phase transition, which can occur under the influence of force fields and precedes a phase transition of the 1st order, there is

no change in entropy, i.e., no heat release or absorption. However, other thermodynamic parameters may change significantly.

Currently, studies of the impact on water of fields of various natures, which can significantly change the thermodynamic characteristics of water and water vapor, are being intensively developed.

Therefore, it seems appropriate to evaluate how such changes that occur during a second-order phase transition will affect the thermal efficiency of the Rankine cycle.

Analytical relations for determining the thermal efficiency of the Rankine cycle when changing the specific heat of water and the hidden heat of vaporization under the influence of a force field are based on classical thermodynamics' laws and the theory of turbomachines.

For the numerical study of changes in the properties of water under the influence of force fields, the results obtained on an experimental stand, which was developed and manufactured at IPMash NAS have been used.

The influence of physical (in particular, magnetic fields) on water and water systems has been studied for a long time, but until now, the works of different researchers often contradict each other due to the lack of a theoretical basis that would allow to explain and to apply the results obtained.

All experimental work in this area can be divided into two large groups:

- research aimed at changing any physical and chemical properties of water to develop the theoretical basis for the influence of external physical fields;
- research aimed at obtaining specific changes in the properties of water systems to use the results in real technological processes.

In our opinion, most of the studies related to the first group over the past decade can be represented by the following few works. Valery Shalatonin et al. [57] in the study of deionized water revealed significant polar-dependent changes in water absorption in the UV range (180 — 350 nm) and water evaporation. Ran Cai et al. [58] showed a decrease in surface tension and an increase in the viscosity of water. Yongfu Wang et al. [59] found that the coefficient of friction in magnetized water at different magnetic field strengths is less than in untreated water. S. Jawad et al. in a study [60] reported the effect of the magnetization process on the chemical and electrical properties of tap water (pH, electrical conductivity). Yanmin Li et al. in their studies [61] showed that a magnetic field can increase the freezing point of water and aqueous solution by about 3.0—5.0 K. Kai-Tai Chang et al. in [62] found that the number of hydrogen bonds increases with increasing magnetic field strength. This means that this field can control the size of the water cluster.

In the second group of studies, we are focused on works related to the thermophysical properties of water. Youkai Wang et al. [63] found an increase in evaporation by 38.98%, a decrease in specific heat capacity by 3.3%, and a de-

crease in boiling point by 2%. J.A. Duenas et al. [64] state that the treatment of deionized water with a magnetic field increases its evaporation by 20%. Yun-Zhu Guo et al. [65] showed an increase in water evaporation. A. Szcześ, et al. [66] showed that the conductivity of water decreases, and this decrease is inversely proportional to the flow rate. E.S. Malkin et al. [67] showed that when treating water with the help of the Ilios-M electromagnetic pulse apparatus, a decrease in the specific heat of vaporization of water by 6...10% and specific heat capacity by 9% was obtained. The maximum effect is obtained at the maximum pulse frequency.

All of the above works have, in our opinion, several significant shortages:

- it is stated that as a result of the action of the field, some parameter quantitatively changes only in one direction, and the magnitude of this change is proportional either to the absolute value (in the case of a constant field), or to the repetition rate of perturbing pulses (in the case of an alternating field);
- received, practically, the same result of the impact of the field in the case of using distilled or tap water as an object of study;
- little attention is paid to the parameters of the water flow and the parameters of the pipelines through which water flows both in the zone of influence of the field and in other zones.

However, the results of all experimental works indicate the possibility of a significant change in the properties of water under the influence of fields of various physical natures.

One of the first tasks of these studies is to prove that these properties can be changed both upwards and downwards, which will make it possible to control the process at different stages of the technological cycle of a steam turbine unit.

For a long time, IPMash NAS of Ukraine has been carrying out work aimed at purposefully changing the thermophysical properties of the working fluid of heat machines [68]. In experimental work, both the input parameters of water and the climatic conditions of the work are controlled. The repeatability of results is up to 60%, because of the lack of accuracy of the measuring equipment and the probable presence of unaccounted factors affect.

The data obtained to this time allow us to assert that the rate of evaporation of distilled water can vary between 11% and +16%. The parameters of water flow and magnetic field induction such as physical and chemical properties, the optical density of water in the infrared range of wavelengths (+4.1% ÷ -1.7%), and the solubility of oxygen in water change were identified. This fact can be used when calibrating magnetic systems for maximum impact efficiency. If we take water with different degrees of purification as an object of study or do not consider the trajectory and flow velocity, then the results differ radically. Thus, we anticipate that the thermophysical properties of the working fluid can be changed due to a second-order phase transition. In this case, under the

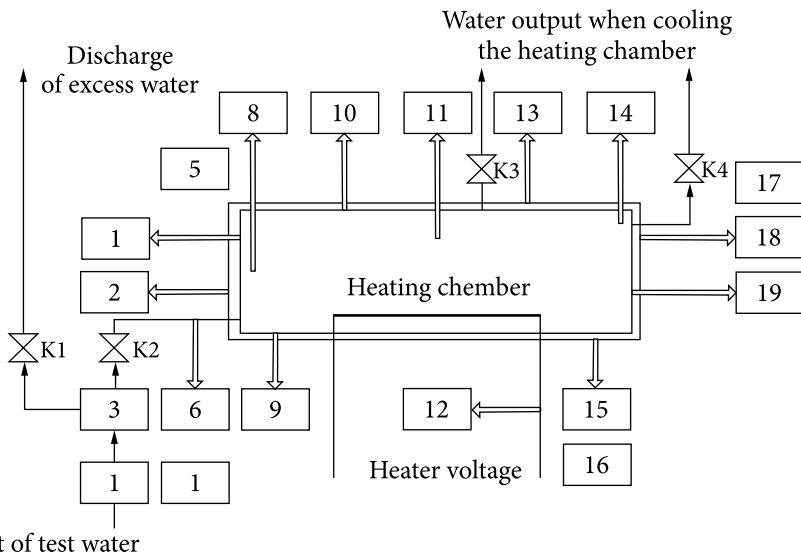


Fig. 5.15. Research stands for measuring the heating rate of liquid media (functional diagram): 1, 9, 10, 19 — temperature sensors of the surface of the heating chamber; 2, 13, 15, 18 — casing surface temperature sensors; 4—magnetic device; 5, 7, 16, 17 — air temperature sensors; 6 — inlet water temperature sensor; 8, 14 — water temperature sensors inside the heating chamber; 11 — conductometric sensor; 12 — voltmeter

action of a force field, hydrogen bonds in a water cluster are replaced by bonds of ion-ion, ion-dipole, and dipole-dipole interactions. As a result, new clusters are formed, but with different properties. The numerical values and the direction of change in properties are determined by the ratio between the number of new and old clusters, their sizes, and the number of «free» water molecules.

Thus, if the goal of the research is to change the properties of water without introducing additional chemical reagents into the water, it is necessary to partially destroy and partially deform water clusters. The destruction or deformation of hydrogen bonds is not particularly difficult due to their low energy. Increasing the return time to the initial state is a significantly more difficult task. Solving this problem will bring this scientific direction to a new qualitative level.

Up to now, there is no information about the reagent-free control of the thermophysical properties of the working body of TPPs and CHPs and the change in the efficiency of the thermodynamic cycle associated with this effect.

This paper presents the results of experimental studies on the influence of a transverse magnetic field on the heat capacity of distilled water. Work was carried out on the stand, the functional diagram of which is shown in Fig. 5.15.

A constant amount of heat was transferred to a constant volume of treated water. The heating rate was chosen as a criterion parameter. Distilled water en-

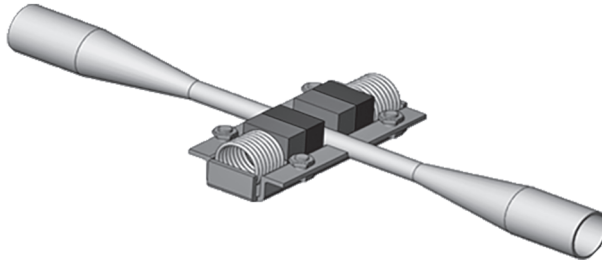


Fig. 5. 16. Device for generating a constant magnetic field

ters the stand input, which has undergone magnetic treatment in a transverse magnetic field generated by permanent magnets (Fig. 5.16). The magnetic field strength can be changed.

The stand works as follows: water enters the heating chamber through tap K2; when tapping K4, structurally located in the upper part of the heating chamber is open; after filling the heating chamber (this is evidenced by the outflow of water through the tap K4), the tap K2 is close; in this way, a certain amount of water is heated. Water can enter the heating chamber at different flow rates, the value of which is determined by the K2 tap. Flow control is carried out by a rotameter. Measurement of magnetic induction is carried out by teslameter EM4305.

The work on the stand was carried out according to the following method. The water was heated from 25 to 70 °C. As an informative temperature value, the arithmetic mean of the readings of the sensors located inside the heating chamber was chosen. All temperature sensors mounted on the stand were selected using an exemplary mercury thermometer with an error of 0.1°C.

To provide measurements in real-time, the iButton TMEX™ SDK software kit by Dallas Semiconductor, US was installed on the PC. To exclude the influence of the supply voltage of heating elements on the heating rate, this parameter was calculated using the formula:

$$V = 45/U \cdot A \cdot \tau,$$

where: V — the reduced heating rate; U — electric voltage supplied to the heating elements; A — electric current consumed by heating elements.

The results of experimental studies are shown in the form of graphs (Fig. 5.17). The final graphs included only those results that were obtained at the same ambient temperature of 20 °C and a supply voltage of heating elements of 50V.

The graph (Fig. 5.17) shows that the reduced heating rate during water treatment with a transverse magnetic field, considering the values of magnetic induction and water flow consumption, established during the research through

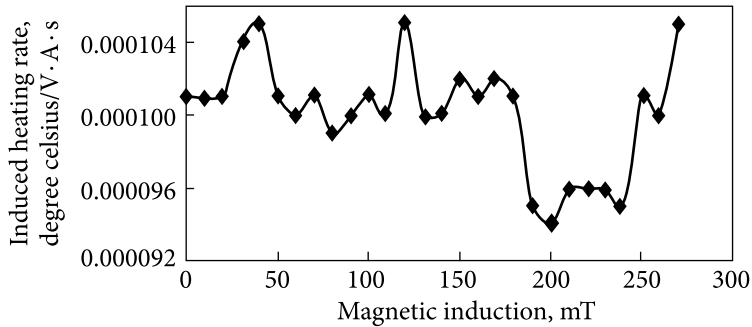


Fig. 5.17. Change in the reduced water heating rate at a flow consumption of 200 dm³/hour

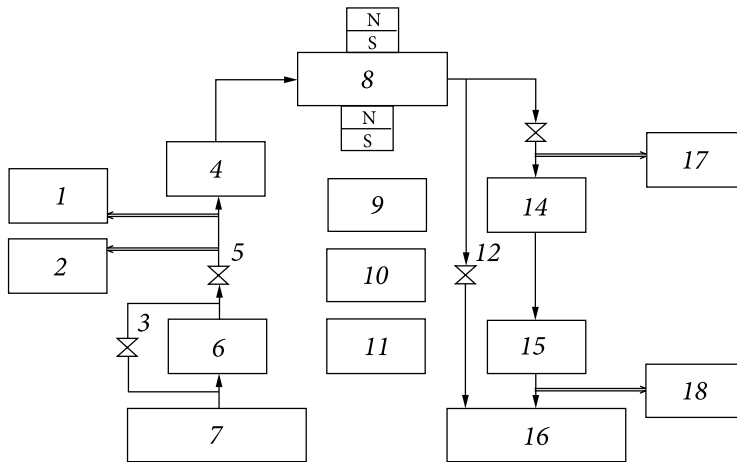


Fig. 5.18. Dynamic evaporation stand (functional diagram): 1 — water pressure sensor; 2 — total water flow sensor; 3 — tap 2; 4 — rotameter; 5 — tap 1; 6 — pump; 7 — expansion tank; 8 — magnetic system; 9 — air temperature sensor; 10 — barometric pressure sensor; 11 — relative humidity sensor; 12 — tap 3; 13 — tap 4; 14 — water flow sensor through the evaporation column; 15 — evaporation column with fan; 16 — expansion tank; 17 — water temperature sensor before cooling; 18 — water temperature sensor after cooling

the working section of the magnetic apparatus, can vary within -6% and $+5\%$. We believe that this corresponds to a change in the heat capacity of water within the same limits.

Along with studies on changing the heat capacity of distilled water on another stand, the functional diagram of which is shown in Fig. 5.18, work was carried out to study the influence of a magnetic field on its evaporation.

The evaporation rate was estimated by an indirect method based on the temperature difference before and after the evaporation column. The results

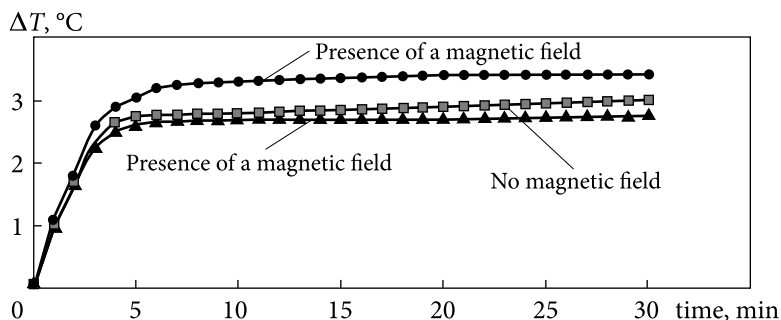


Fig. 5.19. Dependence of the temperature difference before and after the evaporation column in the presence and absence of a magnetic field

obtained are shown in Fig. 5.19. With different magnetic field strengths and different velocities of the water passing through the working section of the magnetic apparatus, the cooling efficiency can change in one direction or the other.

Based on research results, it can be stated that a magnetic field can change the efficiency of water cooling within the range of $-11\% \div +16\%$. We believe that the resulting effect corresponds to a change in water evaporation. Based on an analysis of literary sources [63, 67, etc.] and on the results of our own research, it can be assumed that an increase in evaporation leads to a decrease in the specific heat of vaporization and vice versa.

Consequently, in a reagent-free method, it is possible to significantly change not only such physical and chemical properties of water such as optical density, electrical conductivity, ability to dissolve oxygen, etc., but also change the thermodynamic characteristics of water as a working medium. At the same time, there is a tendency for a simultaneous increase or decrease in specific heat capacity and evaporation or latent heat of vaporization. It should be understood that the degree of water purification as well as the hydrodynamic parameters of the equipment for moving water, along with the magnitude of the magnetic field, are of great importance for achieving a positive effect.

We assume that the thermophysical properties of the working medium can be changed due to a phase transition of the second order. In this case, under the action of the force field, hydrogen bonds in the water cluster are replaced by ion-ion, ion-dipole, and dipole-dipole interaction bonds. As a result, new clusters with different properties are formed. Numerical values and the direction of changes in properties are determined by the ratio of the number of new and old clusters, their sizes, and the number of «free» water molecules.

Thus, if the goal of the study is to change the properties of water without introducing additional chemical reagents into the water, it is necessary to partially destroy and partially deform water clusters. The destruction or deformation of hydrogen bonds does not present particular difficulties due to their low

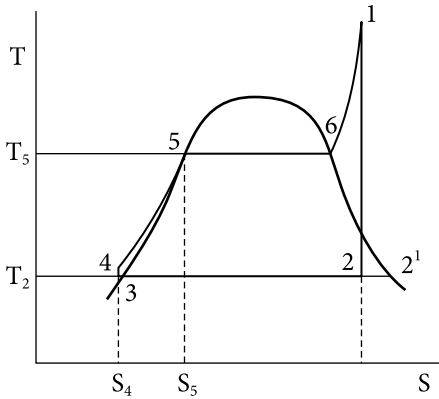


Fig. 5.20. Reversible Rankine cycle in T-S coordinates

Rankine cycle without intermediate overheating of steam and regenerative water heating (Fig. 5.20).

The classical dependence for determining the thermal efficiency of a cycle is written as follows:

$$\eta = 1 - q_1/q_2,$$

where: q_1 — heat supplied in the cycle; q_2 — heat dissipation.

The supplied heat can be represented as the sum of the heat supplied during water heating (process 4—5), its evaporation (the latent heat of vaporization r_p , process 5—6), and steam overheating (process 6—1).

For the simplest reversible Rankine cycle, if we neglect the value of the pump operation due to its smallness in comparison with the available enthalpy difference that occurs in the turbine, the dependence for determining the thermal efficiency of the cycle can be written as follows:

$$\eta_t = 1 - T_3(S_1 - S_3) / \left(\int_{T_4}^{T_5} C_{P_b}(T) dT + T_5(S_6 - S_5) + \int_{T_6}^{T_1} C_{P_{st}}(T) dT \right).$$

Where $C_{P_{st}}(T)$ is the specific heat capacity of steam, which varies in the temperature range T_6 — T_1 ; $C_{P_b}(T)$ — specific heat capacity of water in the range T_4 — T_5 ; S_1, S_3, S_5, S_6 — entropy at the corresponding points of the cycle; $T_5(S_6 - S_5) = r_p$ — latent heat of vaporization;

Accordingly,

$$\eta_t = 1 - T_3(S_1 - S_3) / \left(\int_{T_4}^{T_5} (C_{P_b} dT) + r_p + \int_{T_6}^{T_1} (C_{P_{st}} dT) \right).$$

energy. Increasing the recovery time is a much more difficult task. Solving this problem will bring this scientific direction to a new qualitative level.

Until now, there is no information about reagent-free control of the thermophysical properties of the working medium of TPPs and CHPs and the change in the efficiency of the thermodynamic cycle associated with this effect.

Let us theoretically estimate how this will affect the value of the thermal efficiency of the Rankine cycle.

Consider the simplest reversible

Under the influence of a magnetic field on the working body at the start point of heating (point 4), the specific heat capacity of water C_{P_B} will change by ΔC_{P_B} , and the latent heat of vaporization by Δr_p .

Thus, considering this effect, the expression for determining the efficiency of the thermodynamic cycle will change accordingly and take the form:

$$\eta_t = 1 - T_3(S_1 - S_3) / \left(\int_{T_4}^{T_5} (C_{P_B} + \Delta C_{P_B}) dT + r_p + \Delta r_p \int_{T_6}^{T_1} (C_{P_{H_1}}) dT \right)$$

To verify the obtained dependence, we use the results of calculating the thermal efficiency of the theoretical Rankine cycle of a turbine with the following parameters [69]:

$P_1 = P_4 = P_5 = P_6 = 11 \text{ MPa}$; $P_2 = P_3 = 0.004 \text{ MPa}$; $t_1 = 550 \text{ }^\circ\text{C}$; $t_2 = t_3 = t_4 = 28.98 \text{ }^\circ\text{C}$; $t_5 = t_6 = 318.04 \text{ }^\circ\text{C}$; $q_1 = 3368.6 \text{ kJ/kg}$; $q_2 = 1903.6 \text{ kJ/kg}$; Cycle efficiency = 0.435; $r_p = 1256.16 \text{ kJ/kg-K}$ ($P = 11 \text{ MPa}$, $t_4 = 318.04 \text{ }^\circ\text{C}$); $C_{P_{H_1}} = 2.54$ ($t_1 = 550 \text{ }^\circ\text{C}$).

The efficiency of the cycle, in this case, was determined from the known values of the supplied and removed heat $\eta_t = 1 - q_2/q_1$. Cycle efficiency=0.435.

For the calculation according to this relation, the averaged values of the heat capacity of untreated water and steam $C_{P_B} = 4.19$ and $C_{P_{H_1}} = 3.89$ were chosen.

Such values can be taken only for assessed calculations, for further research it is necessary to approximate the change in the heat capacity of water and steam from the temperature at a given pressure and put the obtained analytical dependences under the integral sign.

The latent heat of vaporization in this process is $r_p = 1256.16 \text{ kJ/kgK}$ ($P = 11 \text{ MPa}$, $t_5 = 318.04 \text{ }^\circ\text{C}$). The resulting calculated efficiency is 0.4348, which coincides with a high degree of accuracy with that given in [65].

Numerical studies have shown that with an increase in C_{P_B} of 5% and η_t by 11%, the thermal efficiency of the Rankine cycle will be 0.467 (an increase of 3.1%).

The results obtained might be regarded as indicative (qualitative). Although a significant effect of changes in the thermodynamic parameters of water on the efficiency of the Rankine cycle has been theoretically proven, in fact, in the process of heating we have a new working medium, the properties of which have not been fully studied, which indicates the need to continue research.

The conducted studies have shown that the use of a second-order phase transition, which occurs when a force field is purposefully applied to water, makes it possible to increase the thermal efficiency of the Rankine cycle. The direction of this action is determined, the results of which should be an in-

crease in the specific isobaric heat capacity of water and a corresponding increase in the heat of vaporization.

Despite traditional methods of increasing the efficiency of the cycle of steam turbine plants (Rankine cycle), the implementation of this method does not require a change in design, replacement of materials used in the creation of equipment and significant material costs. To be able to use a second-order phase transition, it is necessary to continue experimental studies of the effect of force fields on water. The goal is to obtain a positive effect at the actual consumption of the working fluid and temperatures not only at the stage of isobaric heating and evaporation, which was discussed above, but also in the systems of regeneration, deaeration, and chemical water treatment; ensure that the duration of the property change is long enough to be used at any stage of the cycle.

CONCLUSION

During the operation of wet steam turbines, part of its thermal energy is converted into electrostatic energy of the flow due to direct contact of the flow with the metal elements of the flow path. The magnitude of these energy losses is small, however, as the studies have shown, the effect of electrization on the performance of the turbine unit is very tangible and is relevant and important from both practical and scientific points of view.

One of the main tasks of the research presented in this work was to assess the level of electrization of the steam flow at the operating turbines of TPPs and CHPs and to determine the post-factor effects of the charged flow on the performance of the power plant. Comprehensive studies carried out by the employees of IPMash NAS of Ukraine under the leadership of the author at various TPPs and CHPs in Ukraine, the USA and Russia, have shown that in the process of electrization of steam, the charge density in the flow can reach very high values (an order of magnitude higher than in a thundercloud) and these phenomena harm the operation of wet steam turbines: the electric potential of the rotor increases and the risk of bearing destruction increases; electrostatic flow generation downstream of the last stage increases back pressure and dynamic load on the rotor blade, reducing the reliability and efficiency of turbines; dissociation of water droplets in an electric field and electrolytic dissociation lead to hydrogen saturation of the structures of the flow path, etc., the influence of an aggressive electrified steam medium on the surface strength of the rotor blades. It is shown that factors such as the presence of a positively charged steam flow, and constant and alternating electric fields, which were most often recorded during experimental studies on operating turbines of TPPs, significantly (two or more times) intensify erosion-corrosion processes on the metal surfaces of the blades, reducing thus, their working resource. In this case, the change in the surface strength of the material during electrization of the flow occurs mainly due to an increase (5—10 times) of the absorption of hydrogen into the metal and a change in its surface energy under the influence of electric fields, due to a change in the density of electrons.

When considering the degree of influence of natural electrization of the flow on the efficiency of the turbine, it was taken into account that this phenomenon, in principle, could be effective as a factor of additional formation of condensation nuclei in supercooled steam.

However, this assumption was not confirmed when considering the real processes occurring in the turbine. This can be explained by the fact that in the initial phase transition zone when supercooling usually reaches a maximum level, the number of naturally forming charges, as it was experimentally displayed, is insignificant, and they practically do not affect heat and mass transfer processes. In the zone of the last stages, on the contrary, the level of hypothermia is already minimal, and the charge density is maximum, which significantly reduces the possible effect of reducing hypothermia from electrization. Moreover, an additional negative factor is imposed on this process in this zone such as electrostatic forces of flow deceleration. Thus, taking into account all possible processes occurring during the flow of a charged stream (electrostatic forces of deceleration of the flow in the exhaust part, an increase in the non-stationarity of the flow due to the uneven distribution of charges and electric fields in the flow path, the electrostatic force of a drop directed to the grounded sections of the flow path, etc.) it is possible to estimate the amount of heat energy losses from the effect of electrization approximately 0.25—0.30% in the turbine LPC.

The information obtained as a result of comprehensive studies on the electrophysical phenomena in the turbine, including the effect of electrified steam on the surface strength of the blades, was the basic material for the development of new methods and technologies that ensure an increase in the operational efficiency and reliability of wet steam turbines.

On this basis, devices have been developed to neutralize the charged flow; a method for diagnosing erosion-hazardous large dispersed moisture; universal probe for determining the density of charges in the flow, temperature, static and dynamic pressure; evaporative method of reducing erosion-corrosion degradation of metal from the effect of an electrified medium, in which the control of moisture removal from the surface of the blades is carried out by an electric probe; method based on the rational choice of chemistry.

The dynamics of the growth of natural charge formation in the flow path of the LPC, as previously noted, occurs in the direction opposite to the required dynamics of the formation of additional condensation centers, which contributes to a decrease in the level of supercooling of steam. Therefore, the second line presented in the monograph is an artificial ionization of steam that was developed taking into account the accumulated experience and the vision of the disadvantages of natural electrization. The problem of rational control of the processes of charge formation and ionization of steam for this case was formed and solved in the following formulation — increasing the efficiency of the process of expanding the steam flow in a turbine should be carried out by activating (or deactivating) it by local input (or output) into the working environment of electrical and electromagnetic energy.

Numerous bench and partially full-scale tests have shown the high efficiency of the proposed method of artificial ionization of the steam flow. As the calculations and results of experimental tests have shown, the efficiency of wet steam turbines in this case can be increased by two or more percent due to a decrease in the level of overcooling and non-stationary condensation, a decrease in film condensation and concentration of large dispersed moisture, etc. Options for the local input of electrical energy for the ionization of steam in the turbine, as well as elements of devices and structures that ensure reliable and safe operation of the system that ionizes steam were developed such as: high-voltage sources, corona, and barrier type electric dischargers, corona electrodes, bushing, and suspension insulators. The boundary parameters of the steam are determined, at which the ionization of steam can be efficiently carried out. The developed method allows: to intensification of the process of steam condensation in

the form of fine moisture (the droplet size does not exceed 0.4—1.0 microns); to reduce the level of hypothermia and condensation unsteadiness; to reduce film condensation and the concentration of large dispersed moisture.

To reduce the negative influence of the electrostatic forces of deceleration of the flow in the zone of the last stage, local energy removal is provided with the help of charge neutralizers, which have been successfully tested at TPPs and CHPs.

The proposed method of artificial ionization of the steam flow and its use for wet steam turbines is scientifically sufficiently justified, and its effectiveness is confirmed by the results of numerous studies and become a good basis for its further practical refinement and design improvement of promising steam turbines.

The work also investigated and studied the possibilities of controlling thermal processes in a turbine using the correction of water chemistry, more precisely, the pH of the medium. Unfortunately, the results of all specially conducted laboratory and field tests in this direction showed that a change in the pH of the medium has practically no effect on the intensification of the formation of process moisture in the flow path, and hence on the process of steam expansion in the turbine and its efficiency.

At the same time, the fact of the influence of the pH of the medium on the intensity and polarity of the charge formation of the steam flow has been experimentally indicated. These processes, in our opinion, are not associated with process moisture but are a consequence of film condensation on the blade surface, i.e. a factor influencing reliability indicators to a greater extent than efficiency. In this case, a change in the properties (amine content of the medium) leads to a change in the surface tension forces of the water (film) condensate, which in turn contributes to both a change in the dispersion of droplets escaping from the metal and the degree of their electrization and polarity, i.e. parameters that significantly affect the surface strength of the blade.

Understanding these processes opens up broad prospects for the development of recommendations for reducing erosion-corrosion degradation of turbine structural elements. In particular, it is recommended to select the amine content of the feed water from the standpoint of the minimum charge density in the flow (or with negative polarity) and carry out the corresponding control using an electric probe. Studies have shown that such measures lead to a significant extension of the service life of the rotor blades.

The conducted studies have shown that the use of the effect of a second-order phase transition under force action on water may be promising in further research, the goal of which is to increase the thermal efficiency of a turbine unit.

The studies presented in the work on electrophysical phenomena in wet steam turbines are relevant and important information for specialists in the energy-related area. These comprehensive studies can be characterized as a new scientific direction in the theory of steam turbines — heat-electrophysics.

The author is grateful to the management and specialists of the power plants at which the field studies were carried out: TPP-2 “Eskhar”, TPP-5 Kharkov, Zmievskaya TPP, TPP Novakho, TPP Consville, USA.

The author expresses special gratitude to the international partner from USA — Ph.D., Weres O. as well as to all Employees of the Department of General Technical Research in Power Engineering, who at different times took part in these works and, first of all, Doctor of Technical Sciences Sklyarov V.P., Ph.D. Surdu N.V., Ph.D. Nechaev A.V., Ph.D. Annopolska I.E., Ph.D. Tarelin A.A., Engineers: Khinevich A.E., Orlovsky V.P., Lukyanov V.N., Vitkovska T.S., Kryzhenko B.P. et al.

REFERENCES

REFERENCES

1. Tarelin O.O., Sklyarov V.P. Parovyye turbiny: elektrofizicheskiye yavleniya i neravnovesnyye protsessy. SPb.: Enerhotekh, 2012. 292 p. [in Russian].
2. Ryley D. J., Loftus F.P. An investigation of electrostatic phenomena associated with flowing wet steam with particular reference to the wet steam turbine. *Int. J. of Heat and Fluid Flow*. 1980. Vol. 2. 2: 77—84.
3. Semenov V.N., Troyits'kyy O.M., Tarelin A.A., Sklyarov V.P., Duly B.R. Opredeleniye ob»yemnoy plotnosti zaryadov v potoke kondensiruyushchegosya para pri razlichnykh vodno-khimicheskikh rezhimakh. *Probl. mashynostoeniya*. 2001. Vol. 3. 3—4: 12—22 [in Russian].
4. Yevtyeyev B.F. Datchik plotnosti elektricheskogo toka na samolet i analiz yego ekvivalentnoy skhemy. *Tr. Glavnoy geofizicheskoy observatorii: Atmosfernoye elektrichestvo*. — L.: Gidrometeoizdat. 1974. Vyp. 301:130—133 [in Russian].
5. Vorobyov A.A. Sverkhvysokiye elektricheskiye napryazheniya / A.A. Vorob'yev. M.; L.: Gosenergoizdat, 1955. 355 p. [in Russian].
6. Tarelin A.A., Skliarov V.P., Sergienko Yu.I., Weres O. Electrical method to increase power output by improving condensation and flow of steam within the turbine neck and condenser of a steam turbine. *Proc. American Power Conf. 58th Annual (USA, Chicago, April 9—11, 1996)*: 1198 —1203.
7. Povarov O.A., Petrova T.I., Semenov V.N., Tarelin A.O., Skliarov V.P. Turbine Steam Chemistry and Corrosion. *Electrochemistry in Turbines*. EPRI Proceeding TR-100283 (USA August, 2001). 60 p.
8. Petr V., Kolovratnik M. Electrostatic Charge of Fine and Coarse Droplets in LP Steam Turbines. *Proc. of the 14th Int. Conf. on the Properties of Water and Steam (Japan, Kyoto, 2004)*: 606—611.
9. Belotelov A.K. ta in. Povysheniye nadezhnosti zazemleniya valov turboagregatov. *Elektricheskie stantsyi*. 2000. No. 6: 43—46 [in Russian].

10. Rozenberh S.Sh., Safronov L.P., Khomenok L.A. Issledovaniye moshchnykh parovykh turbin na elektrostantsiyakh. M.: Energoizdat, 1994. 270 p. [in Russian].
11. Kurmakayev V.M., Khomenok L.A. Problema elektroerozionnykh povrezhdeniy turboagregatov TETS, GRES i AES. Chast' 2. *Enerhozberezhenie i vodopodgotovka*. 2011. No. 5 (73): 50—53 [in Russian].
12. Palazzolo A.B., Vance J.M., Zeidan F.Y. Electric Shaft Currents in Turbomachinery. *Proc. of the 16th Turbomachinery Symp. Turbomachinery Laboratory. Department of Mechanical Engineering* (Texas A&M University, College Station) Texas, 1987: 11—13.
13. Staroba Y., Shymorda Y. Statychna elektryka u promyslovosti: prov. z ches'koyi. M.; L.: Derzhenerhovydannya, 1960. 284 p. [in Ukrainian].
14. Tarelin A.O. Elektrization of a wet steam flow and its influence on reliability and efficiency of turbines. *Thermal engineering*. 2014. Vol. 61.11. 790—796.
15. Man'kina N.N. Fiziko-khimicheskiye protsessy v parovodyanom tsikle elektrostantsiy. M.: Energiya, 1977. 256 p. [in Russian].
16. Fillipov H.A., Kukhariv O.A. Issledovaniya i raschety turbin vlazhnogo para. M.: Energiya, 1973. 232 p. [in Russian].
17. Kachuriner Y.Ya. Parovyie turbiny: osobennosti raboty vlazhnoparovykh stupenei SPb: Energotekh, 2015. 215 p. [in Russian].
18. Tarelin A.O., Orlovs'kyy V.P., Nechayev V.V. Pat. 113131 Ukrayina, MPK8 F01D5/18, F01D25/32. Sposib zapobihannya utvorenyu velykodispersnoyi volohy bila voloho-parovoho turbinnoho stupenya: vlasnyk Instytut problem mashynobuduvannya im. A.M. Pidhirnoho NAN Ukrainy. No. a201512161; zayavl. 08.12.2015; opubl. 12.12.15, Byul. No. 23. 8 p. [in Ukrainian].
19. Semenov V.M., Troyits'kyy O.M., Tarelin A.A., Sklyarov V.P., Duly B.R. Opredeleniye obyemnoy plotnosti zaryadov v potoke kondensiruyushchego para pri razlichnykh vodno-khimicheskikh rezhimakh. *Problemy mashynostroeniya*. 2000. Vol. 3. 3—4: 12—22 [in Russian].
20. Shylov V.M., Rozen Y.Ya. Polyarizatsiya diffuznogo dvoynogo sloya palochkoo-braznykh chastits i gigantskaya nizkochastotnaya dielektricheskaya pronitsayemost' polielektrolitov. Sb. dokl. konf. po poverkh-nostnym silam. M.: Nauka, 1972: 102—114 [in Russian].
21. Kalsman A.U. Neytral'nyye i zaryazhennyye klasteriy v atmosfere: ikh znacheneye i potentsial'naya rol' v geterogennom katalize. *Geterogennaya khimiya atmosfery / pod red. D.P. Shrayyera*. L.: Gidrometeoizdat, 1986: 33—62 [in Russian].
22. Tenesku F., Kramaryuk R. Elektrostatyka v tekhnike. M.: Energiya, 1980. 296 p. [in Russian].
23. Uzhov V.M. Ochistka promyshlennykh gazov elektrofil'tratsiyey. M.: Khimiya, 1967. 365 p. [in Russian].
24. Perel'man R.H., Pryakhin V.V. Eroziya elementov parovykh turbin. M.: Vysh. shk., 1986. 184 p. [in Russian].
25. Shubenko A.L. ta in. Vliyaniye erozii na osnovnyye ekspluatatsionnyye kharakteristiki rabochey lopatki posledney stupeni tsilindra nizkogo davleniya moshchnoy parovoy turbiny. *Problemy mashynostroeniya*. 2010. Vol. 13. 1: 3—11 [in Russian].
26. Koval's'kyy A. E. Teoreticheskoye obosnovaniye mekhanizma kapleudarnoy erozii rabochikh lopatok osevykh turbomashin. *Aviats.-kosm. tekhnika ta tekhnolohiya*.

- Dvyhuny ta enerhoustanovky: zb. nauk. prats'*. Kharkiv: Nats. aerokosmichnyy un-t «KHAi», 2001. Vyp. 23: 33—41. [in Russian].
27. Sivukhin D.V. Obshchiy kurs fiziki: v 3-kh t. III: *Elektrika*; izd. 4-t, stereotyp. M.: Fizmatlit, 2004. 656 p. [in Russian].
 28. Ulih H.H., Revi R.U. Korroziya i bor'ba s ney. Vvedeniye v korrozionnuyu nauku i tekhniku. L.: Khimiya, 1989. 456 p. [in Russian].
 29. Petrov L.N., Sopronyuk N.H. Korroziionno-mekhanicheskoye razrusheniye metallov i splavov. Kyiv: Nauk. dumka, 1991. 216 p. [in Russian].
 30. Krasnov K.S. ta in. Fizicheskaya khimiya: v 2-kh kn. Kn. 2: Elektrokimiya. Khimicheskaya kinetika i kataliz / 3-tee izd. M.: Vysh. shk., 2001. 319 p. [in Russian].
 31. Tarelin A.A., Surdu N.V. Vliyaniye elektrofizicheskikh yavleniy v protochnoy chasti parovykh turbin na fiziko-khimicheskiye svoystva ikh elementov. *Problemy mashynostroeniya*. 1999. No. 3—4: 100—108 [in Russian].
 32. Tarelin A.O. Post-factor phenomenon of wet-steam flow electrization in turbines. *Thermal engineering*. 2017. Vol. 64. **11**: 810—816.
 33. Fedosov S.A., Pishok L. Opredeleniye mekhanicheskikh svoystv materialov mikroindentirovaniyem: Sovremennyye zarubezhnyye metodik. M.: Fizicheskiy fakul'tet MGU, 2004. 100 p. [in Russian].
 34. HOST 9450-76 Izmereniye mikrotverdosti vdavlivaniyem almaznykh nakonechnikov. M.: Izdatel'stvo standartov, 1993. 35 p. [in Russian].
 35. Ruzhyts'kyy V.V. ta in. Mnogotselevaya eksperimental'naya ustanovka «SKIF». *Voprosy atomnoy nauki i tekhniki. Seriya «Fizika radiatsionnykh povrezhdeniy i radiatsionnoye materialovedeniye»*. 1989. Vyp. 4/5: 84—89 [in Russian].
 36. Soshko V.A., Syminchenko I.P., Lyashkov V.S. Vodородnaya khрупkost' i vodородnaya plastichnost' stali. *Metalofizika i novye tekhnologiyi*. 2014. Vol. 36. **12**: 1701—1710 [in Russian].
 37. Tarelin A.O., Surdu N.V., Nechaev A.V. The Influence of Wet-Steam Flow Electrization on the Surface Strength of Turbine Blade Materials. *Thermal engineering*. 2020. Vol. 67. **1**: 60—67.
 38. Orlova D.V., Filip'yev R.A., Danylov V.I. O vozmozhnykh prichinakh vliyaniya elektricheskogo potentsiala na soprotivleniye metallov mikroindentirovaniy. *Izv. vuzov. Chernaya metalurgiya*. 2012. Vol. 55 (**10**):66—67 [in Russian].
 39. Orlova D.V. ta in. O vliyanii elektrostacheskogo polya na mikrotverdost' monokristallov tsinka. *Obrabotka metallov*. 2012. No. 4: 98—102 [in Russian].
 40. Kinan D. Termodinamika: per. s angl. M.; L.: Gosenergoizdat, 1963. 249 p. [in Russian].
 41. Sklyarov V.P. Izmereniye temperatury vlazhnogo parovogo potoka v parovykh turbinakh. *Probl. mashynostroeniya*. 2005. Vol. 8. **3**: 8—16 [in Russian].
 42. Garmathy G. Grundlagen einer Theorie der Nabdampfturbine. Zurich, 1962. 284 s.
 43. Saltanov H.A. Neravnovesnyye i nestatsionarnyye protsessy v gazodinamike odnofaznykh i dvukhfaznykh sred. M.: Nauka, 1979. 288 p. [in Russian].
 44. Kachuriner Y. Ya., Trevhoda A.M. Raschet neravnovesnykh dvukhfaznykh dvumernykh techeniy v zone nachal'noy kondensatsii. *Inzh.-fiz. zhurnal*. 1992. Vol. 63. **2**: 199—204 [in Russian].
 45. Tarelin A.A., Sklyarov V.P. Pat. 74193 Ukrayina, MKI6 F01D5/28. Sposob uvelicheniya KPD parovykh turbin/ Tarelin A.A., Sklyarov V.P.; zayavitel' i patentoobladatel'

- Institut problem mashinostroyeniya NAN Ukrainy. — № 20030103319; zayavl. 14.012.03; opubl. 15.11.05, Byul. №11
46. Paley A.A., Lapshyn V.B., Zhokhova N.V., Moskalenka V.V. Issledovaniya protsessov kondensatsii parov na elektricheskii zaryazhennykh aerazol'nykh chastitsakh: *Elektron. nauk. zhurn.* 2007: 263—274 [in Russian]. URL: <http://zhurnal.ape.relarn.ru/articles/2007/027.pdf>
 47. Tarelin A.A., Sklyarov V.P., Koval'ov A.S. Vplyv shtuchnykh tsentriv kondensatsiyi na vypadannya volohy pry nerivnovazhnomu rozshyrenni volohoyi pary v sopli Lavalya. *Probl. mashynobuduvannya.* 2008. Vol. 11. 2: 3—7 [in Russian].
 48. Deych M.Ye., Filippov H.A. Dvukhfaznyye techeniya v elementakh teploenergeticheskogo oborudovaniya. M.: Vysh. shk., 1987. 328 p. [in Russian].
 49. Buckley John Richard. A Study of heterogeneous nucleation and electrostatic charge in steam flows: Ph. D. thesis. University of Birmingham, 2004. 246 p.
 50. Martynova O.I. ta in. Utvorenniya korozivno-aktyvnykh seredovysch u zoni fazovoho perekhodu u parovykh turbinakh. *Teploenerhetyka.* 1998. No.7: 37—42 [in Ukrainian].
 51. Tarelin A.O., Nechaev A.V. Influence of Water-Chemical Regime on Electrization of Steam Flow, Reliability and Efficiency of a Turbo Unit. *Thermal engineering.* 2021. Vol. 68. 11: 873—880. <https://doi.org/10.1134/S0040363621110059> [in Ukrainian].
 52. Orlyk V. H., Kachuriner Y.Ya., Averkina N.V., Vaynshteyn L.L., Filaretov M.A., Matyushyn A.St. et al. St. F. Pat. 2267617 RU, MPK F01 D25/32. Sposib vydalennya volohy z kanaliv napravlyayuchoho aparatu voloho-parovoho turbinnoho stupenya / zayavnyk ta patentovlasnyk VAT «NVO TSKTI». No. 2004116091/06; zayavl. 26.05.2004; opubl. 10.01.2006, Byul. No.01. 6 p. [in Ukrainian].
 53. Tarelin A.O., Orlovs'kyi V.P., Nechayev V.V. Pat. № 113131 Ukrayiny, MPK F01D5/18, F01D25/32. Sposib zapobihannya utvorenniyu velykodispersnoyi volohy bilya voloho-parovoho turbinnoho stupenya. Zayavnyk ta vlasnyk patentu Instytut problem mashynobuduvannya im. A.M. Pidhirnoho NAN Ukrayiny. No. a 201512161; zayavl. 08.12.2015; opubl. 12.12.15, Byul No. 23. 5 p.: il. [in Ukrainian].
 54. Dudnik O.M. Novi parogazovi ta gibrydni ustanovki na palyvnykh elementakh. *Zbirka naukovykh prats' XV Mizhnarodnoi konf. «Vugil'na teploenerhetyka: shlyakh rekonstrucii ta rozvytku»* Kyiv, 2019: 40—43 [in Ukrainian].
 55. Robust Design of Multicomponent Working Fluid for Organic Rankine Cycle. Kyeongsu Kim, Jeongnam Kim, Changsoo Kim, Yonggeun Lee, and Won Bo Lee. *Ind. Eng. Chem. Res.* 2019. 58, 10, 4154—4167. <https://doi.org/10.1021/acs.iecr.8b04825>
 56. *Int. J. of Engineering Applied Sciences and Technology.* 2020. Vol. 5. 6: 111—115. URL: https://www.researchgate.net/publication/346495460_Fundamentals_Of_Thermal_Power_Generation. Fundamentals Of Thermal Power Generation Mohammed Elamin Department of Mechanical and Aerospace Engineering (North Carolina State University).
 57. Shalatonin V., Pollack G.H. Effect of Unipolar Magnetic Fields on UV Absorption and Evaporation of Water. *Chemical Physics Impact.* 2022. Vol. 4. 18 p. <https://doi.org/10.1016/j.chphi.2022.100077>
 58. Cai R., Yang H., He J., et al. The effects of magnetic fields on water molecular hydrogen bonds. *J. of molecular structure.* 2009. Vol. 938. 1—3: 15—19. <https://doi.org/10.1016/j.molstruc.2009.08.037>

REFERENCES

59. Wang Y., Zhang B., Gong Z., et al. The effect of a static magnetic field on the hydrogen bonding in water using frictional experiments. *J. of molecular structure*. 2013. Vol. 1052. 1: 102—104. <https://doi.org/10.1016/j.molstruc.2013.08.021>
60. Jawad S., Karkush M., Kaliakin V. Alteration of physicochemical properties of tap water passing through different intensities of magnetic field. *J. of the Mechanical Behavior of Materials*. 2023. Vol. 32. 1, id. 246. 9 p. <https://doi.org/10.1515/jmbm-2022-0246>
61. Yanmin Li, Haifei Lin, Zhendong Yang. The effect of magnetic field on freezing point of water. *Engineering J. of Physics: Conf. Series*. 2022. Vol. 2194, 1. <https://doi.org/10.1088/1742-6596/2194/1/012034>
62. Kai-Tai Chang, Cheng-I Weng. The effect of an external magnetic field on the structure of liquid water using molecular dynamics simulation. *J. of Applied Physics*. 2006. Vol. 100, 4. 043917 <https://doi.org/10.1063/1.2335971>
63. Youkai Wang, Huinan Wei, Zhuangwen Li. Effect of magnetic field on the physical properties of water. *Results in Physics*. 2018. Vol. 8: 262—267. <https://doi.org/10.1016/j.rinp.2017.12.022>
64. Duenas J.A., Weiland C., García-Selfa I., Ruíz-Rodríguez F.J. Magnetic influence on water evaporation rate: an empirical triadic model. *J. of Magnetism and Magnetic Materials*. 2021. Vol. 53. P168377. <https://doi.org/10.1016/j.jmmm.2021.168377>
65. Yun-Zhu Guo, Da-Chuan Yin, Hui-Ling Cao, Jian-Yu Shi, Chen-Yan Zhang, Yong-Ming Liu et al. Evaporation Rate of Water as a Function of a Magnetic Field and Field Gradient. *Int. J. of Molecular Sciences*. 2012. Vol. 13, 12: 16916 —16928. <https://doi.org/10.3390/ijms131216916>
66. Szcześ A., Chibowski E., Hołysz L., et al. Effects of static magnetic field on water at kinetic condition. *Chemical Engineering and Processing: Process Intensification*, 2011. Vol. 50, 1: 124—127. <https://doi.org/10.1016/j.cep.2010.12.005>
67. Malkin E., Furat I.E., Kovalenko N.O., Sepik A.V. Vplyv magnitnoi obrobky na pytomu teplotu paroutvorennya vody. *Ventylyatsia, osvittlennya ta teplog-azopostachannya*. 2014. Vyp. 17: 77—83 [in Ukrainian].
68. Energo i resursosberigayushie tekhnologii v energetike i energomashi-nostroenii / pid. red. A.A. Tarelina. Kyiv: Nauk. dumka, 2017. 272 p. [in Russian].
69. Dubrovska V.V., Shklyar V.I. Teorytychni osnovy teplotekhniki. Vyznachennya efektyvnosti termodynamichnykh cycliv teplovykh dvyguniv: rozrakhunkova robota. Kyiv: KPI im. Igora Sykorskogo, 2021. 31 p. [in Ukrainian].

CONTENTS

FOREWORD.....	5
---------------	---

Chapter 1

ELECTROSTATIC CHARGE IN WET STEAM FLOW WITHIN A TURBINE

1.1. An experimental set-up for the study of electrostatic charge build-up in wet steam flows	9
1.2. Methods for measuring the density of charges in a wet steam flow of a turbine	12
1.3. The main factors affecting the magnitude and polarity of charges in the steam-water flow	14
1.4. A brief chronology of the studies carried out to determine the charge density in the wet steam flow of the turbines of TPP and TPP	17
1.5. Influence of electrization of steam flow on electric currents and potential of the turbine rotor shaft	20
1.6. Electrostatic generator operational mode of the last stage and branch pipe of the turbine	23
1.7. Generation of hydrogen in a steam turbine unit during electrization of a wet steam flow	25
1.8. Electromagnetic fields in the exhaust pipe of a steam turbine	27
1.9. Influence of electrization of the steam flow on the thermodynamic characteristics of the turbine unit	30

Chapter 2

INFLUENCE OF ELECTRIC STEAM FLOW ON THE SURFACE STRENGTH OF BLADE STEEL

2.1. Justification of the physicochemical factors of the influence of a charged steam flow on the strength of the blades	37
2.2. Experimental evaluation of the effect of a charged dispersed medium on the strength properties of blade steel	42

2.2.1. Description of the experimental installation	42
2.2.2. Experimental methodology	44
2.2.3. Experimental results	46
2.2.4. Experimental determination of the influence of the physicochemical properties of the operational medium on the surface strength of blade steel	50
2.3. Study of the effect of a high-speed stream of ionized wet steam on the kinetics of changes in surface strength and hydrogen content in blade steel	53
2.3.1. Stand for studying the effect of a high-speed stream of charged steam on a sample	53
2.3.2. Technique and operating parameters of the experiment	57
2.3.3. Technique, results and analysis of the experiment on thermosorption of hydrogen	58
2.3.4. Study of the surface strength of the sample and the kinetics of changes in microhardness under the action of a high-speed charged steam flow	61
2.4. Study of strength properties of blade steel in a vacuum system under the action of a high-speed ionized flow of steam of different polarization	62
2.4.1. Modernized stand and research methodology	62
2.4.2. Results of the experiment with a high-speed stream in an vacuumed system	65
2.5. Study of the influence of constant and alternating electric field on the microhardness of the surface layer of the blade steel	69
2.5.1. Experimental installation and selection of parameters for electric field exposure to a steel sample	69
2.5.2. Methods and results of the experiment	71
2.6. Conclusion and main outputs in section 2	76

Chapter 3

THERMAL ELECTROPHYSICAL STUDIES OF THE INFLUENCE OF ARTIFICIAL IONIZATION ON THE EFFICIENCY OF EXPANSION OF A WET STEAM FLOW IN A TURBINE

3.1. Features of the thermodynamic process of expansion of the supercooled steam flow in the turbine	79
3.2. Experimental studies on artificial ionization of steam flow	84
3.3. Determination of a rational zone of thermodynamic parameters for artificial ionization of a wet steam flow	85
3.4. Determination of the dispersion of an artificially ionized flow	90
3.5. «Vitality» of condensation nuclei formed during steam ionization	93
3.6. Evaluation of the effectiveness of artificial ionization of the steam flow in the LPC	94
3.7. Field studies of the efficiency of ionization of supercooled steam	95

Chapter 4

INFLUENCE OF WATER-CHEMICAL REGIME (WCR) ON ELECTRIZATION OF WET STEAM FLOW WITHIN CHANGING PH, INDICATORS OF RELIABILITY AND ECONOMIC EFFICIENCY OF THE TURBO UNIT

- 4.1. Influence of water chemistry on electrization of the steam flow 99
- 4.2. Thermal electrophysical studies of the influence of water chemistry (pH) of feed water on the efficiency of the steam expansion process in the flow part of a supersonic nozzle 103
- 4.3. Influence of water chemistry on the reliability indicators of turbine blades 105

Chapter 5

DIAGNOSTIC METHODS AND MEANS OF INCREASING RELIABILITY AND EFFICIENCY INDICATORS DEVELOPED BASED ON ELECTROPHYSICAL PHENOMENA IN A TURBINE

- 5.1. Diagnostics of the concentration of erosive moisture 107
- 5.2. Neutralizer of the volumetric charge of the steam flow in the turbine 110
- 5.3. Methods for reducing erosion-corrosion processes from the effects of electrized large dispersed moisture 112
- 5.3.1. Estimative method for removing moisture from the channels of the guide apparatus of the last stage of a wet steam turbine 112
- 5.3.2. Method of reducing the flow charge by correcting the water-chemical regime and material properties (coatings) 115
- 5.4. Improving the efficiency of the turbine due to artificial ionization of the steam flow of the LPC 117
- 5.5. Study of the possibility of using physical fields (magnetic and electromagnetic) to increase the efficiency of a turbine unit 119
- CONCLUSION 129
- REFERENCES 132

У монографії представлено комплексні дослідження у галузі електризації вологопарового потоку в турбіні. Наведено аналіз, узагальнено досвід проведених досліджень на лабораторних стендах та натурних об'єктах (ТЕЦ та ТЕС) України, США. Розглянуто постфакторні явища електризації та їх вплив на експлуатаційні характеристики турбіни та запропоновано конкретні рекомендації щодо підвищення її ефективності та надійності. Найширше представлені дослідження впливу електризації на поверхневу міцність лопатки, а також методи та засоби діагностики, підвищення економічності та надійності, розроблені на основі електрофізичних явищ у турбіні. Монографія може бути корисна фахівцям енергетичного профілю, які працюють у галузі досліджень, створення та експлуатації парових турбін.

Наукове видання

НАЦІОНАЛЬНА АКАДЕМІЯ НАУК УКРАЇНИ
ІНСТИТУТ ПРОБЛЕМ МАШИНОБУДУВАННЯ
ім. А.М. ПІДГОРНОГО НАН УКРАЇНИ

Анатолій
Олексійович
ТАРЕЛІН

**ТЕПЛО-
ЕЛЕКТРОФІЗИЧНІ
ПРОЦЕСИ
В ПАРОВИХ
ТУРБІНАХ**

Англійською мовою

Редактор-коректор *В.К. Реґо*

Художнє оформлення *Є.О. Ільницького*

Технічне редагування *Н.М. Коваленко*

Виготовлення ілюстрацій *Н.М. Коваленко*

Комп'ютерна верстка *Н.М. Коваленко*

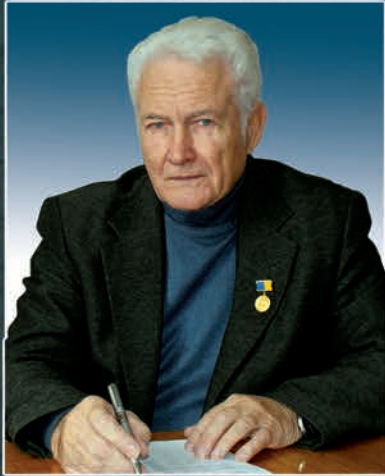
Підп. до друку 18.07.2024. Формат 70 × 100/16.

Гарн. Minion Pro. Ум. друк. арк. 11,38. Обл.-вид. арк. 10,44.

Тираж 107 прим. (у т. ч. 100 за бюджетні кошти). Зам. № 7349.

Видавець і виготовлювач Видавничий дім "Академперіодика" НАН України
01024, Київ, вул. Терещенківська, 4

Свідоцтво про внесення до Державного реєстру суб'єктів
видавничої справи серії ДК № 544 від 27.07.2001 р.



Anatoly Oleksiyovich TARELIN

Doctor of Technical Sciences,
Professor, State Prize Laureate,
Corresponding Member
of the NAS of Ukraine,
Academician of the Engineering
Academy of Ukraine, Chief
Researcher of A. Pidgorniy Institute
of Mechanical Engineering
Problems NAS of Ukraine.

He is well-known scientist in the
field of turbine engineering who
developed methods for complex
optimal automated design of the last
stages of steam turbines. He has
created and headed the new scientific
direction in the theory
and engineering practice of steam
turbines — thermal electrophysics.
Author of more than 200 scientific
works, including 6 monographs
and 31 inventions.